

**REPUBLIC OF TURKEY
HACETTEPE UNIVERSITY
INSTITUTE OF HEALTH SCIENCES**

**THE EFFECTS OF TUMOR MICROENVIRONMENT ON
T CELL RESPONSES IN A RAT CHEMICAL MAMMARY
CARCINOMA MODEL**

Gurcan GUNAYDIN, MD, PhD

**Tumor Biology and Immunology Program
PhD Dissertation**

**ANKARA
2013**

**REPUBLIC OF TURKEY
HACETTEPE UNIVERSITY
INSTITUTE OF HEALTH SCIENCES**

**THE EFFECTS OF TUMOR MICROENVIRONMENT ON
T CELL RESPONSES IN A RAT CHEMICAL MAMMARY
CARCINOMA MODEL**

Gurcan GUNAYDIN, MD, PhD

**Tumor Biology and Immunology Program
PhD Dissertation**

**Advisor of the Dissertation
Prof. Dicle GUC, MD, PhD**

**ANKARA
2013**

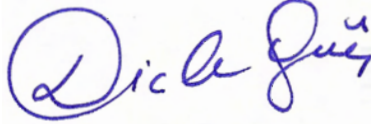
Anabilim Dalı :Temel Onkoloji
 Program :Tümör Biyolojisi ve İmmünolojisi
 Tez Başlığı :Şıçan Kimyasal Meme Kanseri Modelinde Tümör Mikroçevresinin T Hücre Yanıtları Üzerine Etkisi (The Effects of Tumor Microenvironment on T Cell Responses in a Rat Chemical Mammary Carcinoma Model)
 Öğrenci Adı-Soyadı :Gürcañ GÜNAYDIN
 Savunma Sınavı Tarihi :7 Ekim 2013

Bu çalışma jürimiz tarafından Tümör Biyolojisi ve İmmünolojisi Programı'nda Doktora Tezi olarak kabul edilmiştir.

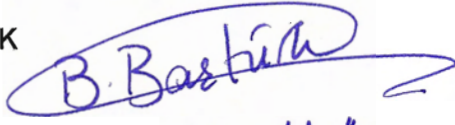
Jüri Başkanı: Prof. Dr. Dicle GÜÇ
 Hacettepe Üniversitesi



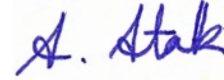
Tez danışmanı: Prof. Dr. Dicle GÜÇ
 Hacettepe Üniversitesi



Üye: Prof. Dr. Bilkay BAŞTÜRK
 Başkent Üniversitesi



Üye: Prof. Dr. Ayşegül ATAĞ YÜCEL
 Gazi Üniversitesi



Üye: Doç. Dr. A. Lale DOĞAN
 Hacettepe Üniversitesi



Üye: Doç. Dr. Güneş ESENDAĞLI
 Hacettepe Üniversitesi



ONAY

Bu tez Hacettepe Üniversitesi Lisansüstü Eğitim-Öğretim ve Sınav Yönetmeliğinin ilgili maddeleri uyarınca yukarıdaki jüri tarafından uygun görülmüş ve Sağlık Bilimleri Enstitüsü Yönetim Kurulu kararıyla kabul edilmiştir.



Prof. Dr. Ersin FADILLIOĞLU
 Müdür

ACKNOWLEDGEMENTS

I would like to express my deepest gratitude and thankfulness to my advisor, Prof. Dicle Güç, MD, PhD, for her support, guidance and understanding during the whole period of my PhD studies. Her continued encouragement led me to the right way.

I cordially thank Prof. Emin Kansu, MD for his encouragement and inspiring advices throughout my studies.

I am indebted to Assoc. Prof. Güneş Esendağlı, PhD for his advices and help in the experimental techniques.

I gratefully acknowledge Assoc. Prof. A. Lale Doğan, MD and Hande Canpınar, PhD for all their continued support and kindness during my research.

Special thanks to S. Altuğ Kesikli, MD, PhD; Yusuf Dölen, PhD; Neşe Ünver, PhD; Seylan Ayan, MSc and all the PhD and MSc students of the Department of Basic Oncology for their help, close friendship, and inspiring scientific discussions.

I would also like to extend my sincere appreciation to my thesis committee member Prof. Ayşegül Atak Yücel, MD for her invaluable advices.

I am deeply grateful to Prof. Ayşegül Üner, MD, PhD for her support in immunocytochemistry experiments.

I am also thankful to all the technicians of the Hacettepe University Laboratory Animals Research and Care Facility for their assistance in the animal experiments and all the staff members of the Department of Basic Oncology for creating a positive working environment.

I am grateful to my grandparents for their support and understanding.

I would like to express my cordial gratitude to my parents Şahin Günaydın, MD and Nilgün Günaydın, MD who have always supported me unconditionally, no matter what I decide to do. I dedicate this dissertation to them.

Finally, I acknowledge *The Scientific and Technological Research Council of Turkey* (Project No: 111S271) for their financial support to this study.

ÖZET

Günaydın, G. Sıçan kimyasal meme kanseri modelinde tümör mikroçevresinin T hücre yanıtları üzerine etkisi. Hacettepe Üniversitesi Sağlık Bilimleri Enstitüsü, Tümör Biyolojisi ve İmmünolojisi Programı, Doktora Tezi, Ankara, 2013. Tümöre infiltre olan T hücrelerindeki fonksiyonel yetersizliğe yol açan hücre ve moleküllerin tespiti ile ilgili araştırmalar birçok etkenin üzerine odaklanmışsa da stromal hücresel elemanların katkısı yeterince aydınlatılmamıştır. Tümör stromasında en fazla bulunan hücre tiplerinden biri olan fibroblastlar, tümör mikroçevresinde kanserle ilişkili fibroblastlara (KİF) ve miyofibroblastlara dönüşürler. Doku fibroblastlarının, T hücre fonksiyonlarını etkilediği daha önce gösterilmiştir. Ancak, kanserle ilişkili fibroblastların T hücreler üzerindeki etkileriyle ilgili literatürdeki çalışmalar kısıtlıdır. Bu çalışmada, kanserle ilişkili fibroblastların (KİF) T hücre efektör fonksiyonlarında ortaya çıkan değişikliklerdeki rolü araştırılmıştır. Bu amaçla, bir sıçan kimyasal meme karsinogenez modeli kullanılmış ve elde edilen kanserle ilişkili fibroblastların splenosit hücreleriyle birlikte kültürleri yapılmıştır. KİF-splenosit kokültür süpernatantlarından yapılan incelemelerde, TGF- β ve IFN- γ düzeyleri değişmemiş olarak gözlenmiştir. Ayrıca KİF ile kokültür yapılmış splenositlerde CD25 ve CD28 gen ekspresyonlarının değişmediği izlenmiştir. Bu araştırmayla, kanserle ilişkili fibroblastların tümör mikroçevresindeki T hücreleri üzerine olan etkileri aydınlatılmaya çalışılmıştır.

Anahtar Kelimeler: Fibroblast, kimyasal karsinogenez, meme kanseri, T hücre, tümör mikroçevresi.

Bu proje, *Türkiye Bilimsel ve Teknolojik Araştırma Kurumu* tarafından desteklenmiştir (Proje No: 111S271).

ABSTRACT

Gunaydin, G. The effects of tumor microenvironment on T cell responses in a rat chemical mammary carcinoma model. Hacettepe University Institute of Health Sciences, Tumor Biology and Immunology Program, PhD Dissertation, Ankara, 2013. The studies that have investigated the nature of the cells and molecules responsible for the functional insufficiency of the tumor infiltrating T cells usually on several components; however, the contribution of stromal cellular elements has not yet been well established. Fibroblasts, one of the most abundant cell types found in the stroma, turn into cancer associated fibroblasts (CAFs) and myofibroblasts in the tumor microenvironment. Tissue fibroblasts have previously been shown to have effects on T lymphocyte functions. However, studies investigating the effects of cancer associated fibroblasts on T cells are limited in the literature. The scope of this study is to determine the role of tumor stromal fibroblasts on the alterations in T cell effector functions. For this reason, cancer associated fibroblasts were isolated from tumors generated by a rat chemical mammary carcinoma model. Then, these cells were cultured together with splenocytes. Supernatants collected from CAF-splenocyte cocultures were shown to have similar levels of TGF- β , and IFN- γ . In addition, splenocytes cocultured with CAFs were found to have similar gene expression levels of CD25 and CD28. This study will help elute the role of cancer associated fibroblasts on the functional changes observed in T cells in the tumor microenvironment.

Keywords: Fibroblast, breast carcinoma, chemical carcinogenesis, T cell, tumor microenvironment.

This project was financially supported by *The Scientific and Technological Research Council of Turkey* (Project No: 111S271).

TABLE OF CONTENTS

APPROVAL OF THE THESIS.....	iii
ACKNOWLEDGEMENTS	iv
ÖZET	v
ABSTRACT	vi
TABLE OF CONTENTS	vii
LIST OF ABBREVIATIONS.....	xi
LIST OF FIGURES.....	xv
LIST OF TABLES.....	xviii
<i>1. INTRODUCTION</i>	<i>1</i>
<i>2. LITERATURE REVIEW</i>	<i>3</i>
2.1. Normal Breast Tissue	3
2.2. Breast Cancer.....	4
2.2.1. Classification of Breast Carcinomas	4
2.2.2. Biology of Breast Carcinogenesis.....	5
2.3. Breast Cancer Microenvironment	7
2.3.1. Components of Breast Cancer Stroma.....	9
2.3.1.1. Fibroblasts.....	9
2.3.1.1.1. Cancer Associated Fibroblasts (CAF)	10
2.3.1.1.2. Origin of CAFs.....	14
2.3.1.1.3. Heterogeneity of CAFs.....	16
2.3.1.1.4. CAF Targeted Therapy.....	17
2.3.1.1.5. Isolation of CAFs from Tumors.....	17
2.3.1.2. Immune Cells and Anti-tumor Immune Responses	18
2.3.1.2.1. Tumor Immunotherapy.....	29
2.3.1.3. Endothelial Cells.....	29
2.3.1.4. Extracellular Matrix.....	30
2.4. Animal Models	32
2.4.1. Experimental Chemical Carcinogenesis	32
2.4.2. Chemical Carcinogenesis in Rats.....	32
2.4.3. N-Nitroso-N-methylurea (NMU) Breast Tumor Model.....	34

2.5. Single Cell Gel Electrophoresis (Comet) Assay to Determine DNA Damage	36
3. <i>MATERIALS AND METHODS</i>	38
3.1. Materials	38
3.2. Media, Solutions and Buffers	40
3.3. Experiments with the Laboratory Animals	41
3.3.1. Induction of Experimental Mammary Carcinoma Formation in Rats	42
3.3.2. Surgical Procedures	45
3.3.2.1. Intracardiac Blood Withdrawal	45
3.3.2.2. Tumor Excision and Mastectomy	45
3.3.2.3. Splenectomy	47
3.3.2.4. Synovial Membrane Excision	47
3.4. Isolation of Normal Fibroblasts and Cancer Associated Fibroblasts	48
3.4.1. Techniques Used for Fibroblast Isolation	49
3.4.1.1. Enzymatic Digestion with Collagenase I and Hyaluronidase (Orimo et al.) (57)	49
3.4.1.2. Enzymatic Digestion with Collagenase II and DNase-I	50
3.4.1.3. Enzymatic Digestion with Collagenase II and DNase I (different protocol) (220)	51
3.5. Isolation of the Immune Cells	51
3.5.1. Isolation of the Splenocytes (Density gradient separation)	52
3.5.2. Isolation of the Peripheral Blood Mononuclear Cells (PBMC) - Density gradient separation	53
3.5.3. Isolation of T Cells	55
3.6. Primary Cell Cultures	56
3.7. Cell Culture	56
3.7.1. Splenocyte, PBMC and T Cell Cultures	56
3.7.2. Subculturing Adherent Cell Cultures with Trypsin-EDTA or HyQTase	57
3.7.3. Cell Counting	58
3.7.4. Freezing and Thawing Cells	59

3.7.5. Quality Control in Cell Cultures: Testing for Mycoplasma Contamination	61
3.8. Morphological Analyses	62
3.8.1. Immunocytochemistry	62
3.8.1.1. Desmin Staining	62
3.8.1.2. Pancytokeratin Staining	65
3.9. Coculture Experiments	65
3.9.1. With Sorted CD4 ⁺ and CD8 ⁺ T cells	65
3.9.2. With Splenocytes or PBMCs	66
3.10. Enzyme-Linked Immunosorbent Assay (ELISA)	66
3.10.1. Rat TGF-beta1 ELISA	67
3.10.2. Rat IFN-gamma (IFN- γ) ELISA	69
3.11. Molecular Techniques	70
3.11.1. Total RNA Isolation	70
3.11.2. Control and Removal of DNA in Isolated RNA Samples	71
3.11.3. Spectrophotometric Analysis of RNA	72
3.11.4. cDNA Synthesis by Reverse Transcription	72
3.11.5. Real-Time Reverse Transcriptase-Polymerase Chain Reaction (Real-Time RT-PCR)	73
3.11.6. Agarose Gel Electrophoresis	76
3.12. Comet Assay	76
3.13. Histopathological Evaluation	77
3.14. Statistical Analyses and Scientific Graphings	77
4. RESULTS	78
4.1. Experiments with the Laboratory Animals	78
4.1.1. Rat Chemically Induced Mammary Carcinoma Model	78
4.2. Tumor Excision and Mastectomy	85
4.2.1. Normal and Cancer Associated Fibroblast Isolation	86
4.2.1.1. Enzymatic Digestion with Collagenase I and Hyaluronidase (Orimo et al.) (57)	86
4.2.1.2. Enzymatic Digestion with Collagenase II and DNase-I	88

4.2.1.3. Enzymatic Digestion with Collagenase II and DNase-I (different protocol) [2]	88
4.3. Morphological Analyses	89
4.3.1. Immunocytochemistry - Fibroblast Characterization	89
4.4. Isolation of T Cells	90
4.5. Coculture Experiments	92
4.6. Gene Expression Analyses (PCR)	92
4.7. Assessment of Cytokine Levels with Enzyme-Linked Immunosorbent Assays	96
4.8. Comet Assays	98
4.9. Quality Control in Cell Cultures: Testing for Mycoplasma Contamination	105
5. <i>DISCUSSION</i>	107
6. <i>RESULTS AND RECOMMENDATIONS</i>	113
REFERENCES	115
APPENDICES	142
<i>Appendix 1. Research ethics approval for animal experimentation</i>	144
<i>Appendix 2. Award received</i>	145
<i>Appendix 3. Scientific meetings where the data of the thesis was presented</i>	146

LIST OF ABBREVIATIONS

APC	Allophycocyanin
APC	Antigen presenting cell
bFGF	Basic fibroblast growth factor
BMC	Bone marrow cells
BMDC	Bone marrow derived cells
bp	Base pair
BSA	Bovine serum albumin
BD	Becton Dickinson
CAF	Cancer associated fibroblast
CCL	Chemokine (C-C motif) ligand
CD	Cluster of differentiation
cDNA	Complementary DNA
CTGF	Connective tissue growth factor
CTL	Cytotoxic T cells
CXCL	Chemokine (C-X-C motif) ligand
DAB	Diaminobenzidine
DC	Dendritic cell
DCIS	Ductal carcinoma in situ
dH ₂ O	Distilled water
DMBA	7,12-Dimethylbenz(a)anthracene
DMEM	Dulbecco's modified eagle medium
DMEM HG	DMEM High glucose
DMSO	Dimethyl sulfoxide
DNA	Deoxyribonucleic acid
dNTP	Deoxyribonucleotide triphosphate
DTH	Delayed type hypersensitivity
EBV	Epstein–Barr virus
ECM	Extracellular matrix
ED-A	Extra domain A (alternatively spliced domain)

EDTA	Ethylenediaminetetraacetic acid
EGF	Epidermal growth factor
EGFR	Epidermal growth factor receptor
ELISA	Enzyme-linked immunosorbent assay
EMT	Epithelial mesenchymal transition
EndMT	Endothelial mesenchymal transition
ER	Estrogen receptor
FACS	Fluorescence-activated cell sorting
FBS	Fetal bovine serum
FCS	Fetal calf serum
FITC	Fluorescein isothiocyanate
FOXP3	Forkhead box P3
FSC	Forward scatter
FSP1	Fibroblast specific protein 1
h	Hour
Ha- <i>ras</i>	Harvey- <i>ras</i>
HCl	Hydrochloric acid
HER2	Human Epidermal Growth Factor Receptor 2
HGF	Hepatocyte growth factor
HLA	Human leukocyte antigen
HPV	Human papillomavirus
HRP	Horseradish peroxidase
i.v.	Intravenous
i.p.	Intraperitoneal
ICAM	Intercellular adhesion molecule
IDO	Indoleamine 2,3-dioxygenase
IFN	Interferon
Ig	Immunoglobulin
IGF	Insulin-like growth factor
IL	Interleukin
iNOS	Inducible nitric oxide synthase
kb	Kilobase

kDA	KiloDalton
LCIS	Lobular carcinoma in situ
LDH	Lactate dehydrogenase
LLC	Lewis lung carcinoma
MDSC	Myeloid derived suppressor cell
MHC	Major histocompatibility complex
MICA	MHC class I chain-related protein A
MICB	MHC class I chain-related protein B
MMP	Matrix metalloproteinase
MMT	Mesenchymal mesenchymal transition
mRNA	Messenger RNA
MSC	Mesenchymal stem cell
NAC	N-acetylcysteine
NaOH	Sodium hydroxide
NCBI	National Center for Biotechnology Information
NF	Normal fibroblast
NG2	Neuron-Glial antigen-2
NK	Natural killer cell
NKG2D	NK cell receptor D (Natural killer group 2, member D)
NKT	Natural killer T cell
NMU	N-Nitroso-N-methylurea
No	Number
OD	Optical density
PBMC	Peripheral blood mononuclear cell
PBS	Phosphate buffered saline
PCR	Polymerase chain reaction
PDGF	Platelet derived growth factor
PDGFR	Platelet derived growth factor receptor
PE	Phycoerythrin
Pen/Strep	Penicillin Streptomycin
PerCP	Peridinin chlorophyll
PGE	Prostaglandin

RA	Rheumatoid arthritis
RNA	Ribonucleic acid
ROS	Reactive oxygen species
rpm	Revolutions per minute
RT	Reverse transcriptase
SD	Standard deviation
SDF1	Stromal derived factor 1
SDS	Sodium dodecyl sulphate
SE	Standard error
SFRP1	Secreted frizzled-related protein 1
SSC	Side scatter
TAP	Transporter associated with antigen processing
TBE	Tris Borate EDTA
TCR	T cell receptor
TEB	Terminal end buds
TGF	Transforming growth factor
T _H	Helper T lymphocyte
T _{H0}	Naive CD4 ⁺ T cell
TIL	Tumor infiltrating lymphocyte
TMB	3,3',5,5'-Tetramethylbenzidine
TNF	Tumor necrosis factor
Treg	Regulatory T cell
TSLP	Thymic stromal lymphopietin
ULB	UL-16 binding protein
USA	United States of America
UV	Ultraviolet
V	Volt
VCAM	Vascular cell adhesion molecule
v/v	Volume/volume
w/v	Weight/volume

LIST OF FIGURES

2.1.	Stages of mammary gland development in a mouse model.....	3
2.2.	Stromal contribution to neoplastic progression.....	7
2.3.	Crosstalk between CAFs and tumor cells.....	12
2.4.	Multiple Origins of Cancer Associated Fibroblasts.....	15
2.5.	“CAFcentric” View of the Tumor Microenvironment.....	17
2.6.	The polarity of CD4 ⁺ helper T cells and its consequences.....	26
2.7.	Angiogenic switch is essential for tumor progression to malignant state.....	30
2.8.	Eight mechanisms of ECM functions to change cell behavior.....	31
2.9.	Color coded 2D and 3D molecular structures of N-Nitroso-N-methylurea.....	34
3.1.	NMU Induced Mammary Carcinoma Protocol.....	42
3.2.	Three months old Sprague Dawley rat with a mammary tumor.....	43
3.3.	Time Scale of NMU Injections.....	44
3.4.	Sacrificiation of the animal and excision of the induced tumor in a safety cabinet.....	44
3.5.	Dissection of the ventral skin and exploration of the mammary tissue regions and mammary tumors in a Sprague Dawley rat.....	46
3.6.	Fibroblast isolation steps.....	48
3.7.	Tumor tissue was split into pieces mechanically with the cross-cutting technique.....	49
3.8.	Densities of various blood cells are shown.....	52
3.9.	Formation of the <i>buffy coat</i> after centrifugation.....	54
3.10.	Isolation of PBMC and splenocytes from blood or spleen.....	55
3.11.	Improved Neubauer Haemocytometer.....	59
3.12.	Nalgene Mr. Frosty achieves a rate of cooling close to -1°C per minute.....	60

3.13.	Eight chamber-well culture slides (BD).....	62
3.14.	Comparative threshold cycle method ($\Delta\Delta Ct$).....	75
3.15.	Fifty bp DNA ladder (50-1000 bp).....	76
4.1.	The molecular structure of N-Nitroso-N-methylurea (NMU).....	78
4.2.	NMU induced breast tumor.....	79
4.3.	Normal fibroblasts (200X) obtained by enzymatic digestion with collagenase I and hyaluronidase.....	87
4.4.	Carcinoma Associated Fibroblasts (200X) obtained by enzymatic digestion with collagenase I and hyaluronidase.....	87
4.5.	Gating strategy used in T cell sorting.....	91
	<i>a. Discrimination of doublets</i>	
	<i>b. Selection of the lymphocyte gate</i>	
	<i>c. CD3 (APC) intensity histogram and selection of CD3⁺ cells</i>	
	<i>d. CD4 (PE) vs. CD8 (PerCP) signal dot-plot and selection of positively stained cells</i>	
	<i>e. Percentages of cells in specified gates</i>	
4.6.	Post-sort evaluations.....	92
	<i>a. CD4 (PE) staining of CD4⁺ cells</i>	
	<i>b. CD8 (PerCP) staining of CD8⁺ cells</i>	
4.13.	IFN- γ levels in supernatants from NF-splenocyte and CAF-splenocyte cocultures (mean and \pm standard error are shown).....	97
4.14.	TGF- β levels in supernatants from NF-splenocyte and CAF-splenocyte cocultures (mean and \pm standard error are shown).....	98
4.15.	Results of the blood sample taken from the negative control animal.....	99
4.16.	Results of the blood sample taken from an animal 24 hours after the last NMU injection.....	100
4.17.	Results of the blood sample taken from another animal 2 months after the last NMU injection.....	100
4.18.	Tail length results of the blood samples taken from a control animal, from an animal 24 hours after the last NMU injection and from animals 2 and 3 months after	

the last NMU injections.....	102
4.19. Tail migration results of the blood samples taken from a control animal, from an animal 24 hours after the last NMU injection and from animals 2 and 3 months after the last NMU injections.....	103
4.20. Tail moment results of the blood samples taken from a control animal, from an animal 24 hours after the last NMU injection and from animals 2 and 3 months after the last NMU injections.....	104
4.21. Comet Assay results of four animal groups.....	105
4.22. Mycoplasma contamination assessment.....	106

LIST OF TABLES

3.1.	Antibodies used in T cell sorting.....	56
3.2.	Steps of the immunocytochemistry protocol are explained in detail.....	63
3.3.	ELISA kits used for the experiments.....	67
3.4.	Conditions and compounds used for Cdna synthesis.....	73
3.5.	Primer sequences designed for real time RT-PCR.....	74
3.6.	Quantities and final concentrations of real time RT-PCR reagents.....	74
3.7.	Real-Time RT-PCR thermal cycler conditions.....	75
4.1.	Dates of NMU injections and the average weights of the animals at the times of injections.....	79
4.2.	The order of sacrifices, excised tissues, tumor locations & sizes at the time of sacrifices.....	80
4.3.	Statuses of tumors and ages of the animals at sacrifices.....	83
4.4.	Ages of control animals at sacrifices.....	85
4.5.	IFN- γ levels in supernatants from NF-splenocyte and CAF-splenocyte cocultures.....	97
4.6.	TGF- β levels in supernatants from NF-splenocyte and CAF-splenocyte cocultures.....	98

1. INTRODUCTION

The estimate for the expected new cases of breast cancer among women during 2012 in the US is 226,870 and the estimate for men is 2,190 new cases (1). Approximately 39,920 deaths are estimated to occur in 2012 due to breast cancer (2).

Carcinogenesis is thought to be a multistep process of gain or loss of different gene functions. This *seed-centric* model; however, does not take into account the probable impact of the microenvironment, "*soil*", that the tumor cells reside in. Tumor cells are not isolated elements; they rather reside in a rich microenvironment consisting of fibroblasts, endothelial cells, pericytes, leukocytes and extra-cellular matrix (3).

Effector T cells play crucial roles in immune responses against tumors, which are described in three stages as elimination, equilibrium and tumor escape. Even though the effector T cells are known to recruit to the tumor microenvironment, these T cells give a weaker response to the stimuli via CD28 receptors. The studies that have investigated the nature of the cells and molecules responsible for this functional insufficiency of the tumor infiltrating T cells, usually focused on tumor cells themselves, tolerogenic dendritic cells and regulatory T cells (Treg); however, the contribution of stromal cellular elements has not yet been well established. In fact, recent studies in the field of oncology have underlined the crucial roles of microenvironment in cancer progression and metastasis.

Activated fibroblasts found specifically in the tumor microenvironment are defined as cancer associated fibroblasts (CAFs) (4). CAFs originate primarily by activation of tissue fibroblasts by cancer derived growth factors. This mechanism is similar to that seen in myofibroblasts during wound healing. CAF derived factors are able to promote a tumor permissive microenvironment and contribute to the metastatic properties of cancer cells (5).

Actually, the effects of CAFs on tumor progression are diversified. Cancer associated fibroblasts are also thought to be involved in ineffectiveness of anti-tumor immune responses by taking an important part in T cell functional losses. Yet the hallmarks of this interplay are vague.

Indeed, CAFs might be utilized as potential targets for therapy (6, 7).

Rats can be useful hosts for cancer studies, since various features of human cancers have been modeled in them (8). Chemically induced experimental carcinogenesis models are commonly used in *in vivo* cancer studies. Furthermore, the potential of N-Nitroso-N-methylurea (NMU) induced rat breast adenocarcinoma model to simulate human breast carcinoma histopathology is better than similar models utilized in mice (9-11).

For this reason, an experimental rat chemical breast carcinogenesis model was utilized. The cancer associated fibroblasts were isolated from the tumors generated in the animals and cocultured with splenocyte cells. The effects on T cell responses could then be assessed.

To the best of our knowledge, our study is the first in the literature in terms of investigating the influence of cancer associated fibroblasts which were obtained directly from breast cancer tissues on T cell functions.

2. LITERATURE REVIEW

2.1. Normal Breast Tissue

The mammary tissue is composed of the epithelial parenchyma and stroma which includes stromal cells and the matrix. This stroma has profound effects on mammary gland development, survival and proliferation (12). In addition, mammary stromal cells play a crucial role in tumorigenesis (12). The gland contains many ducts which consist of cuboidal epithelium. The inner layer is composed of the ductal epithelial cells, while the outer layer is a layer of myoepithelial cells (13). The mammary gland goes through multiple cycles and changes over the life of a female; which includes rapid development at puberty, cycles of proliferation and apoptosis during the menstrual period of a woman's life, and differentiate into lobular alveoli for lactation (14). Stages of mammary gland development in a mouse model is shown in Figure 2.1.

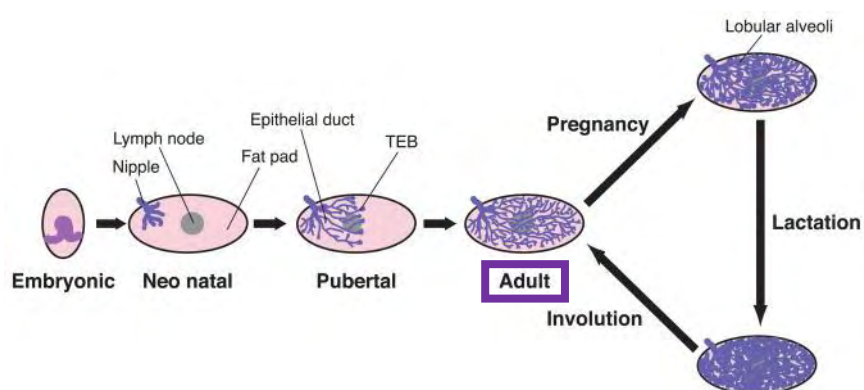


Figure 2.1. Stages of mammary gland development in a mouse model. Adapted from Wiseman et al. (12). TEB: Terminal end buds.

At each stage of embryonic and pubertal development, various signals are needed to promote changes in both the epithelium and the surrounding stroma. A recent surprising finding is that mammary epithelial cells commit to different lineages by using the same signaling pathways that regulate lineage determination of helper T cells (15). The mesenchymal stroma is an important factor for determining the mammary tissue fate during the developmental stages. The primary fibroblastic mammary mesenchyme determines the cell fate of the mammary gland. The secondary preadipocyte mesenchyme; however, is crucial for the characteristic branching ductal morphology (16). In summary, stroma plays a pivotal role for the development, morphology, physiology and also the pathologies of the mammary tissue.

2.2. Breast Cancer

The estimate for the expected new cases of breast cancer among women during 2012 in the US is 226,870 and the estimate for men is 2,190 new cases (1). It is estimated that 39,920 deaths (39,510 women, 410 men) are to occur in 2012 due to breast cancer (2). Breast cancer is a multifactorial disease with numerous types in terms of histopathology, grade and hormone receptor status. As conventional treatment modalities such as chemotherapy and radiotherapy cause dose limiting serious toxic side effects, new modalities like adjuvant hormonal treatments, targeted therapies and immunotherapy have emerged (17, 18).

2.2.1. Classification of Breast Carcinomas

It has been reported that various types of lesions can result in breast tumors. About 57 % of breast tumors are due to fibrocystic changes and about 7 % of them are because of fibroadenomas. While the benign neoplastic lesions constitute about 19 %, malignant lesions are about 14 % of all mammary tumors (19). Although malignant lesions are not the most common causes of breast tumors, they are one of the most common

cancers in women worldwide. Adenocarcinoma is the most frequent type of breast cancer. The other types (i.e. squamous cell carcinoma, phyllodes tumor, lymphoma and sarcoma) constitute only about 5 % of total breast tumors.

Breast cancer can be divided into two main categories as in situ carcinoma and invasive carcinoma. While the invasive type penetrates through the basement membrane, neoplastic cells of in situ type are confined to mammary ducts and lobules by an intact basement membrane (20). As a result, carcinoma in situ lesions do not invade tissues, lymphatics and blood vessels and thus cannot metastasize. The invasive types first invade the stroma at the outer side of basement membrane. Then gaining access to reach and invade lymphatics and blood vasculature; thus can metastasize to regional lymph nodes, distant lymphatics and even reach distant body sites. The in situ cancers can be subdivided into ductal carcinoma in situ (DCIS) and lobular carcinoma in situ (LCIS). The invasive type can be further divided into tubular carcinoma, colloid carcinoma (mucinous carcinoma), medullary carcinoma, invasive lobular carcinoma, and invasive ductal carcinoma, which makes up the majority of cancers (70 - 80 %) (20).

2.2.2. Biology of Breast Carcinogenesis

The steps of carcinogenesis have extensively been studied over the last 50 years. By the help of advancements in identification and characterization of many oncogenes and tumor suppressor genes, carcinogenesis is now thought to be a multistep process of gain or loss of different gene functions. These models suggesting a pivotal role for the genome have also been supported by Weinberg and Hanahan (21). They described the six hallmarks of cancer that are essential for a normal cell for its transformation to any type of cancer. These are evasion of programmed cell death (apoptosis), self sufficiency in growth signals, insensitivity to inhibitors of growth, limitless replicative potential, ability to develop blood

vessels, tissue invasion and metastasis (21). Acquiring these functions can be achieved by a change in one of many genes. For example, self sufficiency in growth signals can be achieved by an alteration in ER, EGF-R, Ras or HER2/*neu* genes. Even an alteration in one gene like p53 might result in gaining more than one of these capabilities; since p53 has pivotal roles in cell cycle control, DNA repair and apoptosis (20). These hallmarks have already been established usually even at the early stages like in situ lesions.

However, the *seed*-centric model described above does not take into account the probable impact of the microenvironment, "*soil*", that the tumor cells reside in. Tumor cells are not isolated elements; they rather reside in a rich microenvironment consisting fibroblasts, endothelial cells, pericytes, leukocytes and extra-cellular matrix (3). The microenvironment of a tumor is highly sophisticated, which has a vast impact on cancer progression (22). It has been more than a century since Paget mentioned about his "Seed and Soil" hypothesis; however, most of the molecular mechanisms of the soil are still unknown (23). Though we have a huge knowledge about the molecular characteristics of the *seed*; the significance of the crosstalk of tumor cells and their surrounding stroma-*soil* as a prognostic factor for tumor progression has only recently been recognized (24).

The epithelial cells are well separated from the stroma by a basement membrane consisting of normal fibroblasts and other supportive cell types in the normal mammary tissue. Transition from normal to preneoplastic state involves the loss of organization in epithelial cells; and then hyperplasia / aplasia (Figure 2.2). The basement membrane stands intact. The paracrine crosstalk between the epithelium and the stroma results in activation of stromal members such as fibroblasts and maturation of blood vessels (25).

Progression to neoplastic status is characterized with further epithelial proliferation together with the incorporation of the activated stromal cells (Figure 2.2). This, in turn, causes reciprocal secretory communication with the activated stroma and thus extracellular matrix (ECM) remodeling. Increased angiogenesis and degraded basement

membrane helps facilitate tumor invasion and metastasis. Stromal cells such as activated fibroblasts may even directly facilitate the metastatic movement at this state (25).

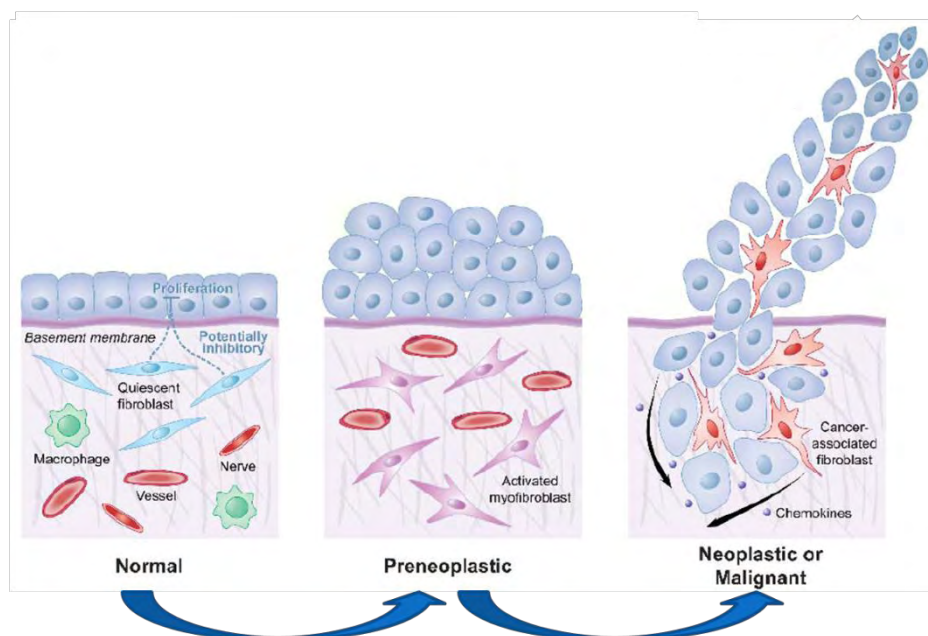


Figure 2.2. Stromal contribution to neoplastic progression. Adapted from Schauer et al. (25).

Tumor cells are in fact changing their microenvironment with growth factors, interleukins, colony stimulating factors, etc. via utilizing mechanisms like induction of angiogenesis (26, 27), inflammatory cell recruitment (28), and ECM remodeling (29); in a way that will help support tumor progression in the end.

2.3. Breast Cancer Microenvironment

In addition to serious side effects, conventional treatment modalities seem to be not very effective against advanced stage tumors which are extremely heterogeneous, metastasize, exhibit drug resistance and progress rapidly. Even though mainly cancerous cells are responsible for

the tumor formation, the impact of the surrounding stroma should not be ignored.

DeCosse et al. had previously shown that normal breast microenvironment is able to revert the malignant characteristics of mammary carcinoma cells back by promoting a more differentiated status. They commented that neoplastic cells could only proliferate in an abnormal microenvironment (30, 31).

Although there are numerous convincing results and reports today suggesting a very strong role for the microenvironment in mammary carcinogenesis process, the exact genes, proteins and pathways that orchestrate the complex cellular communication network among different types of cells in healthy and cancerous mammary tissues are still not completely clear (32).

Allinen et al. characterized the genome wide gene expression profiles of numerous cell types such as epithelial cells, endothelial cells, infiltrating leukocytes from normal mammary tissues, in situ and invasive mammary cancers in order to evaluate molecular changes in members of the microenvironment in a thorough and objective way (33). Allinen et al. concluded that alterations in expressions of genes occur in all cell types during the mammary carcinogenesis process. The clonally selected genetic changes are restricted to tumor epithelial cells.

Ma et al. used a different technique of laser capture microdissection and array-based profiling and they also demonstrated similar results. They evaluated variations in expressions of genes in epithelial cells and stromal cells by studying healthy breast, in situ and invasive mammary cancers. They showed that the alterations in gene expressions are associated with tumor progression (34).

It is of crucial importance to reveal the molecular mechanisms of cellular interactions and characterize the microenvironment members in mammary carcinomas, in order to be able to target them in the clinical setting.

2.3.1. Components of Breast Cancer Stroma

Members of the tumor microenvironment, especially the stromal components, strongly influence the course of metastatic events (35). Various cells are recruited by cancer cells to support their growth, survival and later invasion and metastasis (35). Examples of such cells that promote tumor progression are endothelial cells lining the blood and lymphatic circulatory systems; various types of bone marrow derived cells such as mesenchymal stem cells (MSCs), myeloid derived suppressor cells (MDSCs), macrophages, neutrophils, mast cells; pericytes and fibroblasts. In summary, components of the tumor microenvironment (mainly: 1-fibroblasts, 2-immune cells, 3-endothelial cells and 4-extracellular matrix) play crucial roles.

2.3.1.1. Fibroblasts

Fibroblasts are among the most common types of cells found in connective tissues. They secrete collagen that is used to maintain the structural framework of various tissues. Fibroblasts also play critical roles in wound healing processes.

Fibroblasts have a branched cytoplasm surrounding an elliptical nucleus. The molecular characteristic *signature* of fibroblast cells is not very clear and a widely accepted fibroblast specific molecular marker is lacking. Most of the proposed markers are either not specific only to fibroblasts or are not expressed in all types of fibroblasts. A filament associated calcium-binding protein, fibroblast-specific protein 1 (FSP1), was proposed to be relatively specific to fibroblasts (36). However, some types of activated fibroblasts might not express FSP1 (37).

Fibroblasts can secrete ECM constituents like type I, type III, type IV collagen and fibronectin (38). However, they are not just basic construction workers, they rather take active parts in many crucial processes. They can help direct leukocyte behavior such as leukocyte accumulation,

differentiation and survival in a variety of physiological stromal niches (39). They also play critical roles in regulation of ECM turnover with matrix metalloproteinases (40) and wound healing / scar formation (41). Fibroblasts at the site of a healing wound or fibrotic tissue were shown to secrete higher amounts of ECM products and proliferate more than the normal fibroblasts at healthy tissues (42). This phenomenon of increased bioactivity is defined as fibroblast *activation* (42).

2.3.1.1.1. Cancer Associated Fibroblasts (CAF)

As a type of fibroblast, CAFs are tumor connective tissue cells that secrete ECM rich in collagen, which is the structural framework for animal tissues. CAF is one of the most common type of cell found in tumor stroma.

Activated fibroblasts found specifically in the tumor microenvironment are defined as cancer associated fibroblasts (CAFs) (4). Loose definitions of CAF include "cells that surround cancer epithelia". More precise definitions of CAF involve those fibroblast cells that have the ability to promote tumorigenesis (43).

Furthermore, approximately 80 % of stromal fibroblasts are thought to show such an activated phenotype in breast carcinomas (44).

Normal fibroblasts become activated during wound healing and fibrosis and turn into myofibroblasts (45). After completion of the wound healing, activated fibroblasts are removed from the granulation tissue by a particular type of programmed cell death called nemosis (46, 47).

As "tumors are wounds that do not heal" (48), CAFs are similar to myofibroblasts. Some researchers; however, propose that they differ for their duration (they are not removed by apoptosis) and their activation is not reversible (49). On the contrary, Orimo et al. suggest that CAFs are stromal fibroblast populations which are present within tumor and these CAFs include populations of both myofibroblasts and fibroblasts. CAFs are the most prominent cell type within the tumor microenvironment of various

cancers (3, 43). CAFs express several activation markers within different tumors.

The main activation markers in stromal fibroblasts of solid tumors were reported as fibroblast specific protein (FSP) and platelet-derived growth factor (PDGF) receptors- β (43, 50). However, there also exists a controversy, just like in the case of definition of CAFs. Various fibroblastic markers are used to reveal stromal fibroblasts in tumor such as NG2 (Neuron-Glial Antigen-2) chondroitin sulfate proteoglycan, PDGFR- β , fibroblast-associated antigen, prolyl 4-hydroxylase and fibroblast specific protein 1 (FSP-1).

On the other hand, Sugimoto et al. found unique FSP1 expressing CAF subpopulations are present in the tumor microenvironment (Figure 2.4) (51). These FSP1 expressing CAF subpopulations should be further investigated in terms of promoting tumor progression compared to FSP1 negative counterparts.

The effects of CAFs on tumor progression are diversified. CAFs become activated by several tumor originated factors and then promote tumor progression (Figure 2.3). Cirri et al. summarized the crosstalk between cancer and stromal cells by two interactive pathways. According to their model, cancer cells induce a reactive response in stromal cells in the microenvironment (efferent pathway); which in turn affect cancer cell responses (afferent pathway) (Figure 2.3) (52, 53). Several factors including TGF- β are thought to be among tumor cell derived factors altering the activation status of CAFs (54).

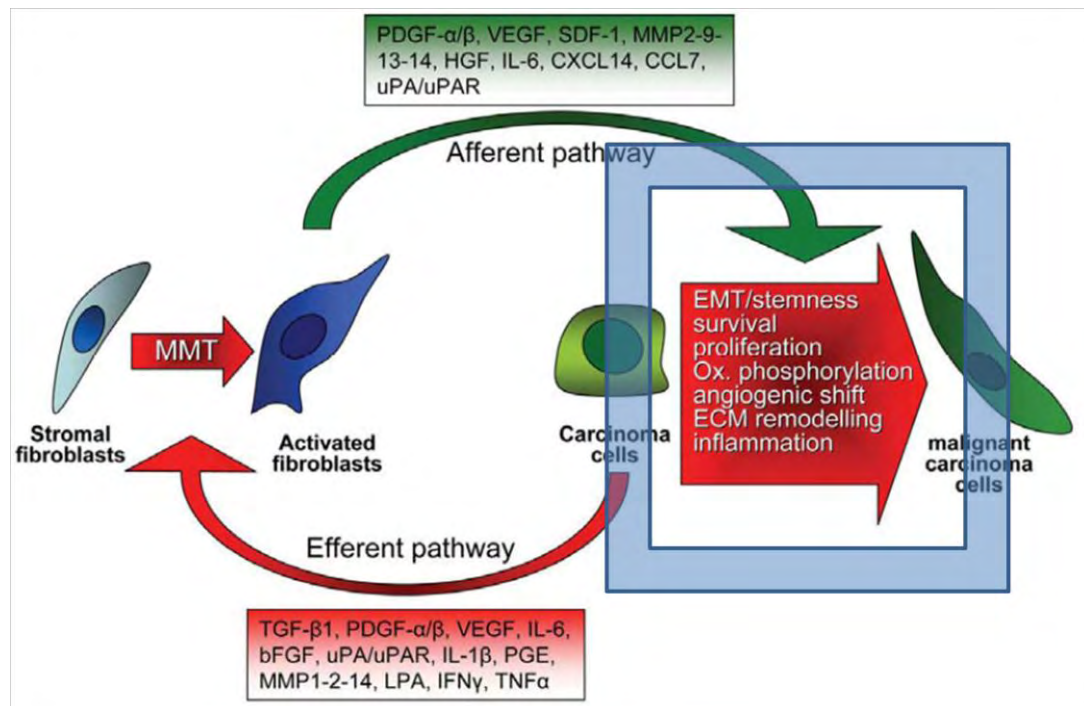


Figure 2.3. Crosstalk between CAFs and tumor cells. Adapted from Cirri et al. (49). MMT: mesenchymal–mesenchymal transition, EMT: epithelial–mesenchymal transition.

Furthermore, CAFs were demonstrated to directly promote tumor progression in various studies. CAFs take active role in the process of cancer cell invasion and metastasis (55). It was demonstrated that cancer cells move within tracks, which are generated by fibroblasts via ECM remodeling, behind fibroblast cells (56). Coimplantation tumor xenograft model experiments revealed that CAFs are able to promote the growth of breast carcinoma cells significantly more than do normal mammary fibroblasts (57).

Attempts on discovering the cells and molecules responsible for the functional insufficiency of the tumor infiltrating T cells mostly concentrate on tumor cells, tolerogenic dendritic cells and regulatory T cells (Treg). Natural Killer T (NKT) cells are also known to have complicated roles in regulation of the tumor immunosurveillance process (58). Berezhnaya N. M. (59) reported that tumor cells have roles in determining the number and activities

of various suppressor cells such as myeloid derived suppressor cells (MDSC), Treg cells and M-2 macrophages. In addition, tumor metabolites have been shown to be effective in suppression of T cell responses (60). It was reported that Treg cells impair proper immunological responses to tumor cells and promote tumor metastasis as soon as the gastric tumorigenesis is initiated (61). Hamai et al. (62) reported the inhibition of T cell effector functions via Treg cells. Since this functional insufficiency is thought to be usually related to tumor progression, T cell - tumor cell interactions have been investigated in many studies. On the other hand, our knowledge about the implications of other stromal elements in the tumor microenvironment; especially the fibroblasts which are the most abundant cell type in stroma; on anti-tumor immune responses is unsatisfactory. The effects of fibroblasts in tumor microenvironment on cancer pathogenesis has just recently been the topic of studies (43).

The suppression of anti-tumor immune responses have been studied relatively more often in Tregs and MDSCs. Most of these immunosuppressive mechanisms that are utilized by Tregs and MDSCs have been shown to be relevant also for fibroblasts. Secretion of soluble factors like Transforming Growth Factor- β (TGF β) and production of hormones like Prostaglandin E₂ (PGE₂) are among the probable immunosuppressive mechanisms described in fibroblasts. Fibroblasts have also been reported to secrete chemokines that regulate the accumulation of immune cells (63). Hence, fibroblasts are not solely structural cells. At present, they are thought to be involved in a dynamic and dense crosstalk with other cells of the tumor microenvironment (64).

As mentioned previously, fibroblast cells turn into myofibroblasts after activation in the tumor microenvironment. These cells then secrete high amounts of Extracellular Matrix (ECM) elements (65). Studies with pre-activated T cell cultures in plates coated with ECM proteins, have reported the increase of T cell proliferation (66, 67). Thus, ECM products originating from fibroblasts, have been shown to be able to result in T cell activation and increase in inflammatory responses.

2.3.1.1.2. Origin of CAFs

Despite many studies investigating the characteristics and functions of CAFs, there is still a huge debate about the possibility of multiple origins for CAFs. Their origin might vary even within different sites of tumors. The line of evidence about origins of CAFs might roughly be classified in: 1-resident; 2-mesenchymal stem cell (MSC)-derived; 3-mutational (Figure 2.4) (49).

CAFs originate primarily by activation of tissue fibroblasts by cancer derived growth factors. This mechanism is similar to that seen in myofibroblasts during wound healing. Growth factors such as TGF- β , PDGF and bFGF secreted by tumor cells activate tissue fibroblasts, smooth muscle cells, immune cells, adipocytes and pericytes (Figure 2.4). The trans-differentiation MMT process is accompanied by the expression of CAF specific genes in fibroblasts (68, 69) such as collagens, etc (70, 71). Toullec et al. reported that SDF- 1 is an important player involved in activation of resident fibroblasts of human adenocarcinoma (72).

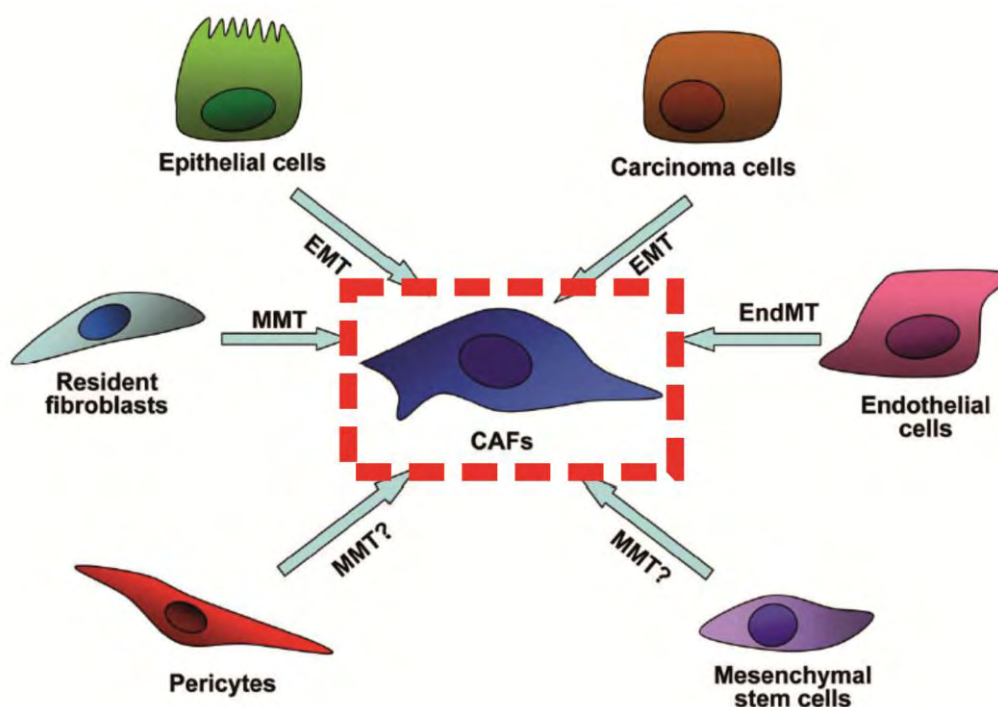


Figure 2.4. Multiple Origins of Cancer Associated Fibroblasts. Adapted from Cirri et al. (49).

Another source of CAFs is bone marrow derived MSCs. MSCs are able to differentiate into various cells in many physiological and pathological processes (73, 74). MSCs have also been shown to differentiate into CAFs within tumor mass.

In addition, epithelial cells might gain mesenchymal characteristics and become fibroblasts through an EMT process (43, 75). They indeed can undergo a specialized EMT in which they transdifferentiate into activated myofibroblasts (43, 76). EMT is induced by many factors (i.e. PDGF, TGF β , EGF, etc) (77, 78) and causes polarized epithelial cells to gain a mesenchymal cell phenotype in terms of migration and invasion capabilities by losing E-cadherin expression (77, 79).

Endothelial cells might also turn into CAFs via endothelial to mesenchymal transition (EndMT) which is similar to EMT. This process is characterized by the loss of endothelial markers like CD31, the expression of mesenchymal markers like FSP-1 under the stimulation of TGF β . This

results in passing of the cells through their basal membrane (80). Zeisberg et al. reported that approximately 40 % of FSP1 positive perivascular cells in the tumor periphery were also positive for CD31, an endothelial marker (80).

As mentioned before, the debate about the relative contribution of each of these models in generating the CAF population is still ongoing.

2.3.1.1.3. Heterogeneity of CAFs

It is proposed that even normal stromal fibroblasts from different locations in the body should be considered distinct differentiated cell types based on the finding of differential gene expression profiles (81). The anatomical origin of the fibroblast cells seem to affect their gene expression patterns. This heterogeneity is also consistent for CAFs, as most markers do not represent the whole population. Instead, markers like FSP-1 define diverse populations of CAFs (37).

Tumors usually have disorganized structures that contain many different cell types. Fibroblasts and myofibroblasts are important constituents of primary tumor tissues (43, 51). However, identification of cancer associated fibroblasts in cancerous tissues comprises many difficulties. Markers like Collagen I have frequently been used to distinguish these fibroblasts. Since these cells have great variations in expressing these markers, Sugimoto et al. (51) defined cancer associated fibroblasts as a group, representing in fact a heterogeneous population of cells.

The large heterogeneity of CAFs originating from different tumors in terms of expressing various markers might be explained by their possible diverse origins. As mentioned above, CAFs are variously reported to originate from resident local fibroblasts, bone marrow derived progenitor cells or transdifferentiating epithelial/endothelial cells through epigenetic modifications (5, 65, 82, 83).

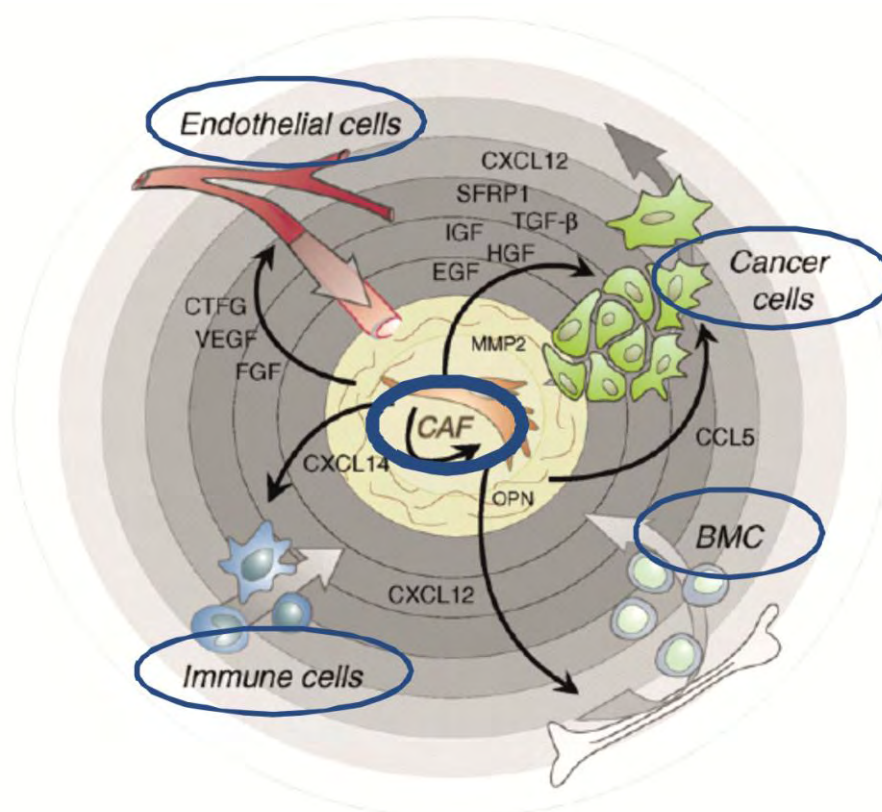


Figure 2.5. "CAFcentric" View of the Tumor Microenvironment. Adapted from Ostman et al. (5).

2.3.1.1.4. CAF Targeted Therapy

There is increasing evidence that the stromal compartments of tumors play important roles in tumor progression and metastasis and CAFs are protumorigenic. These findings led to the idea that CAFs might be utilized as potential targets for therapy (6, 7).

In summary, such strategies specifically targeting CAFs might help discover novel therapeutic approaches for cancer.

2.3.1.1.5. Isolation of CAFs from Tumors

The difficulties in specifically characterizing the cancer associated fibroblasts, make it even harder to isolate fibroblasts from the tumor tissue. Orimo et al. (57) published a method of isolating fibroblasts from breast

cancer tissues, by using a protocol that utilizes enzymes collagenase I and hyaluronidase. Although there are other protocols that have been published in the literature, it has usually been reported that these protocols have difficulties in achieving a pure cell population.

2.3.1.2. Immune Cells and Anti-tumor Immune Responses

The entire mechanisms that are responsible for protection against diseases, especially the infections, are referred to as immunity. The cells and molecules taking part in immunity comprise the immune system. The coordinated responses initiated by the immune system elements after an encounter with foreign molecules are called the immune responses (84). Although the immune system has crucial physiological roles in defending the organism against microorganisms that cause infections, immune responses might also be established against foreign molecules that do not cause infections; or even against the organism's self molecules.

Substances that cause the initiation of specific immune responses and that are the targets of these responses are called as antigens (85). These molecules can be proteins, lipids or nucleic acids. They can be organic or inorganic; having simple or complicated structures. The proteins that are secreted in vertebrates after an encounter with antigens and that help the recognition and elimination of these antigens by binding to them are referred to as antibodies.

Immune system responses to foreign organisms are executed by two complementing manners: the early responses of innate immunity and the late responses of adaptive immunity (86). Innate immunity is responsible for very rapid responses to infections, as it exists prior to the infections (87). These mechanisms respond to foreign organisms in the same way at every event of infection. Components of the innate immune system are physical (epithelium) and chemical barriers; phagocytic cells like neutrophils and macrophages; Natural Killer (NK) cells; complement system proteins and other inflammatory mediators; cytokines that regulate the immune cell

functions. Although the innate immune system recognizes the foreign organisms, it is not capable of differentiating the slight differences between foreign molecules (88).

On the other hand, adaptive immunity is initiated in case of an encounter with the organism. Its strength and versatility improves with each subsequent encounter with the pathogen (89). Adaptive immune responses can differentiate even the slightest differences between molecules. Lymphocytes and antibodies secreted from them comprise the adaptive immunity.

Adaptive immunity utilizes two different types of responses: cellular and humoral; which have different functions via using different members of the immune system. Humoral immunity comprises B lymphocytes, plasma cells and antibodies secreted from these cells. Its primary goal is the defense against extracellular pathogens (90). Cellular immunity components are various T cell subtypes and the cytokines secreted from these cells. It has crucial roles in eliminating intracellular microorganisms (91).

Adaptive immune responses are late onset, but they are capable of distinguishing even very closely related microorganisms and molecules. The specific immune responses of adaptive immunity also create memory. This feature gives rise to very rapid and efficient immune responses in cases of subsequent encounters with the same antigen (88). Both the humoral and the cellular responses of adaptive immunity involve lymphocytes (92). Antibodies, which are produced by B cells, are the mediators of humoral immunity. They are secreted to the blood stream or mucosal fluids and function against extracellular microorganisms. As the main effectors of the cellular immunity, T cells, are responsible for the immune responses against intracellular microorganisms like viruses. Both cell types originate from the bone marrow but mature at different sites (93).

T cells are responsible from the specificity of the cell-mediated immunity. They recognize intracellular antigens expressed on target cell surfaces by Major Histocompatibility Complex (MHC) molecules (94). In addition to responses against intracellular pathogens, T cells also function in

other processes such as delayed type hypersensitivity (DTH), graft and tumor rejections. These lymphocytes all express CD3 molecules and recognize antigens via T cell receptors (TCR) (95). This receptor is highly specific and varied (96).

There exists two main types of T cells: 1- CD8⁺ cytotoxic T cells (CTLs) that have the ability of direct cellular killing and 2- CD4⁺ helper T cells (T_H) that can secrete various cytokines. The activation of naive T cells requires the recognition of peptide-MHC complexes. TCR recognizes the antigens presented by class I and II MHC molecules (97). Peptides presented on class I MHC molecules are recognized by CD8⁺ T cells and peptides presented on class II MHC molecules are recognized by CD4⁺ T cells. While class I MHC molecule is composed of a heavy α chain and a non-covalently attached non-polymorphic β_2 -microglobulin polypeptide (98), class II MHC is composed of a polymorphic α and a polymorphic β chain (94). The MHC molecule has an extracellular peptide binding groove, a non-polymorphic Ig-like domain, a transmembrane region and a cytoplasmic region.

CD8⁺ T cells react with target cells that express the class I MHC molecules on their cell surfaces. Class I MHC molecule is expressed on all nucleated cells. Class I MHC presents antigens as peptides of 8-10 aminoacids. These peptides are degraded from intracellular proteins by the proteolytic activity of specific cytoplasmic proteasomes. A single CD8⁺ T cell's CD3/TCR complex recognizes only one type of peptide/MHC complex specifically. Then, that T cell is activated to kill the target cell by means of the interactions of a series of molecules. The chief mechanism of CTL mediated cellular killing is via secretion of perforin and granzyme that results in target cell cytolysis.

CD4⁺ helper T cells interact with cells that express class II MHC molecules, which are professional antigen presenting cells (APC) like dendritic cells and B cells. Class II MHC molecule presents 12-20 aminoacid long peptides originating from exogenous proteins. These proteins are taken up by the antigen presenting cells and processed for proper presentation.

When the specific T cell receptor of a CD4⁺ helper T cell is activated, cytokines are secreted. These cytokines from T_H cells stimulate antibody production from B cells, support T cell responses, and activate other immune cells. CD4⁺ helper T cells are studied in two different subgroups as T_H1 and T_H2, based on their biological functions and cytokine secretion patterns. While T_H1 cells take active part in cell-mediated immunity and generation of inflammatory responses, T_H2 cells are more important for the IgE and eosinophil/mast cell mediated allergic reactions and immune responses effective against helminthic infections (99).

CD4⁺ T cells result in various effector functions by secreting different types of cytokines. In addition to the T_H1 and T_H2 cells that have been described above, interleukin-9 (IL-9) secreting T_H9 cells and interleukin-22 (IL-22) secreting T_H22 cells are also among the CD4⁺ helper T cell subgroups (100-102).

The antigen presented by antigen presenting cells to T lymphocytes, activates these T cells. T cells require two signals in order to be activated. First signal is the result of binding of MHC/peptide complex to TCR. After activation with a specific antigen, T cells differentiate either into IFN- γ secreting T_H1 cells or IL-4, IL-5 and IL-13 secreting T_H2 cells. These cytokines have pleotropic effects like growth, proliferation, activation, alteration in membrane expression profiles on immune cells (103).

The advancements in immunological techniques over the last 30 years, have also led to a better understanding of the interaction between the cancers and the immune system (104-106). This, in turn, has resulted in identification of novel and specific targets for immunotherapy applications in cancer (107).

Macfarlane Burnet proposed a crucial physiological role for the immune system, called immunosurveillance, back in the 1950's. This idea implicated the recognition and elimination of transformed cell clones before or after tumor formation (108). The existence of immunosurveillance has been proven by the increase in incidence of certain types of tumors observed in experimental immunodeficient laboratory animals and also in

immunodeficient patients. Immune responses are mounted against many different types of tumors in various stages. It is crucial for tumors to find ways of evading these host responses in order to progress (107).

Anti-tumor immune responses have some basic features. Tumor cells express antigens that are recognized as foreign by the host's immune system. Even though chiefly T lymphocytes are responsible for the anti-tumor immune responses; NK cells, macrophages, plasma cells and antibodies have been shown to have crucial roles in these responses, too. However, these immune responses are frequently insufficient in preventing tumor progression. Immune system can be activated by external stimuli to effectively eliminate the tumor cells (109, 110).

The interaction between the tumors and host immune system is explained by the "Tumor Immunoediting" hypothesis (111). Even though it has been shown that a functional immunosurveillance process suppresses tumor progression during the early stages of cancer, it is also known that immune system elements might also be involved in an immunoediting process which results in cancer progression (112). In experimental carcinogenesis models, the immunoediting, which starts as the immune system encounters the tumor cells, involves three different stages: elimination, equilibrium and tumor escape (112).

Tumor cells can be eliminated at the early stages of carcinogenesis by the immune system components. Host immune cells recognize and eliminate the transformed tumor cell clones in the host. This recognition is either due to various tumor specific tumor antigens or due to lack of normal antigens; which are expressed on all normal cells; on tumor cells. By this way, most of these transformed cells are eliminated before they can form tumors.

In instances when all of these transformed cells cannot be eliminated, the next phase of equilibrium is seen. Although the proliferating tumor cells are eliminated in the equilibrium phase, some variants of these tumor cells cannot be eliminated. At this phase, tumor and host immune cells reside together in the tissues in a state of balance.

However, these tumor cells might suppress the immune system at later stages and gain rapid growth and metastasis potentials (113). When they achieve this evasion from the immunosurveillance of the host immune mechanisms, they also modify the microenvironment for their advantage. Though some of the tumor cells are recognized by the immune system at this phase, immune system cannot prevent tumor formation and tumor cell proliferation. Tumor cells might then invade the tissues and metastasize to distant sites.

Effector mechanisms of innate and adaptive immunity were actually shown *in vitro* to be capable of eliminating tumor cells (104, 105). The mechanisms that are effective in preventing tumor formation and progression *in vivo*; however, is still not exactly known. In addition, the attenuation of specific anti-tumor immune responses is the goal of many studies.

Innate immunity elements NK cells and macrophages are also capable of directly killing tumors in cell cultures. NK cells are capable of killing virus infected cells and various tumor cells including hematopoietic tumor cells. They are capable of killing cells with decreased class I MHC expression and that express MICA, MICB or ULB ligands for the NK cell activating receptors like NKG2D (114). The tumoricidal activities of NK cells are enhanced with the presence of interferons and cytokines like IL-2 and IL-12 (115).

Although the role of macrophages in anti-tumor immune responses is explained by the fact that tumor cells are eliminated much more efficient with activated macrophages than normal cells, how tumor cells activate the macrophages is still unknown (116). IFN- γ produced by tumor specific T cells and direct recognition of some of the antigens expressed on tumor cell surfaces might be responsible from this activation. Macrophages have been shown to eliminate tumor cells by means of secretion of various lysosomal enzymes, reactive oxygen species, nitric oxide and TNF- α (117).

It has been shown that anti-tumor T cell-mediated and humoral immune responses develop together. In addition, T cell effector functions

might have preventive effects on tumor initiation. The effector T cells, which are thought to be suppressors of cancer progression, have been shown to be present in the tumor microenvironment (118, 119). The results of various experiments in both laboratory animals and humans have shown the role and the importance of CD8⁺ cytotoxic T cells and CD4⁺ helper T cells (T_H) in anti-tumor immune responses (62, 107, 119-124). Though it has been reported that the dominant T_H subtype in the tumor microenvironment is the T_H1 group, IL-17 secreting CD4⁺ T_H17 cells have also been shown to have important roles in tumor pathogenesis (125, 126).

The chief immune mechanism of anti-tumor immunity is the elimination of tumor cells by CD8⁺ CTLs (62). CTLs recognize mutant cellular proteins or oncogenic viral proteins that are processed and presented on class I MHC molecules as part of immunosurveillance. When CTLs recognize malignant cells expressing these molecules, they eliminate these tumor cells (127). Tumor specific CTLs have been isolated from human melanomas and experimental animal tumors. The presentation of tumor antigens by professional APCs such as dendritic cells is very crucial for the tumor antigen specific CD8⁺ T cell responses (128). Tumor antigens become suitable for recognition by TCR of CD8⁺ T cells, when processed by professional APCs and presented with class I MHC molecules. These APCs express the costimulatory molecules necessary for the conversion of CD8⁺ T cells into anti-tumor CTLs. They also carry the class II MHC molecules crucial for the CD4⁺ helper T cells to recognize the antigen, so that they will be activated (129). Once the CTLs develop, they recognize and kill the tumor cells without a need for costimulation. On the other hand, CD4⁺ T cells help the development of active CTLs and activate the macrophages by secreting cytokines like TNF- α and IFN- γ .

Antibodies against tumor antigens have also been discovered in some patients with cancer. In serums of patients with EBV associated lymphomas, antibodies against antigens that are coded by EBV and expressed on lymphoma cells have been detected. In *in vitro* studies, antibodies have been shown to help eliminating tumor cells by means of

complement system activation or by antibody-dependent cell-mediated cytotoxicity via Fc receptor bearing macrophages and NK cells (130, 131). Several antibodies specific to oncogenic viruses like HPV, might avoid viral induced tumors by preventing the host from viral infections (132).

Tumor infiltrating lymphocytes (TIL) have been shown to be present also in breast cancer (133). CD3⁺ cells constitute the major leukocyte population detected in breast tumors, with CD4⁺ cells being the predominant among TIL (134). Although there is evidence showing the presence of a T cell mediated immune response against breast cancer, breast tumor derived factors may impair these T lymphocyte functions. When the intratumoral cytokine production was analyzed in breast cancer, the level of cytokine production was found to be low both in normal breast tissue (135) and benign lesions (136). On the other hand, Camp et al. (136) also showed the production of immunoinhibitory cytokines by TIL in 44 % of breast cancers, by using immunohistochemical staining techniques. Venetsanakos et al. (135) showed the production of IL-10 in 60 % of breast cancers by RT-PCR. They concluded that the TIL activity reduction might be due to the inhibitory effects of this cytokine.

There appears to exist a polarity of the CD4⁺ helper T cell responses in breast cancer tissues (137). The polarity of CD4⁺ helper T cells and its consequences are demonstrated in Figure 2.6.

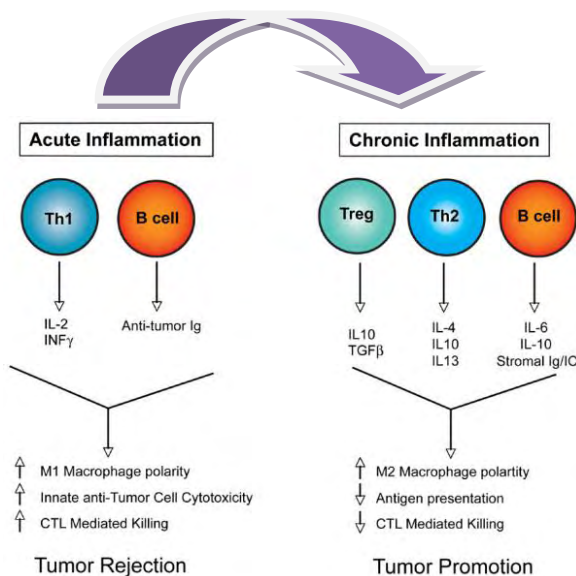


Figure 2.6. The polarity of CD4⁺ helper T cells and its consequences. Adapted from DeNardo et al. (137).

After activation, T_{H1} polarized CD4⁺ helper T cells secrete IFN- γ , TGF- β , TNF- α and IL-2 (138). These cytokines then take part in cytotoxic functions of CD8⁺ T cells (139), induce expressions of class I and II MHC molecules, upregulate antigen processing in proteasome, and also induce antigen presentation. In addition, secretion of IFN- γ from T_{H1} cells attenuates anti-tumor immune responses via inducing the activation of macrophage cytotoxic functions (140). On the other hand, T_{H2} polarized CD4⁺ helper T cells secrete IL-4, IL-5, IL-6, IL-10 and IL-13, which result in induction of T cell anergy and loss of T cell-mediated immune responses. In addition, they enhance humoral immunity (141). In summary, while T_{H1} responses work for anti-tumor immunity (142), T_{H2} responses work against it by hindering cell-mediated anti-tumor responses (143).

Neoplastic tissues also promote the expansion of a T cell subset called regulatory T cells (Treg). This, in turn, results in tumor escape from CD8⁺ T cell cytotoxicity. In addition, it has been stated that regulatory T lymphocyte functions are disordered in breast cancer patients (137, 144). Treg mediated immunosuppression has also been demonstrated in patients

with breast cancer (145). Allan et al. (133) showed the association between the impairment of breast cancer specific T cell functions and the expansion of Tregs in breast cancer patients. Though the mechanisms responsible for this immunosuppression are not very clear, Treg cells have been shown to actively inhibit CD8⁺ T cells, dendritic cells, NK cells in a cell-to-cell contact manner (146).

As a general rule, T lymphocyte activation is achieved by presentation of the antigen on a MHC molecule, expression of appropriate costimulatory molecules and the involvement of cytokines. Frequent alterations in class I MHC molecule expressions in breast cancer has been observed (147). In addition, it has been demonstrated that the increase in breast tumor grade is correlated with the down regulation of transporter associated with antigen processing (TAP1 and TAP2) proteins (148). These mechanisms render breast tumor cells poorly immunogenic and thus might allow for their escape from the host anti-tumor immune responses.

Contrary to the concept of effective anti-tumor responses, vast majority of the effector T cells go into a state of functional arrest after arriving to the tumor microenvironment (149, 150). The importance of various cells and molecules at the tumor microenvironment in suppressing anti-tumor immune responses has already been known. The mechanisms responsible for this event must be investigated and understood, in order to be able to revert this effect. The functional arrest in T cells in the tumor microenvironment is thought to be responsible for the T cells' insufficient anti-tumor immune responses. As a result, the tumor cannot be eliminated (151).

Most malignant tumors possess mechanisms for either resisting host immune responses or evading them. Evidence from mouse models suggest that anti-tumor immune responses exert a selective immunoediting process that results in survival and growth of tumor cell variants with low immunogenic character (152). Tumor's evasion of host immune responses and immunoediting might be the result of several different mechanisms (153, 154). Tumor antigens might cause specific immunological tolerance.

The regulatory T cells are capable of altering anti-tumor T cell responses. Tumor cells may decrease or completely cease expressing immunogenic antigens. The tumor cells usually do not express costimulatory or class II MHC molecules, thus cannot initiate CD8⁺ cytotoxic T cell responses. Products such as TGF- β , Fas ligand, and indolamine-2,3-dioxygenase (IDO) from tumor cells can suppress anti-tumor immune responses. Tumor cell surface antigens might hide from immune system by glycoalyx molecules such as sialic acid containing mucopolysaccharides. This is called antigen masking.

It has also been shown that the majority of tumor infiltrating T cells respond weakly to the activation through CD3/CD28. The changes in T cell receptor/ CD28 pathway are also thought to be one of the mechanisms responsible for the loss of potent responses in effector T cells (151).

Various mechanisms that are effective on immune cell functions have been proposed to be responsible for the decreased responses to T cell receptor in the tumor microenvironment. Among these mechanisms are decreased Ca⁺² flux, dysregulated protein kinase activities, alterations in protein tyrosine kinase expressions in signal transduction. In addition, significant decreases of T cell receptor associated zeta chain expressions are thought to have a role in ineffectiveness of the T cell responses (155). Singer et al. (60) indicated that tumor metabolites also have roles in suppression of T cell responses. They reported the suppressive effects of factors like indolamin-2,3-dioxigenase, arginase, inducible nitric oxide synthase (iNOS) and lactate dehydrogenase (LDH)-A; which are upregulated in human tumors; on the adaptive immune system. Alterations in cytokine influences (156) and IL-10 levels (157) have also been reported to have roles in the T cell hyporesponsive state in the tumor microenvironment.

Although some of the mechanisms responsible for the functional alterations of tumor infiltrating lymphocytes have been explained, all mechanisms related to the regulation of immune cells have not yet been fully discovered. Shedding light on mechanisms responsible for suppression

of anti-tumor immune responses will clearly help finding out novel therapeutic targets for cancer immunotherapy (158).

2.3.1.2.1. Tumor Immunotherapy

Tumor immunotherapy is utilized in order to attenuate active anti-tumor immune responses or to transfer tumor specific immune effectors to patients. Immune responses can actively be attenuated by means of vaccinating with tumor cells or antigens, by injecting tumors that are modified to highly express cytokines and costimulatory molecules which stimulate T cell proliferation and differentiation, by systemic administration of cytokines to patients, and by blocking the inhibitory pathways of immune regulation (159-163). Approaches for passive immunotherapy are administration of anti-tumor antibodies or immunotoxin conjugated antibodies to patients, readministration of tumor reactive T cells and NK cells that have been isolated from the patients back to the patients after being proliferated with growth factors in cell cultures (164, 165).

2.3.1.3. Endothelial Cells

Endothelial cells of the tumor microenvironment play crucial roles in the carcinogenesis process (166). They support the tumors by angiogenesis via providing the necessary factors for the cancerous growth. Furthermore, they act as an active interface between the blood and the tumor microenvironment. As a result, they are critically involved in key process as leukocyte recruitment and tumor cell metastasis. Hypoxia induced in the tumor microenvironment is one of the key regulators of angiogenesis. The mechanisms underlying angiogenesis have been mostly discovered over the last years (167, 168).

In fact, angiogenic vessel formation is a reaction of the stroma and is a vital requirement for cancer progression (169, 170). In addition to promoting tumor growth by supplying necessary oxygen and nutrients, tumor vasculature also accommodates metastasis by paving the way for

cancer cell entry into the blood stream. It has long been known that tumors lacking sufficient angiogenesis are unable to grow to volumes more than a few mm^3 (26). The initiation of the angiogenesis in tumor is called as "angiogenic switch", which is regulated by the collective effects of tumor cells, stromal components and the emergence of hypoxia in the tumor microenvironment (27, 28). It is thought that such an "angiogenic switch" is a crucial borderline event between premalignant and malignant tumor states (171) (Figure 2.7).

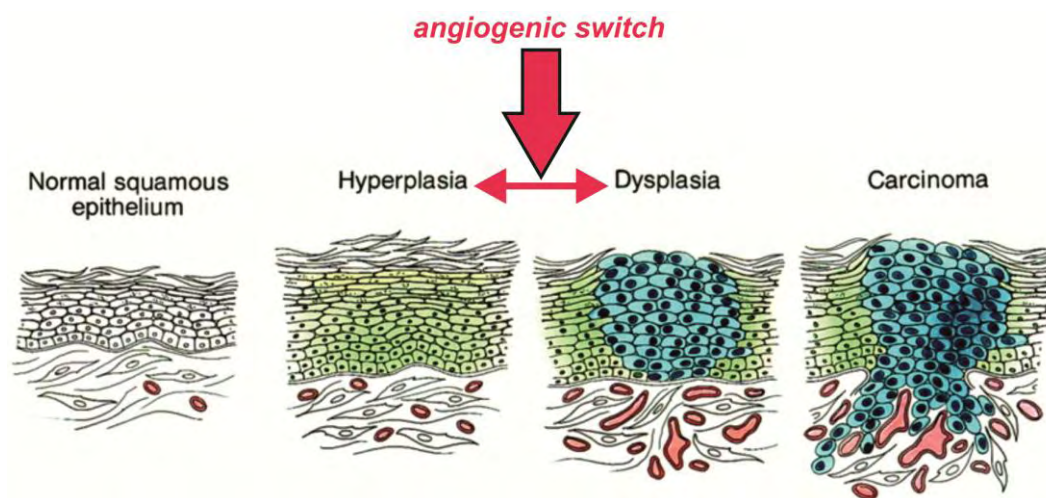


Figure 2.7. Angiogenic switch is essential for tumor progression to malignant state. Adapted from Hanahan and Folkman (171).

2.3.1.4. Extracellular Matrix

Extracellular matrix (ECM) consists of various components such as proteins, glycoproteins, proteoglycans and polysaccharides (172, 173). Even though, ECM had previously been thought as a static structure whose main role was to support the tissues, recent findings clearly showed the importance of this non-cellular part of the niche, ECM, in carcinogenesis (174-178). Furthermore, it is a very dynamic element of the microenvironment and is capable of critically affecting the biology of the

residing cells (179). Figure 2.8 demonstrates eight mechanisms of ECM to change cell behavior.

ECM might also influence the differentiation and invasion capabilities of neoplastic cells. It may promote carcinogenesis by directly inducing the transformation and metastasis of the cells. Dysregulated ECM disrupts stromal cell functions, promotes angiogenesis and inflammation; therefore, results in a tumor permissive microenvironment (180).

ECM components also take part in local immune regulation. An example is Osteonectin, a matricellular glycoprotein. Osteonectin was shown to be expressed in remodeling tissues and tumors (181, 182). It induces T_H1 polarization via modulating the expression of TGF- β 1 and fine-tunes TNF- α production of macrophages (183). In the absence of Osteonectin, macrophages do not down regulate TNF- α in response to TGF- β 1.

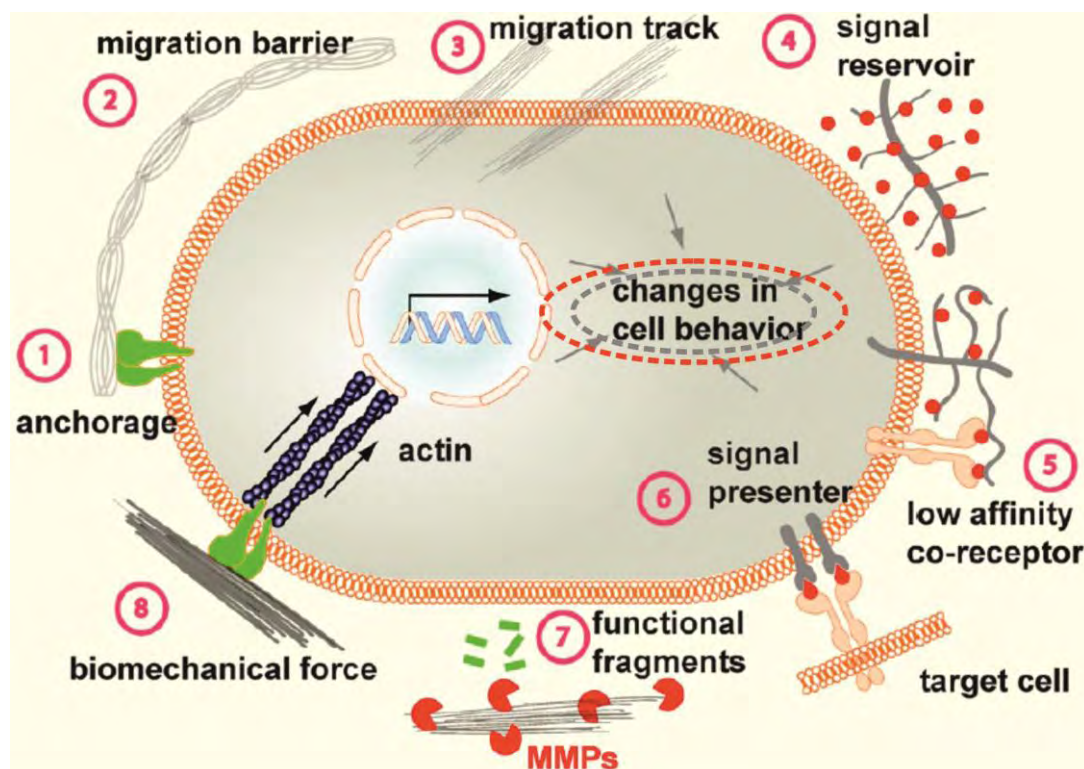


Figure 2.8. Eight mechanisms of ECM functions to change cell behavior. Adapted from Lu et al. (180).

2.4. Animal Models

The value of animal models in tumor immunology is priceless, since *in vivo* experiments simulate the diseases much better than *in vitro* ones. Most of the fundamentals of tumor immunity have been discovered by the use of such animal models. The type of animal model that will be used for the experiments is also very important. Many researchers are now abandoning the transplantation type tumor models, as they do not sufficiently represent the human tumors (184).

2.4.1. Experimental Chemical Carcinogenesis

The abundantly found chemical carcinogens are able to induce tumors in humans and many animals. The administration of purified carcinogens to laboratory animals is a frequently used method of animal tumor model. Tumors developing in such ways are very useful for cancer studies. Chemical carcinogens might be divided into two subgroups: 1- directly acting agents and 2-indirectly acting agents (19). Directly acting agents do not require a conversion to become metabolically active. Instead, they can directly act on DNA as a mutagen. The indirectly acting agents; on the other hand, require a way of metabolic conversion in the body in order to be able to act on DNA (19). These DNA damages caused by the carcinogens result in accumulation of mutations and loss of cell cycle control. This in turn causes cell proliferation and then carcinogenesis. The type and site of the tumor is determined by the type of carcinogen, way of administration, species of the animal, time and amount of the administration.

2.4.2. Chemical Carcinogenesis in Rats

Rats might prove to be useful hosts for tumor immunology studies, since various features of human tumor immunology have been modeled in rats (8). Chemically induced experimental carcinogenesis models are

frequently used in *in vivo* cancer studies. Huggins et al. (185) reported a method of inducing a high incidence of breast tumors in female rats in 1961 by using a single dose of a carcinogen called 7,12-Dimethylbenz(α)anthracene (DMBA). DMBA was reported to be one of the most potent and specific carcinogens for induction of breast cancers (185, 186). Later, N-Nitroso-N-methylurea (NMU) was also shown to specifically and reproducibly induce a high incidence of breast carcinomas after a single i.v. or i.p. dose (187).

Both of these carcinogens induce tumors reliably and organ site specific. The resulting tumors are of ductal histology that are predominantly carcinomas. These tumors show varying responses to hormones. They both promise a potential to investigate the process of tumor initiation and progression (187, 188).

On the other hand, there are several differences between these models. NMU model provides an experimental approach for examining breast carcinogenesis induced by a directly acting carcinogen. DMBA model; however, provides a method for investigating breast carcinogenesis induced by a carcinogen requiring metabolic activation (187). Even though the carcinomas induced by both carcinogens rarely metastasize, NMU mediated breast cancers appear to be more aggressive histologically than DMBA induced ones. The tumors induced by NMU has a higher proportion of malignant to benign breast tumors than DMBA. While DMBA induced mammary carcinomas are more prolactin dependent, NMU induced breast cancers appear to be more estrogen dependent (187). The NMU model has several advantages which include the nature of the carcinogenic responses, simplicity of the tumor induction methodology, histological characteristics of the tumors induced, and the flexibility of the NMU model in experiment design (189).

NMU induced mammary tumor models originate from ductal epithelial cells, might carry altered TGF- β , erbB2, cyclin D1 expressions and have similar histopathological lesions with their human counterparts (189). Thus, NMU mediated tumor models are relevant to human breast carcinomas.

These features might explain the reason why this model has been extensively used in oncological studies (190). In addition, NMU mediated mammary carcinomas show consistencies with the local immune status of human breast cancers (9, 191, 192).

2.4.3. N-Nitroso-N-methylurea (NMU) Breast Tumor Model

N-Nitroso-N-methylurea (NMU) is a highly carcinogenic substance (Figure 2.9). It has been previously reported that periodical intraperitoneal injections of NMU result in mammary adenocarcinomas with a high incidence in female Sprague-Dawley rats (189, 193, 194). The development and spread of tumor tissues that develop with this technique can easily be followed up in a context of time. The ability of this NMU induced rat breast adenocarcinoma model to simulate human breast carcinoma histopathology is better than similar models utilized in mice (9-11). The probable changes in T cells that interact with cancer associated fibroblasts can therefore be investigated in great detail with this model.

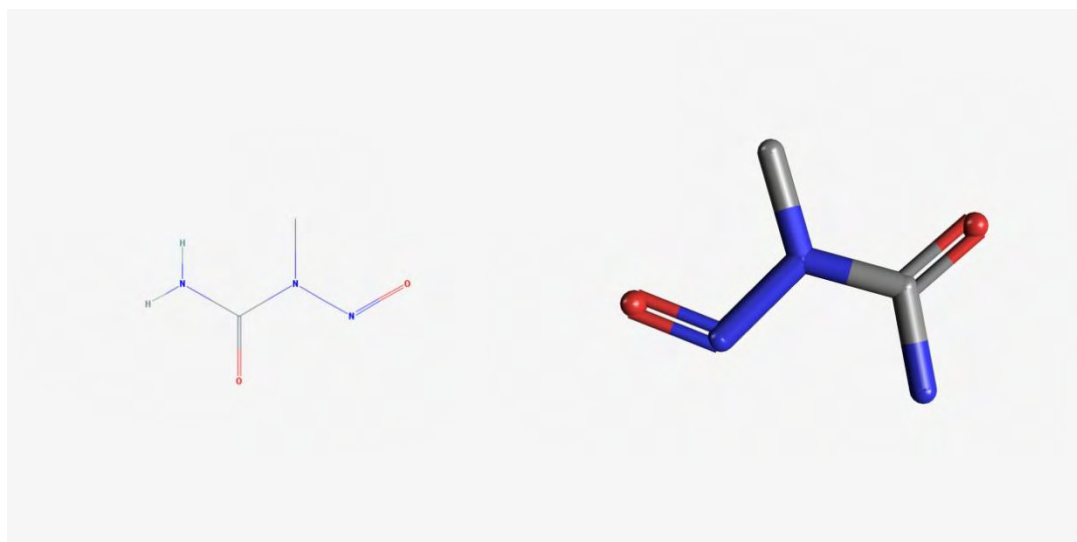


Figure 2.9. Color coded 2D and 3D molecular structures of N-Nitroso-N-methylurea. Adapted from PubChem Compound (195).

NMU is a nitrous amide substance which is highly mutagenic and teratogenic, besides being carcinogenic (196, 197). It directly alkylates DNA and can induce experimental cancers in various organs when administered to animals.

Cox et al. reported that NMU administration to rats results in O⁶-methylguanine accumulation in DNA of mammary glands (198). Similar to other experimental chemical carcinogens, type and site of the tumor is determined by the species of the animal, route, time and amount of the administration. NMU has been reported to induce tumors in breast, thymus, skin, endometrium, ovary and colon tissues (189, 199-203). Intraperitoneal, intravenous and subcutaneous administrations of NMU show carcinogenic effects on mammary glands in Sprague Dawley rats (204). Increasing the dose and/or frequency of carcinogen injections results in a decreased latent period for tumor formation (204).

NMU shows suppressive effects on host immune system. NMU shows marked genotoxicity on proliferating lymphocytes, followed by increased apoptotic death (205). Furthermore, the toxic effects of NMU on spleen and bone marrow may continue about three more weeks after the injection (206).

Immature Sprague Dawley rats are more sensitive to carcinogenic effects of NMU than multiparous ones. Differentiation of mammary terminal end buds prevents cells from transformation. Each estrous cycle causes a decrease in these structures and pregnancy causes terminal end buds to turn into alveolar buds. Therefore, the frequency of tumor formation due to NMU is decreased in ovariectomized or aged animals (207, 208). High proliferative index of cells might contribute to sensitivity to the agent (204). The highest frequency of tumor formation is seen at the rats that are injected when they are 30-55 days old.

Although the diversity of lesions seen in rats is limited (189), NMU induced experimental neoplastic breast lesions show great similarities in terms of histopathology with their premalignant and advanced stage counterparts in humans (209, 210). Furthermore, NMU induced neoplasias

simulate the characters of multi step carcinogenesis process (211). Thompson et al. reported that the lesions' occurrence pattern was consistent with intraductal proliferations being a precursor lesion for ductal carcinomas in situ and adenocarcinomas (212). NMU induced neoplasias were reported to possibly bear mutations in Harvey-*ras* (*Ha-ras*), Kirsten-*ras*, *neu*, *oncR3*, *RAR-b* genes (194, 204, 207, 213); of which *Ha-ras* mutation is the most frequent one. This mutation leads to persistent activation of the ras GTPase pathway (204, 207). However, frequent high dose NMU administration decreases the frequency of this mutation (214).

2.5. Single Cell Gel Electrophoresis (Comet) Assay to Determine DNA Damage

DNA is a fragile molecule that might be the target of various reactive molecules. Damage to the cellular DNA can occur due to several environmental determinants. Damage in the nuclear DNA can lead to several diseases including cancer, diabetes and atherosclerosis. On the other hand, such damages in DNA might be useful as a marker in terms of monitoring chemo/radiotherapy efficacy or determining radiation induced genotoxicity (215). Therefore, there is a crucial need for specific techniques that determine DNA damage precisely. Single cell gel electrophoresis (Comet Assay) is a fast, precise and reliable technique to determine the level of DNA damage at cellular level by utilizing the fluorescent microscopy.

As genotoxicity is characterized by DNA strand breaks, it can be evaluated with Comet Assay (216, 217). Furthermore, this technique does not require radioactive labeling, it is widely used for evaluating the extent of DNA damage. Cells in question are embedded in an agarose gel on a microscope slide. Then the cells are lysed to release the supercoil DNA. Alkali medium causes loosening of the supercoil structure, thereby showing up the DNA breaks. The following electrophoresis causes migration of these DNA breaks towards the anode, resulting in an appearance similar to a comet (218, 219).

The Comet Assay procedure is a relatively delicate process; thus, standard assay guidelines should be strictly followed for each sample in order for the results to be precise and reliable (217).

For this reason, cancer associated fibroblast are obtained by using the rat chemical breast carcinogenesis model. The probable effects of these cells on T cell responses are then examined.

3. MATERIALS AND METHODS

This work was performed during the period of August, 2010 — October, 2013 at the Research Laboratories of the Department of Basic Oncology, Cancer Institute, Hacettepe University in Ankara, Turkey.

3.1. Materials

The chemical and biological materials used in this work are listed below:

Phosphate buffered saline (PBS) (Oxoid Limited, UK); Ethylenediaminetetraacetic acid (EDTA), Trypan Blue, Sodium Hydroxide (NaOH), Collagenase, Crude, General Use-Type I from *Clostridium histolyticum* (C0130-100MG, C0130-500MG), Hyaluronidase from bovine testes (H3506-100MG), N-Nitroso-N-methylurea, Agarose, Histopaque-1077 (similar to Ficoll), Hydrogen peroxide, Collagen Type I solution from rat tail (C3867), 1 kb DNA marker, Bovine serum albumin (BSA) (New England Biolabs-NEB, USA); primer oligonucleotides (Alpha DNA, Canada); DNA-Free DNase Kit (Ambion, USA); 50 base-pair DNA marker, 6X DNA loading buffer, *Taq* DNA polimerase, dNTP-mix solution, QuantiTect Reverse Transcription Kit (Fermentas, Lithuania); Pure Ethyl Alcohol (Reidel-de Haën, Germany); GeneClean Turbo Kit (Q-biogene, Canada); Methyl Alcohol, Hydrochloric acid, Brome Phenol Blue, Entellan, Immersion Oil (Merck, Germany); Diethyl Ether (Kimetsan, Turkey); FACSCFlow Sheath Fluid, APC Mouse Anti-Rat CD3 Mouse (BALB/c) IgM, κ (557030), APC Mouse IgM, κ Isotype Control (550883), Cytofix/Cytoperm™ Fixation/Permeabilization Solution Kit, 8 Well Chamber Slides, Pasteur

Pipettes, 70 μm and 40 μm cell strainers, APC Mouse Anti-Rat CD3 Antibody - Mouse (BALB/c) IgM, κ (557030), APC Mouse IgM, κ Isotype Control (550883) (Becton Dickinson, USA); Serological Pipettes (5ml, 10ml and 25ml), Tissue Culture Flasks (75cm² and 25cm²), Centrifuge Tubes (15ml and 50ml), Microcentrifuge Tubes, Culture Dish (100mm x 20mm) (Corning, USA); Cell Scraper, Tissue Culture Plates (6, 12, 24, 48, 96 well) (Sarstedt, Germany); Formaldehyde, Hematoxylin-Eosin, Nile Red (Santa Cruz Biotechnology, USA); Giemsa (Biostain, Australia); QIAmp RNA Blood Mini Kit (Qiagen, USA); TBE Buffer Solution (AppliChem, Germany); L-glutamine, Fetal Bovine Serum (FBS), Fetal Calf Serum (FCS) (Biological Industries, Israel); Penicillin / Streptomycin (PAA, Germany); Biocoll (Biochrom AG, Germany); HyClone HyQTase (Thermo Scientific, USA); Desmin Clone D33 (ready to use), Cytokeratin (Pan) Cocktail (ScyTek Laboratories, USA); DAB chromogen, DAB Substrate, Polyvalent Biotinylated Secondary Antibody, Streptavidin (Lab Vision, USA); Heparin Sodium (Nevparin) (Mustafa Nevzat Ilac, Turkey); SYBR Green PCR Kit, Protease Inhibitor Cocktail (Roche Diagnostics, Germany); Interleukin-2 (Proleukin) (Hoffmann-La Roche, Switzerland); *Pfu* DNA Polimerase (Promega, USA); RPMI-1640 Cell Medium, DMEM High Glucose Cell Medium, Trypsin-EDTA (1X) (Hyclone, ThermoFisher Scientific, USA and Lonza Group, Switzerland); Dimethyl sulfoxide (DMSO) (Ambresca, USA); PE anti-rat CD4 (domain 2) Mouse IgG1, κ (203308), PE Mouse IgG1, κ Isotype Control Antibody (400112), PerCP anti-rat CD8a Antibody Mouse IgG1, κ (201712), PerCP Mouse IgG1, κ Isotype Control Antibody (400148), Rat TGF-beta1 Platinum ELISA (BMS623/2), Rat IFN-gamma Platinum ELISA (BMS621) (eBioscience, USA).

All of the buffers and solutions were prepared with the water obtained from Millipore (Milli Q) distillation and ultrafiltration system. In addition, same water was used in all of the biological reactions carried out.

3.2. Media, Solutions and Buffers

Full RPMI Medium: RPMI-1640 medium was supplemented with 10 % fetal bovine serum, 2mM L-glutamine, 100 units/ml penicillin and 100µg/ml streptomycin. The medium was aliquoted (50 ml) and stored at 4°C.

Full DME Medium (Fibroblast medium): DME High Glucose medium (with 1mM Sodium Pyruvate) was supplemented with 2mM L-glutamine, 10 % fetal calf serum, 100 units/ml penicillin and 100µg/ml streptomycin. The medium was aliquoted (50 ml) and stored at 4°C.

1X PBS Solution: One tablet of PBS was added to 100 ml of distilled water and the solution was mixed thoroughly and sterilized.

Collagenase Type I Solution: 100 mg of lyophilized Collagenase type I was dissolved in 10 ml 1 X PBS and aliquoted to 1 ml (10 mg/ml) in microcentrifuge tubes. The aliquots were stored at -20°C until used. For the digestion experiments, 1 ml (10 mg/ml) of Collagenase I was mixed with 500 µl (~2500 units/ml) of Hyaluronidase and 8.5 ml of cell medium in order to achieve a 1 mg/ml final concentration of Collagenase I. This solution was prepared freshly just before the experiments each time.

Collagenase Type II Solution: 100 mg of lyophilized Collagenase type II was dissolved in 10 ml 1X PBS. Then, 123.3 ml of RPMI1640 was added on it, resulting in the working solution with the concentration of 0.075 % (w/v). This solution was distributed in aliquots of 10 ml and these aliquots were stored at -20°C.

Hyaluronidase Solution: 29 mg of lyophilized Hyaluronidase (Type I-S, lyophilized powder, 866 units/mg solid) was dissolved in 10 ml 1 X PBS and distributed in aliquots of 500 µl in microcentrifuge tubes. The aliquots were stored at -20°C until used. For the digestion experiments, one aliquot of Hyaluronidase (500 µl) was mixed with one aliquot of Collagenase I (1 ml) and 8.5 ml of cell medium in order to achieve a 125 units/ml final

concentration of Hyaluronidase. This mixing was performed freshly just before the experiments each time.

N-Nitroso-N-methylurea (NMU) Solution: NMU was prepared by dissolving the lyophilized chemical at the concentration of 100 mg/ml (w/v) in saline solution (0.9 % NaCl). The pH of the solution was adjusted to be 5 via buffering with HCl. This solution was prepared freshly just before the experiments each time.

Cell Medium for Freezing in Liquid Nitrogen: Full cell medium was supplemented with additional 20 % FBS and 10 % Dimethyl sulfoxide (DMSO). This solution was prepared freshly just before the freezing procedure each time.

3.3. Experiments with the Laboratory Animals

Sprague-Dawley out-bred rats were used for the experiments. Research ethics approval for animal experimentation was received from "Hacettepe University Institutional Animal Care and Use Ethics Committee, Ankara" before the initiation of the animal experiments (Approval Number: 2011/28-3).

All rats were housed under environmentally controlled standard conditions in "Hacettepe University Laboratory Animals Research and Care Facility" at about 25°C temperature and 30-70 % humidity. The day / night cycle was adjusted to be 12 hours with light and 12 hours in the dark conditions. The rats were given ad libitum access to food and water. The Guiding Principles in the Care and Use of Laboratory Animals together with those described in the Declaration of Helsinki were strictly followed in the conduct of all experimental procedures described within this manuscript.

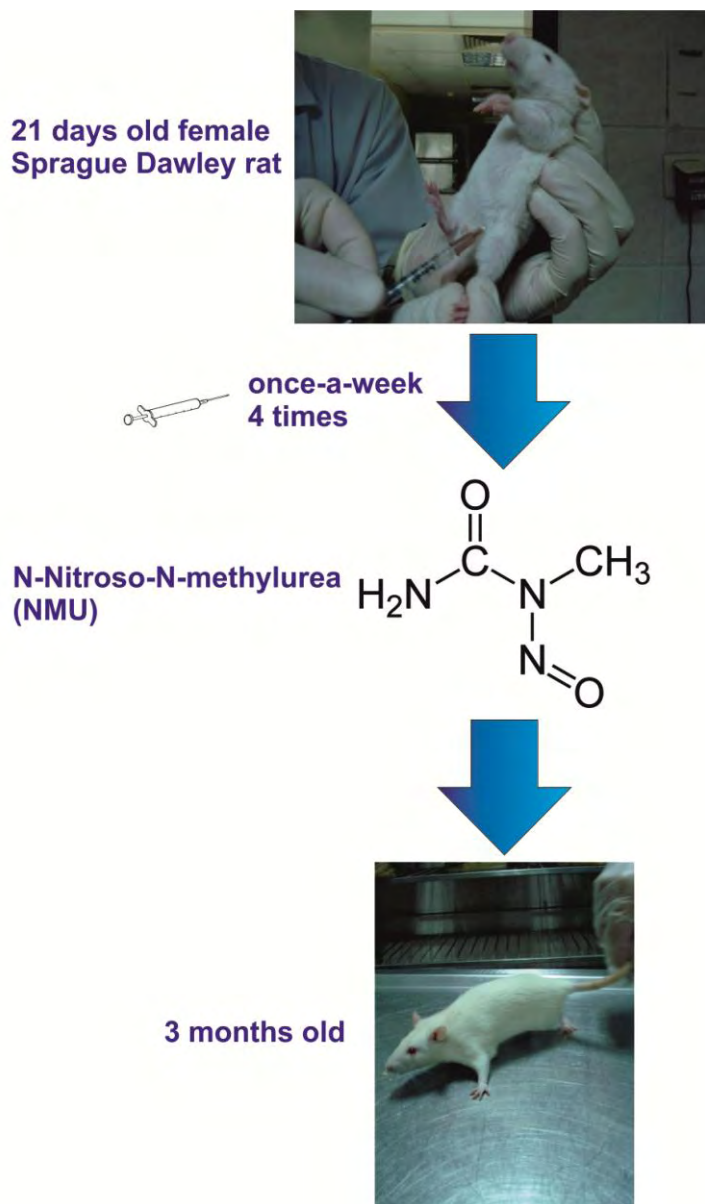


Figure 3.1. NMU Induced Mammary Carcinoma Protocol.

3.3.1. Induction of Experimental Mammary Carcinoma Formation in Rats

N-Nitroso-N-Methyl Urea (NMU) induced experimental mammary carcinogenesis model was utilized (9). Twenty-one days old 20 female Sprague-Dawley albino rats were enrolled to be injected with 50 mg/kg

NMU once-a-week for four weeks via intraperitoneal route; in order to induce mammary carcinoma formation (Figure 3.1 and 3.3).

The breast tissue of the animals were palpated routinely twice a week. General health status of all animals were monitored routinely both before and after the development of tumors. No abnormality except a decrease in mobility was observed in the rats that have developed tumors. All of the animals that were injected with NMU developed tumors.

When the animals were about 3 months old (Figure 3.2 and 3.4) and when the developed mammary tumor reached approximately more than 1 cm in diameter, the animals were sacrificed by the cervical dislocation technique. Developed tumors were harvested surgically under sterile conditions for use in further experiments (Figure 3.4).



Figure 3.2. Three months old Sprague Dawley rat with a mammary tumor.

Even though periodical i.p. injections of NMU result in mammary adenocarcinomas with a high incidence in female Sprague-Dawley rats, some studies using this model have also previously reported that there is also a probability of benign neoplasia and hyperplasia development at the early phases. However, it has also been reported that most of these tumors turn into adenocarcinomas at later phases. Therefore, it was desirable for

the tumor sizes to be greater than 1 cm in diameter. On the other hand, the tumors were never allowed to grow greater than 4 cm in diameter not to cause any disturbances in the general well-being of the animals. The animals that have developed necrosis on their skin over the tumor area were sacrificed as soon as possible and thus were involved in the experiments.

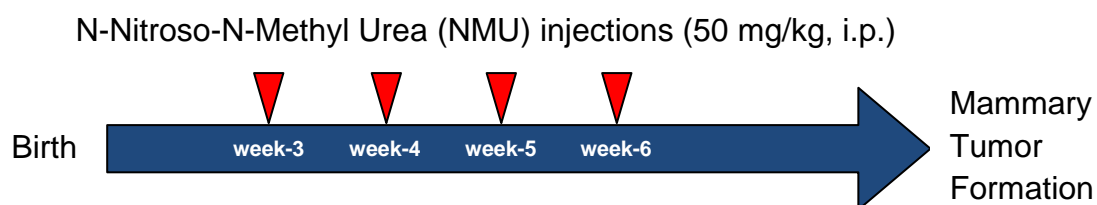


Figure 3.3. Time Scale of NMU Injections.



Figure 3.4. Sacrification of the animal and excision of the induced tumor in a safety cabinet.

For the control experiments, seven rats were injected with isotonic saline using the same protocol.

3.3.2. Surgical Procedures

Female Sprague Dawley rats that were about three months old were used for the surgical procedures. The animals were sacrificed by the cervical dislocation technique. The rats were sterilized by soaking into 70 % ethanol supplemented with iodine solution. After the sterilization, the animals were stabilized on to the dissection board and taken immediately to the safety cabinet (HERA Safe, THERMO/Electron Corporation) (Figure 3.4).

3.3.2.1. Intracardiac Blood Withdrawal

For the intracardiac blood sampling, the rats were first anesthetized by being put inside an air-tight big-enough glass container supplemented with a piece of pad immersed in diethyl ether (Kimetsan). After the rat was anesthetized, it was taken out of the glass container and its chest was wiped with a sterile solution of 70 % ethanol. The intracardiac blood was aspirated from the beating heart by a heparinized syringe (gauge 22). The heparin (Nevparin-Mustafa Nevzat, Turkey) was aspirated from the glass vial to the syringe and injected back to the vial several times before using the syringe for blood withdrawal. The aspiration process was continued until the heart stopped beating and no further blood came to the syringe. The blood was then taken into a 15 ml-centrifuge tube.

3.3.2.2. Tumor Excision and Mastectomy

By using scalpels, scissors and blunt-nosed thumb forceps (with serrated tips); a median incision was made on the ventral side of the animal

during the necropsy. The incision was extended from the cervical region all the way to the inguinal region, also including the abdominal area. From the lowest point of this median incision, two lateral incisions were made toward the lower limbs of the rat. By using the scalpel and the thumb forceps, the skin of the animal was separated from the underlying muscular tissue. This separated skin is fixated tightly onto the dissection board (Figure 3.5).

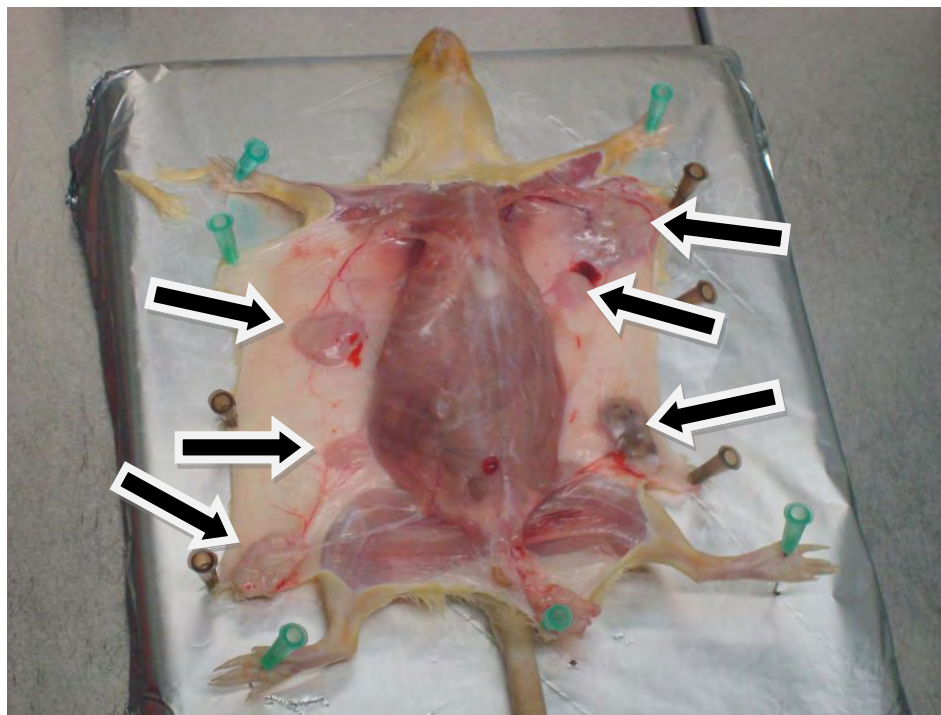


Figure 3.5. Dissection of the ventral skin and exploration of the mammary tissue regions and mammary tumors in a Sprague Dawley rat (arrows indicate the mammary tumors).

The tumor masses were picked up carefully by a tissue forceps and excised from the surrounding connective tissue.

The tumor tissues that were to be used for enzymatic digestion studies, were placed on a Petri dish containing 15 ml of 1 X PBS. Further experiments and cell isolations were carried out with only one of tumors, in case there were more than one tumor in one animal.

All of the internal organs were inspected and examined carefully and the tissues with probable foci of metastasis were noted and also stored in Formaldehyde solutions for further histopathology investigations.

For the control experiments, seven healthy rats that were injected with isotonic saline were sacrificed and the above mentioned mastectomy protocol was also performed on their mammary tissues for further protocols of normal fibroblast cell isolation.

3.3.2.3. Splenectomy

By using scalpels, scissors and blunt-nosed thumb forceps (with serrated tips); a median incision was made from the xiphoid process of sternum down to the inguinal area. The skin lateral to the median incision was separated from the muscular layer and fixated onto the dissection board (Figure 3.4). An incision is made to the anterior abdominal wall by the scalpel; thus allowing the entry to the peritoneum. The abdominal organs, especially the intestines, were retracted in order to reach the spleen in the cavity. By using a thumb forceps, the spleen was picked up and its pedicle containing the splenic artery and vein was finely dissected. The excised spleen was then placed on a sterile Petri dish containing 30 ml of sterile 1 X PBS.

3.3.2.4. Synovial Membrane Excision

By using scalpels and thumb forceps, an incision was made over the upper limb of the rat which extended from the shoulder of the animal to its

forearm. The muscular tissue was dissected over the elbow joint area. The skin and muscles over elbow were retracted as much as possible and fixated onto the dissection board. An incision was made on the ligaments and capsule of the elbow joint, separating the bones forming the joint apart. The distal end of the humerus and the proximal ends of the radius and ulna bones were shaved with a scalpel and the excised tissues were placed on a sterile Petri dish.

3.4. Isolation of Normal Fibroblasts and Cancer Associated Fibroblasts

Normal fibroblasts were obtained from healthy mammary tissues of control female Sprague-Dawley rats. Cancer Associated Fibroblasts (CAFs) were obtained from mammary carcinomas excised from NMU injected rats (Figure 3.6).

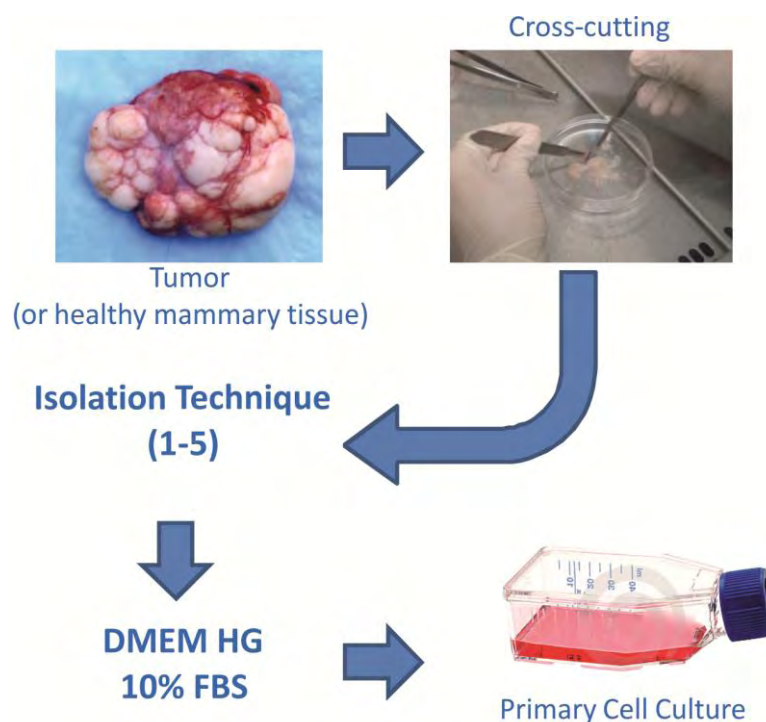


Figure 3.6. Fibroblast isolation steps.

3.4.1. Techniques Used for Fibroblast Isolation

3 different protocols were utilized for fibroblast and CAF isolation.

1. Enzymatic Digestion with Collagenase I and Hyaluronidase
(Orimo et al.) (57)
2. Enzymatic Digestion with Collagenase II and DNase I
3. Enzymatic Digestion with Collagenase II and DNase I (different protocol)
(220)

3.4.1.1. Enzymatic Digestion with Collagenase I and Hyaluronidase (Orimo et al.) (57)

First, normal mammary tissue or the excised mammary tumor was mechanically dissected into 1-3 mm pieces in a Petri dish via cross-cutting technique; before the enzymatic digestion steps (Figure 3.7).



Figure 3.7. Tumor tissue was split into pieces mechanically with the cross-cutting technique.

Then the tumor was enzymatically digested with 1 mg / ml of Collagenase I and 125 units / ml of Hyaluronidase. The enzymatic digestion process was performed at 37°C for 5 hours with mild agitation in DMEM HG

containing 10 % FBS. The resulting digested tissue suspension was passed through a 70 μ m nylon cell strainer; the part passing through the strainer was collected. The collected fraction was centrifuged for 5 minutes at 250 G. The resulting pellet was resuspended in full DMEM medium and cultured in a flask.

In efforts to optimize the protocol, duration of the digestion was performed in several different ways ranging from 2 hours to 24 hours. In addition, the concentration of the Collagenase I digestion enzyme was used in different doses of either 0.5 mg / ml or 1 mg / ml. The same digestion process was also performed only with the Collagenase I and without utilizing the Hyaluronidase enzyme; in order to eliminate any possible harmful effects of Hyaluronidase. Finally, different levels of centrifugation with various different G values were also tried.

3.4.1.2. Enzymatic Digestion with Collagenase II and DNase-I

First, normal mammary tissue or the excised mammary tumor was mechanically dissected into 1-3 mm pieces in a Petri dish via cross-cutting technique; before the enzymatic digestion steps (Figure 3.7).

Then the tumor was enzymatically digested with 0.075 % Collagenase type II and 0.01 % DNase I. The enzymatic digestion process was performed at 37°C for 5 hours with mild agitation in DMEM HG containing 10 % FBS. The resulting digested tissue suspension was passed through a 70 μ m nylon cell strainer; the part passing through the strainer was collected. The collected fraction was centrifuged for 5 minutes at 250 G. The resulting pellet was resuspended in full DMEM medium and cultured in a flask.

3.4.1.3. Enzymatic Digestion with Collagenase II and DNase I (different protocol) (220)

First, normal mammary tissue or the excised mammary tumor was mechanically dissected into 1-3 mm pieces in a Petri dish via cross-cutting technique; before the enzymatic digestion steps (Figure 3.7).

Then the tumor was enzymatically digested with 400 IU / ml Collagenase type II and 0.01 % DNase I. The enzymatic digestion process was performed at 37°C for 2 hours with mild agitation in DMEM HG containing 10 % FBS. The resulting digested tissue suspension was centrifuged for 2 minutes at 90 G and the (stromal rich) supernatant was collected. The collected fraction was centrifuged for 10 minutes at 800 G. The resulting pellet was resuspended in full DMEM medium and cultured in a flask.

3.5. Isolation of the Immune Cells

The immune cells were isolated from five of the NMU injected and from all seven healthy female Sprague-Dawley rats. Spleens and peripheral bloods of the control animals were used in order to obtain splenocytes and peripheral blood mononuclear cells (PBMC), respectively. Density gradient separation technique was utilized (221, 222). Ficoll like separating solutions such as Histopaque-1077 are very helpful for cell isolation via density gradient centrifugation (Figure 3.8).

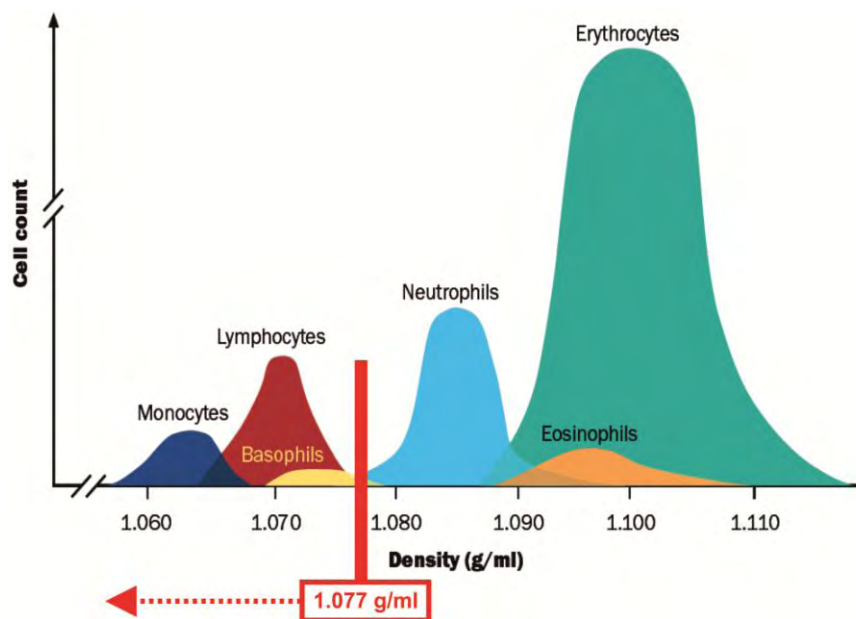


Figure 3.8. Densities of various blood cells are shown. 1.077 g/ml was the density of the solution that was used for density-gradient-separation. (Adapted from Biochrom AG (221).)

3.5.1. Isolation of the Splenocytes (Density gradient separation)

After splenectomy, the excised spleen was placed on a sterile Petri dish containing 30 ml of sterile 1 X PBS. By using a scalpel, the spleen was cut into 4 to 5 pieces gently, without harming the tissue. A sterile 70 μ m nylon cell strainer (BD) was put on a 50 ml centrifuge tube. The intact tissue pieces of the spleen were put on the mesh and were pushed through the filter by the help of a handle of a syringe piston. The spleen tissues were never grinded; since it was highly recommended to avoid doing so, in order to prevent generation of many dead cells. The splenic cell suspension that passed through the filter was used for further experiments.

10 ml of Histopaque-1077 (similar to Ficoll) (with density of 1.077 g/ml, Figure 3.8) was added into a 50 ml centrifuge tube. The splenic cell suspension was poured very slowly and carefully over the Histopaque-1077 phase by using a Pasteur pipette, preventing the mixing of these two fluids

(splenic cell suspension & Histopaque-1077). The centrifuge tube containing the overlaid splenic cell suspension and the Histopaque-1077 was centrifuged for 30 minutes at 20°C with 1800 rpm (400 x G) without brakes. Centrifugation at lower temperatures like 4°C might cause clumping and poor recovery (222).

After centrifugation, the formed phase of cell layer (mononuclear cell *buffy coat*, Figure 3.9) was collected together with the media and Histopaque-1077 (similar to Ficoll) with a Pasteur pipette and transferred to a new 50 ml centrifuge tube. Then, this suspension was washed 2 times (by adding 1 X PBS to the tube which contained the collected part of the cell suspension and then centrifuging for 5 minutes at 20°C with 1800 rpm) (Figure 3.10).

3.5.2. Isolation of the Peripheral Blood Mononuclear Cells (PBMC) - Density gradient separation

Heparinized blood that was collected from the animals was taken into a 15 ml-centrifuge tube. The blood was washed 1 time (for 5 minutes at 20°C with 1800 rpm). Twenty to thirty ml warm full RPMI cell medium at 37°C was used to resuspend the pellet.

10 ml of Histopaque-1077 (similar to Ficoll) (with density of 1.077 g/ml, Figure 3.8) was added into a 50 ml centrifuge tube. The diluted blood was overlaid onto the Histopaque-1077 (similar to Ficoll) phase very slowly and carefully by using a Pasteur pipette, preventing the mixing of these two fluids (Diluted blood & Histopaque-1077). The centrifuge tube containing the overlaid diluted blood and the Histopaque-1077 (similar to Ficoll) was centrifuged for 30 minutes at 20°C with 1800 rpm (400 x G) without brakes. After centrifugation, the formed phase of cell layer (plasma/Histopaque-1077 interface) was collected together with the media and Histopaque-1077 (similar to Ficoll) with a Pasteur pipette and transferred to a new 50 ml centrifuge tube. Then, this suspension was washed 2 times (by adding 1 X

PBS to the tube which contained the collected part of the cell suspension and then centrifuging for 5 minutes at 20°C with 1800 rpm) (Figure 3.10).

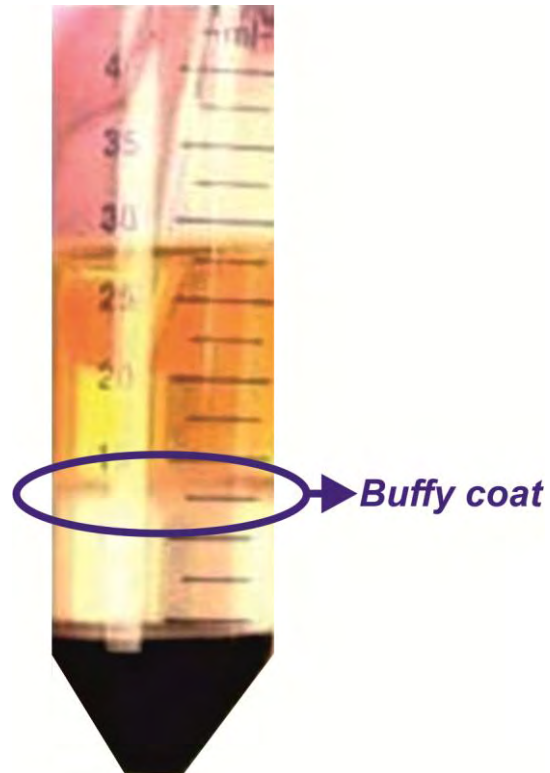


Figure 3.9. Formation of the *buffy coat* after centrifugation. Adapted from Assistance publique – Hôpitaux de Paris (223).

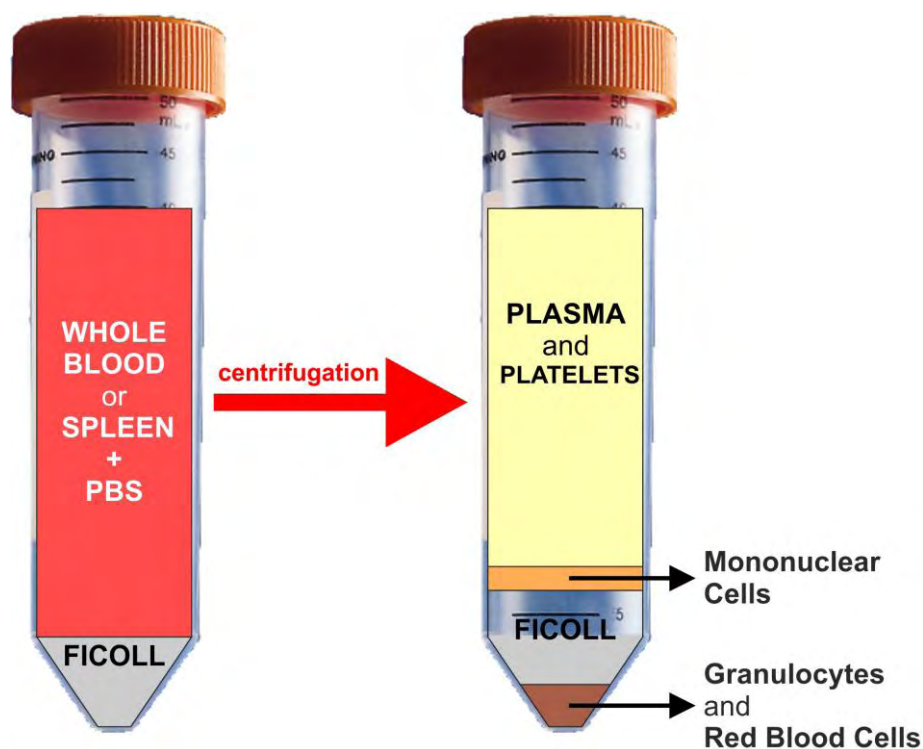


Figure 3.10. Isolation of PBMC and splenocytes from blood or spleen.

3.5.3. Isolation of T Cells

As mentioned before, rat PBMCs and splenocytes were obtained by intracardiac blood withdrawal and splenectomy.

CD4⁺ T cells and CD8⁺ T cell populations were obtained by fluorescence activated cell sorting with the use of proper fluorescent dye-tagged specific anti-rat CD3, CD4 and CD8 antibodies. For this reason, "APC Mouse Anti-Rat CD3" from BD with catalog number 557030, "PE anti-rat CD4" from Biolegend with catalog number 203308 and "PerCP anti-rat CD8a" from Biolegend with catalog number 201712 antibodies were utilized (Table 3.1). Figure 4.5 demonstrates the gating strategy.

The sorted T cells were then incubated in full RPMI1640 medium containing 1 % Pen/strep, 1 % L-Glutamine, 10 % FBS. Post-sort evaluations were also performed (Figure 4.6).

Table 3.1. Antibodies used in T cell sorting.

Manufacturer	Antibody	Catalog No
BD	APC Mouse Anti-Rat CD3	557030
Biolegend	PE anti-rat CD4	203308
Biolegend	PerCP anti-rat CD8a	201712

3.6. Primary Cell Cultures

Primary cell cultures of fibroblasts and Cancer Associated Fibroblasts were performed. The isolation techniques of these cells were described in section 3.4. Fibroblasts and CAFs were incubated in T25 cell culture flasks with full DME medium at the environmental conditions of 37°C, 5 % CO₂ and 60 % humidity.

The subculturings were performed with Trypsin-EDTA or HyQTase when the cells reached a surface confluency of approximately 80 % in their flask.

3.7. Cell Culture

3.7.1. Splenocyte, PBMC and T Cell Cultures

Primary splenocyte, PBMC and T cells that were obtained from the spleen and peripheral blood of healthy and NMU injected female Sprague Dawley rats were cultured. The isolation techniques of these cells were described in section 3.5 in detail. These cells were incubated in T25 or T75 cell culture flasks with full RPMI medium supplemented with 50 IU / ml Interleukin-2 (Proleukin) at the environmental conditions of 37°C, 5 % CO₂ and 60 % humidity.

The subculturings and transfers of cells were performed mechanically with the liquid flushing effect of a serological pipette, without employing Trypsin-EDTA or HyQTase.

3.7.2. Subculturing Adherent Cell Cultures with Trypsin-EDTA or HyQTase

Subculturings were performed when the cell culture monolayers were nearly confluent.

Trypsin-EDTA:

Trypsin-EDTA was used for most of the cell culture subculturings. First, growth medium was decanted from the cell culture flask. Then, the flask containing the cells was washed gently a few times with 1 X PBS. Trypsin-EDTA solution (1:250) was added onto the cell monolayer, making sure that it dispersed evenly and covered all of the surface. The flask was placed in a 37°C incubator until the adherent cells detached from the surface (about 1 to 2 minutes). The detachment of cells was further facilitated by tapping the side of the flask a few times. Detached cells were examined under an inverted microscope. The detached cells were resuspended in their growth medium which halted the action of the trypsin. The cell suspension was gently aspirated and mixed a few times with a Pasteur pipette to achieve a single-cell suspension. The new culture flasks were then placed in a 37° incubator (224).

HyQTase:

HyQTase was used only a few times for subculturing primary fibroblast and primary Cancer Associated Fibroblast cells obtained from healthy and NMU injected Sprague-Dawley rats, respectively. The cell medium was decanted and the cells were covered with 4 ml of HyQTase solution. The flask was placed in a 37°C incubator for about 15 minutes. The detachment of cells was facilitated by tapping the side of the flask a few

times. The detached cells in the solution were then centrifuged and resuspended in their growth medium. This fresh cell suspension was then transferred to a new flask.

3.7.3. Cell Counting

The numbers of the cells were calculated by counting the cells in a haemocytometer (i.e. Improved Neubauer) (225, 226). Cell suspension was first pipetted up and down with a Pasteur pipette in order to disperse the cells thoroughly. 20 μ l from the cell suspension was mixed well with 20 μ l of "Trypan Blue" (0.1 % w/v Trypan Blue in PBS solution), which stained the non-viable cells in blue. 20 μ l of this mixture was aspirated and loaded to the Neubauer haemocytometer chamber with capillary effect (Figure 3.11). The cells were counted under a light microscope (100x magnification). The viable (non-blue) cells in each of the four corner squares bordered by triple lines were counted (cells lying on these lines were omitted). The arithmetic mean count of the total viable cells per four corner squares was calculated. Formula 3.1 was used to calculate the viable cell concentration per ml (224).

$$\begin{aligned} \text{(Initial cell concentration per ml)} = & \text{(total viable cell count of four} \\ & \text{corner squares)} \times [\text{correction for the trypan blue dilution (counting} \\ & \text{dilution was } 1 / \text{tb)}] \times 1/4 \times 10^4 \end{aligned} \quad (3.1)$$

Total number of the cells was calculated by simply multiplying the cell concentration per ml by the total volume of the cell suspension.

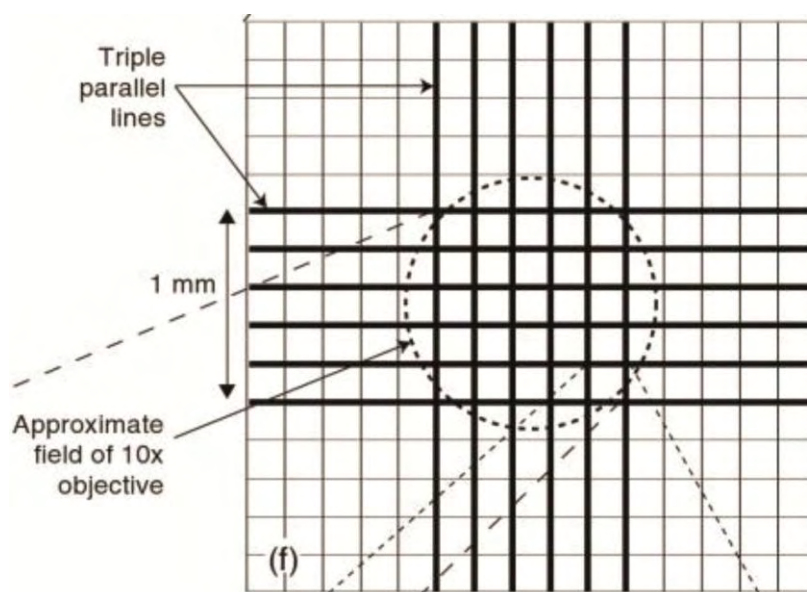


Figure 3.11. Improved Neubauer Haemocytometer. Adapted from "Culture of Animal Cells: A Manual of Basic Technique and Specialized Applications" (225).

3.7.4. Freezing and Thawing Cells

Freezing:

The adherent fibroblast and CAF cells were detached with Trypsin-EDTA. Splenocytes and peripheral blood mononuclear cells were just mechanically suspended in growth medium by using a Pasteur pipette, without employing Trypsin-EDTA. The total number of cells in suspension was calculated by using the technique described in section 3.7.3. (The final total number of fibroblast or CAF cells in a 1 ml cryopreservation vial was adjusted to be 2×10^6 cells/ml. The final total number of splenocyte cells or PBMC in a 1 ml cryopreservation vial was adjusted to be 30×10^6 cells/ml.)

Then, the cells in suspension (either fibroblasts or mononuclear cells) were centrifuged at 1800 rpm for 5 minutes. The supernatant was discarded and the cells in pellet were then thoroughly resuspended in their respective pre-chilled growth mediums (full DMEM or full RPMI1640) containing 20 %

fetal calf serum and 10 % (v/v) dimethyl sulfoxide. Screw-capped cryopreservation vials were labeled properly and 1 ml of the cell suspensions for freezing were dispensed in each of the vials (1 ml freezing media / cryotube).

The vials were frozen slowly using the Nalgene Freezing container "Mr. Frosty" which provided the critical and repeatable $-1^{\circ}\text{C}/\text{minute}$ cooling rate required for successful cell cryopreservation and recovery (Figure 3.12). The cells were first stored at -80°C for 24 hours. After 24 hours in -80°C , the vials were taken out of Mr. Frosty and transferred to the special container that stored them in the gaseous phase (-150°C to -180°C) of the liquid nitrogen vessel (224).



Figure 3.12. Nalgene Mr. Frosty achieves a rate of cooling close to -1°C per minute. Adapted from Thermo Scientific (227).

Thawing:

The vials were removed from the nitrogen tank and transferred immediately to a water bath of sterile water in a beaker at 37°C . When suspensions in vials were completely thawed, outsides of the vials were wiped with alcohol to reduce bacterial contamination. The cells were then transferred to a 50 ml centrifuge tube containing growth medium. The cell suspension was then centrifuged for 5 minutes at 1800 rpm. The

supernatant containing DMSO was discarded and cell pellet was resuspended in sufficient growth medium and incubated at 37°C (224).

3.7.5. Quality Control in Cell Cultures: Testing for Mycoplasma Contamination

Reliability of cell culture studies depends strongly on continuous supply of healthy cell cultures. Mycoplasma contamination of the cell cultures results in a critical problem in the cell culture laboratory.

Mycoplasma contamination does not display visible signs such as turbidity of the cell medium, cytopathic effects or pH changes. However, it may deplete arginine in media, change nucleic acid synthesis and RNA profiles and growth rate of the cells. It might also affect the phenotypic characteristics of the cells and can negatively impact the study results.

Therefore, 3-monthly testing of all cell cultures for mycoplasma was introduced as a means of internal quality control program of the study. For this reason, mycoplasmas were detected via Biological Industries EZ-PCR Mycoplasma Test Kit. This is a ready-to-use PCR Mix for the detection of mycoplasma in cell cultures. The results are obtained within a few hours with PCR testing. The presence of contaminant mycoplasma can be easily detected by analyzing the bands of amplified DNA fragments in electrophoresis. The primer set allows detection of various mycoplasma species (*M. fermentans*, *M. hyorhinae*, *M. arginini*, *M. orale*, *M. salivarium*, *M. hominis*, *M. pulmonis*, *M. arthritis*, *M. bovis*, *M. pneumoniae*, *M. pirum* and *M. capricolum*), as well as *Acholeplasma* and *Spiroplasma* species with high sensitivity and specificity.

Manufacturer's guidelines were followed for the test protocol (228). Briefly, test sample was prepared first. Then, the PCR amplification was performed in thermal cycler. Finally, amplified products were analyzed by gel electrophoresis.

3.8. Morphological Analyses

All of the cells in question; including the normal tissue fibroblasts that were obtained from healthy Sprague-Dawley rats and the Cancer Associated Fibroblast that were isolated from the tumors of NMU injected animals as described previously; were cultured in 8 chamber-well culture slides (BD) (Figure 3.13). A biotin/streptavidin/horseradish peroxidase detection system was utilized and bindings of antibodies was demonstrated with diaminobenzidine (DAB) substrate and examined under a light microscope.



Figure 3.13. Eight chamber-well culture slides (BD) (229).

3.8.1. Immunocytochemistry

At the end of the incubation period, the 8 chamber-well culture slides were taken to the room temperature and the cell media were decanted. The protocol described in the next section was followed strictly (230).

3.8.1.1. Desmin Staining

After the removal of the cell media, the slides were washed once with 1 X PBS. Then, cold 70 % methanol with 0.3 % H₂O₂ solution was added and incubated for 15 minutes at room temperature. This solution both fixed the cells and also blocked the peroxidase activity by its H₂O₂ content. The

slides were then washed twice with 1 X PBS. The fixed cells in each well were then covered with 100 µl solution of primary antibody against desmin in 1 X PBS and incubated for 90 minutes at room temperature in the dark. After the washing process, the cells were then covered with 150 µl solution of polyvalent biotinylated secondary antibody in 1 X PBS and incubated for 30 minutes at room temperature in the dark.

After the washing process, the cells were then covered with 150 µl solution of Streptavidin and incubated for 15 minutes at room temperature in the dark. 150 µl solution mixture of DAB is added onto each of the wells after the washing step and incubated for 5 minutes. 100 µl of Hematoxylin is added and incubated for 1 minute after the washing step. A series of incubations with increasing concentrations of ethyl alcohol was used to dehydrate the cells. After the last 100 % alcohol incubation, the chamber walls were removed by the help of a special key supplied by the manufacturer (BD). One minute of incubation in xylene is followed by a step of covering with entellan (for mounting) and a cover-slip. The slides were stored in the dark at +4°C (Table 3.2).

Table 3.2. Steps of the immunocytochemistry protocol are explained in detail.

Immunocytochemistry Protocol - Stepwise	
1	Removal of the cell media
2	Washing with 500 µl 1 X PBS (1 time 5 minutes)
3	Addition of 200 µl cold 70 % methanol with 0.3 % H ₂ O ₂ solution (15 minutes of incubation at room temperature)
4	Decanting the solution
5	Washing with 500 µl 1 X PBS (2 times 5 minutes)
6	Addition of 100 µl solution of primary antibody in 1 X PBS (90 minutes of incubation at room temperature in the dark)

7	Decanting the primary antibody solution
8	Washing with 500 μ l 1 X PBS (4 times 5 minutes)
9	Addition of 150 μ l solution of polyvalent biotinylated secondary antibody in 1 X PBS (30 minutes of incubation at room temperature in the dark)
10	Decanting the secondary antibody solution
11	Washing with 500 μ l 1 X PBS (4 times 5 minutes)
12	Addition of 150 μ l solution of Streptavidin (15 minutes of incubation at room temperature in the dark)
13	Decanting the Streptavidin solution
14	Washing with 500 μ l 1 X PBS (4 times 5 minutes)
15	DAB substrate and DAB chromogen are mixed (1 to 2 drops of DAB chromogen for each 1 ml of DAB substrate)
16	Addition of 150 μ l solution mixture of DAB onto each of the wells (5 minutes of incubation at room temperature in the dark)
17	Decanting the DAB solution mix
18	Washing with 500 μ l 1 X PBS (4 times 5 minutes)
19	Addition of 100 μ l Hematoxylin onto each of the wells (1 minute of incubation at room temperature in the dark)
20	Decanting the Hematoxylin
21	Washing with 500 μ l 1 X PBS (4 times 5 minutes)
22	Addition of 1 ml 70 % ethanol onto each of the wells to dehydrate the cells (1 minute of incubation at room temperature in the dark)
23	Decanting the 70 % ethanol
24	Addition of 1 ml 90 % ethanol onto each of the wells to dehydrate the cells (1 minute of incubation at room temperature in the dark)
25	Decanting the 90 % ethanol
26	Addition of 1 ml 100 % ethanol onto each of the wells to dehydrate the cells

	(1 minute of incubation at room temperature in the dark)
27	Decanting the 100 % ethanol
28	Addition of 1 ml 100 % ethanol onto each of the wells to dehydrate the cells (1 minute of incubation at room temperature in the dark)
29	Decanting the 100 % ethanol
30	Removal of the chamber walls by the help of a special key supplied by the manufacturer (BD)
31	Immersion of the microscope slide in xylene (1 minute of incubation in xylene at room temperature in the dark)
32	Mounting the slide with 3 drops of entellan (no bubbles)
33	Putting of a cover-slip on top
34	Examination with a light microscope
35	Storage of the microscope in the dark at +4°C

3.8.1.2. Pancytokeratin Staining

The same protocol described in section 3.8.1.1 and Table 3.2 was used; except the fact that 100 µl solution of primary antibody in 1 X PBS against "pancytokeratin" was used.

3.9. Coculture Experiments

3.9.1. With Sorted CD4⁺ and CD8⁺ T cells

Rat normal mammary primary fibroblasts and rat primary cancer associated fibroblasts from mammary tumors were separately cocultured with CD4⁺ and CD8⁺ T cells; as a result in total of 4 different coculture settings. The setup is described below.

- i. Rat primary normal mammary fibroblast cells + CD4⁺ T cells
- ii. Rat primary normal mammary fibroblast cells + CD8⁺ T cells
- iii. Rat primary Cancer Associated Fibroblast Cells + CD4⁺ T cells
- iv. Rat primary Cancer Associated Fibroblast Cells + CD8⁺ T cells

3.9.2. With Splenocytes or PBMCs

Rat normal mammary primary fibroblasts and rat primary cancer associated fibroblasts from mammary tumors were separately cocultured with healthy splenocytes or PBMCs; as a result in total of 2 different coculture settings. The setup is described below.

- i. Rat primary normal mammary fibroblast cells + Splenocytes / PBMCs
- ii. Rat primary cancer associated fibroblast cells + Splenocytes / PBMCs

3.10. Enzyme-Linked Immunosorbent Assay (ELISA)

Supernatants collected from coculture settings (explained in section 3.9) were used for cytokine analyses. Splenocyte supernatants that were collected at various times from tissue culture plates containing either NF or CAF cells were stored at -80°C until they were analyzed by ELISA. All supernatants were investigated for IFN- γ and TGF- β . These experiments helped comparatively identify the effects of normal fibroblasts and CAFs on splenocytes. Table 3.3 demonstrates the ELISA kits that were used during these experiments. All procedures were conducted according to the manufacturers' instructions.

Table 3.3. ELISA kits used for the experiments.

No	Producer	Product Name	Catalog Number
1	eBioscience	Rat TGF-beta1 Platinum ELISA	BMS623/2
2	eBioscience	Rat IFN-gamma Platinum ELISA	BMS621

3.10.1. Rat TGF-beta1 ELISA

All the samples, standards and controls were assayed in duplicate.

Reagent Preparation: All of the reagents were brought to the room temperature just before use.

Wash Buffer (1x): 50 ml of "**Wash Buffer Concentrate (20x)**" was added into 950 ml of distilled water to prepare 1000 ml of Wash Buffer (1x) for one plate.

Assay Buffer (1x): 5 ml of "**Assay Buffer Concentrate (20x)**" was added to 95 ml distilled water to prepare 100 ml of Assay Buffer (1x).

Biotin-Conjugate: Biotin-Conjugate was diluted 1:100 in Assay Buffer (1x).

Streptavidin-HRP: Streptavidin-HRP was diluted 1:100 in Assay Buffer (1x).

Rat TGF- β 1 Standard: Lyophilized rat TGF- β 1 standard was reconstituted with distilled water. (Reconstitution volume is stated on the label of the standard vial.)

Test Protocol Summary: First, there was a pretreatment step for cell culture supernatant samples. According to this step, 20 μ l of sample

was mixed with 180 μl of Assay Buffer (1x). Then, 20 μl of 1N HCl was added to 200 μl prediluted sample and mixed. This mixture was incubated for 1 hour at room temperature. Then, 20 μl of 1N NaOH was added.

The number of required microwell strips were determined. Microwell strips were washed twice with Wash Buffer. Rat TGF- β 1 standard was diluted on the microwell plate. For this, 100 μl Sample Diluent was added, in duplicate, to all standard wells. Then, 100 μl of prepared standard was pipetted into the first wells and standard dilutions were created by transferring 100 μl from well to well. 100 μl was discarded from the last wells. 100 μl of Sample Diluent was added, in duplicate, to the blank wells. 60 μl of Sample Diluent was added to sample wells. 40 μl of cell culture supernatant sample was added, in duplicate, to designated sample wells. Microwell strips were covered and incubated for 2 hours at room temperature (Shaking is absolutely necessary for an optimal test performance.). Biotin-Conjugate was prepared as described above. Microwell strips were emptied and washed 5 times with Wash Buffer. 100 μl of Biotin-Conjugate was added to all wells. Microwell strips were covered and incubated 1 hours at room temperature (18° to 25°C) (Shaking is absolutely necessary for an optimal test performance.). Streptavidin-HRP was prepared as described above. Microwell strips were emptied and washed 5 times with Wash Buffer. 100 μl of diluted Streptavidin-HRP was added to all wells. Microwell strips were covered and incubated 1 hour at room temperature (18° to 25°C) (Shaking is absolutely necessary for an optimal test performance.). Microwell strips were emptied and washed 5 times with Wash Buffer. 100 μl of TMB Substrate Solution was added to all wells. Microwell strips were incubated for about 30 minutes at room temperature (18° to 25°C). 100 μl of Stop Solution was added to all wells. Microwell reader was blanked and color intensity was measured at 450 nm. The optical density of each well was determined by using the microplate reader (Spectramax Plus, Molecular Devices, USA). The standard curve was drawn according to the standards' concentrations and then the concentrations of the samples were calculated (231).

3.10.2. Rat IFN-gamma (IFN- γ) ELISA

All the samples, standards and controls were assayed in duplicate.

Reagent Preparation: All of the reagents were brought to the room temperature just before use.

Wash Buffer (1x): 50 ml of "**Wash Buffer Concentrate (20x)**" was added into 950 ml of distilled water to prepare 1000 ml of Wash Buffer (1x) for one plate.

Assay Buffer (1x): 5 ml of "**Assay Buffer Concentrate (20x)**" was added to 95 ml distilled water to prepare 100 ml of Assay Buffer (1x).

Biotin-Conjugate: Biotin-Conjugate was diluted 1:100 in Assay Buffer (1x).

Streptavidin-HRP: Streptavidin-HRP was diluted 1:100 in Assay Buffer (1x).

Rat IFN- γ Standard: Lyophilized rat IFN- γ standard was reconstituted with distilled water. (Reconstitution volume is stated on the label of the standard vial.)

Test Protocol Summary: The number of required microwell strips were determined. Microwell strips were washed twice with Wash Buffer. Rat IFN- γ standard was diluted on the microwell plate. For this, 100 μ l Sample Diluent was added, in duplicate, to all standard wells. Then, 100 μ l of prepared standard was pipetted into the first wells and standard dilutions were created by transferring 100 μ l from well to well. 100 μ l was discarded from the last wells. 100 μ l of Sample Diluent was added, in duplicate, to the

blank wells. 50 μ l of Sample Diluent was added to sample wells. 50 μ l of sample was added, in duplicate, to designated sample wells. Biotin-Conjugate was prepared as described above. 50 μ l of Biotin-Conjugate was added to all wells. Microwell strips were covered and incubated 2 hours at room temperature (18° to 25°C). Streptavidin-HRP was prepared as described above. Microwell strips were emptied and washed 3 times with Wash Buffer. 100 μ l of diluted Streptavidin-HRP was added to all wells. Microwell strips were covered and incubated 1 hour at room temperature (18° to 25°C). Microwell strips were emptied and washed 3 times with Wash Buffer. 100 μ l of TMB Substrate Solution was added to all wells. Microwell strips were incubated for about 10 minutes at room temperature (18° to 25°C). 100 μ l of Stop Solution was added to all wells. Microwell reader was blanked and color intensity was measured at 450 nm. The optical density of each well was determined by using the microplate reader (Spectramax Plus, Molecular Devices, USA). The standard curve was drawn according to the standards' concentrations and then the concentrations of the samples were calculated (232).

3.11. Molecular Techniques

3.11.1. Total RNA Isolation

Total RNA was extracted from all the cell types cultured alone or cultured in the coculture settings. The isolation was performed by using QIAamp Blood Mini Kit (7, 233). First, the cells were detached from the flasks with trypsin-EDTA or by the help of a scraper and centrifuged at 4°C for 5 minutes at 18000 rpm. The pellet was resuspended with 400 μ l of Buffer RLT (containing β -mercaptoethanol) and was vortexed rigorously. The content was transferred to "purple columns" and centrifuged for 2 minutes at 1300 rpm. The lisate was mixed well with 400 μ l of 70 % ethanol and transferred into white columns. Following the centrifugation at 10000 rpm for 20 seconds, 350 μ l of Buffer RW1 was added to the white columns

and another centrifugation at 10000 rpm for 20 seconds was performed. For each sample, 80 μ l (which consists of 70 μ l Buffer RDD and 10 μ l RNase free DNase I) was added and then incubated at room temperature for 45 minutes. After the incubation, 350 μ l of Buffer RW1 was added and centrifuged at 10000 rpm for 20 seconds. The "white columns" were inserted into new collection tubes after each centrifugation. Buffer RPE (500 μ l) was added and centrifuged at 10000 rpm for 20 seconds. This was repeated again but then centrifuged at 13000 rpm for 4 minutes. "White columns" were taken to new collection tubes and dried by centrifugation at 13000 rpm for 1 minute. The columns were then taken to RNase free tubes and 30 μ l RNase free water was added and centrifuged at 10000 rpm for 1 minute. The eluate containing total RNA was stored at -80°C .

RNA isolations were performed from cultured rat splenocytes or rat splenocytes cocultured with normal fibroblast / CAFs. In addition, RNA isolations were also performed from cultured rat normal fibroblasts and CAFs.

3.11.2. Control and Removal of DNA in Isolated RNA Samples

In order to ensure that DNA is not present in isolated RNA samples, PCRs directly from RNA samples (no reverse transcription controls) were performed with β -actin primers. If amplicons were detected, treatment with "Ambion DNA-free DNase Treatment & Removal Reagent set" was performed (234). All reagents were kept on ice during the procedure. From each RNA sample, 20 μ l was taken into a RNase free PCR tube and mixed with 2 μ l of DNase I Buffer (10x). rDNase I (2.2 μ l) was added to the mixture and then placed at 37°C for an incubation of 45 minutes. After the incubation, 4.8 μ l of DNase I Inactivation Reagent was added, mixed well and incubated for 2 minutes at room temperature. Then, the tubes were centrifuged for 90 seconds at 10000 rpm and the supernatants were

collected to RNase free PCR tubes, rechecked for DNA presence and stored at -80°C.

3.11.3. Spectrophotometric Analysis of RNA

Concentrations and qualities of the isolated RNAs were determined by the measurement of the optical density (OD) using Nano Drop Spectrophotometer (ND-100, USA) at the wavelengths of 260 nm and 280 nm. The quality of RNA was evaluated by using A_{260}/A_{280} and A_{230}/A_{280} ratios (range: 1.5-2.1). The concentrations of RNAs were also measured and recorded as ng / μ l, which were further used for cDNA synthesis.

3.11.4. cDNA Synthesis by Reverse Transcription

Complementary DNA (cDNA) was synthesized from RNA by using oligo(dT) primers and RevertAid First Strand cDNA Synthesis Kit (Thermo Scientific) according to the manufacturer's instructions (235). cDNA was synthesized from total RNA in a reaction shown in Table 3.4. The cDNAs were stored at -20°C.

Table 3.4. Conditions and compounds used for cDNA synthesis.

<i>Compound</i>	<i>Quantity</i>	<i>Final Concentration</i>
RNA	0.66 µg	33 ng/µl
Oligo(dT) Primer (10 µM)	1 µl	0.5 µM
dH ₂ O	Completed to 12 µl	
<i>Incubation</i>		<i>70°C, 5 min.</i>
dNTPmix (10 mM)	2 µl	1 mM
RNase Inhibitor (20 u/µl)	1 µl	1 u/µl
RT Buffer (5x)	4 µl	1 x
<i>Incubation</i>		<i>37°C, 5 min.</i>
Reverse Transcriptase M-MuLV (200 u/µl)	1 µl	10 u/µl
<i>Incubation</i>		<i>42°C, 60 min. & 70°C, 10 min.</i>
Final Volume	20 µl	

3.11.5. Real-Time Reverse Transcriptase-Polymerase Chain Reaction (Real-Time RT-PCR)

Synthesized cDNAs were used to determine the gene expression levels. In the experiments, gene expression levels of CD25 and CD28 were analyzed. In addition, expression levels of TGFβ and IFN-γ genes were investigated in normal fibroblasts and CAFs. β-actin expression was used as housekeeping reference to normalize the expression levels of the genes for real time RT-PCR. The primer sequences for rat CD25, CD28, TGFβ, IFN-γ and β-actin genes are demonstrated in Table 3.5.

Table 3.5. Primer sequences designed for real time RT-PCR.

Gene	Oligo Name	Forward & Reverse Primer Nucleotide Sequences (5'-3')	Product Size
CD25	rCD25_F (2 nd)	CCTGGAGCAACAACACTGTCAGTGC	113 bp
	rCD25_R (2 nd)	TGATTTCTGCGTGTCCGTGG	
CD28	rCD28_F (1 st)	CGGGCATCCCTTTACAAGGGCGT	152 bp
	rCD28_R (1 st)	AGATTCCAGAGACGGAACGTCAC	
TGF-β1	TGFb1_F (T)	CCAGATCCTGTCCAAACTAAGGC	103 bp
	TGFb1_R (T)	GCGGGTGCTGTTGTACAAAGC	
IFN-γ	IFNg_F (\mp , 2 nd)	TGGCAAAGGACGGTAACACG	196 bp
	IFNg_R (\mp , 2 nd)	TCACCTCGAACTTGGCGATGCT	
β-Actin	bActin_F (T)	ACCAGGGTGTGATGGTGGGTATG	118 bp
	bActin_R (T)	CAGTTGGTGACAATGCCGTGTTC	

All of the reactions were carried out at Rotor-Gene 6000TM Cycler (Corbett Research, Australia) with using LightCycler DNA Master SYBR Green I real-time PCR kit (Roche) (236). The reaction conditions are listed in Table 3.6.

Table 3.6. Quantities and final concentrations of real time RT-PCR reagents.

Reagents	Quantity	Final Concentration
DNA Master SYBR (10x)	2 μ l	1 x
MgCl₂ (25 mM)	2 μ l	3,5 mM
Primer Fw (5 pmol/μl)	0,3 μ l	0,075 μ M
Primer Rv (5 pmol/μl)	0,3 μ l	0,075 μ M
dH₂O	12,4 μ l	
cDNA (1/3 diluted)	3 μ l	
Final Volume	20 μ l	

Real time RT-PCR controls with distilled water (dH₂O) instead of a cDNA template (negative control) were performed to ensure the absence of contamination. A *mastermix* was prepared: dH₂O, DNA Master SYBR Green (10x), primers (forward and reverse for each one), MgCl₂ solution (25 mM) were placed in a 1.5 ml tube and mixed thoroughly by pipetting. The mixture was then distributed to microtubes (200 µl) and the respective template cDNA (1/3 diluted) was added. Each sample was studied in duplicate.

The tubes were then placed into Rotor Gene and the thermal cycler conditions were adjusted according to Table 3.7. The number of cycles was set 40.

Table 3.7. Real-Time RT-PCR thermal cycler conditions.

Initial Denaturation	95°C	1 min.	
Denaturation	95°C	30 sec.	} 40 cycles
Annealing	60°C	20 sec.	
Extension	72°C	30 sec.	
Final Extension	40°C	30 sec.	

Relative expression levels of target genes were measured by the "Comparative threshold cycle" (Ct) ($\Delta\Delta\text{Ct}$) method (237) (Figure 3.14).

$$2^{-\Delta\Delta\text{Ct}} = 2^{-(\Delta\text{Ct target gene} - \Delta\text{Ct target gene normalizer})}$$

$$= 2^{-[(\text{Ct target gene} - \text{Ct reference gene}) - (\text{Ct target gene normalizer} - \text{Ct reference gene})]}$$

Figure 3.14. Comparative threshold cycle method ($\Delta\Delta\text{Ct}$).

3.11.6. Agarose Gel Electrophoresis

Agarose gel (2 % w/v) was prepared by adding 4 gr of agarose to 200 ml of 1xTBE solution. Then, it was melted in a microwave oven for 4 minutes and left to cool. Ethidium bromide (5 mg/ml) was added in order to have a final concentration of 500 µg/ml followed by mixing. It was poured into a casting tray, a comb was placed and incubated at room temperature for gelling. The gel was placed in the 1xTBE containing electrophoresis tank. The PCR products (15 µl) were mixed with 3 µl of 6x loading dye solution and were loaded into the gel. DNA size marker (50-1000 bp) was also loaded and electrophoresis was run at 150V (Figure 3.15) (238).

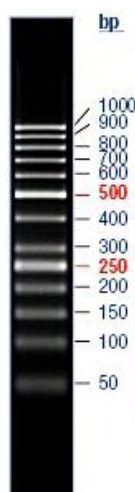


Figure 3.15. Fifty bp DNA ladder (50-1000 bp). Adapted from Thermo Scientific (238).

The gels were then visualized and documented with UV light (Kodak Gel Logic 1500 Imaging System, USA).

3.12. Comet Assay

Standard assay guidelines were followed for all 100 µl of blood samples taken from the tail vein of each rat (217). For comparative analyses, 4 groups of animals were enrolled in these experiments.

1. Control rats without any NMU injections.
2. Twenty-four hours after the last NMU injection (total of 4 injections) of NMU injected rats
3. Two months after the last NMU injection (total of 4 injections) of NMU injected rats
4. Three months after the last NMU injection (total of 4 injections) of NMU injected rats

Analyses of the Comet experiments were performed with the guidance of Hacettepe University, Faculty of Pharmacy, Department of Pharmaceutical Toxicology; where the assay is routinely performed with the help of a computer software.

3.13. Histopathological Evaluation

The mammary tumors excised from the NMU injected Sprague-Dawley rats were fixed in 10 % formalin solution, embedded in paraffin for further histopathological evaluations. The tumor specimens were examined under light microscopy following hematoxylin - eosin staining.

3.14. Statistical Analyses and Scientific Graphings

Statistical analyses were performed using the SPSS software version 18. All values were expressed by arithmetic mean \pm either standard error (SE) or standard deviation (SD). A 5 % type-I error level was used to infer statistical significance. Statistically significant differences between experimental and control groups were determined using one sample, Student's paired or unpaired *t*-tests where applicable.

Scientific graphings were performed using the GraphPad Prism software version 5.

4. RESULTS

4.1. Experiments with the Laboratory Animals

4.1.1. Rat Chemically Induced Mammary Carcinoma Model

21 days old female Sprague Dawley out-bred rats were used for the mammary carcinoma model experiments. All animals were housed at Hacettepe University Laboratory Animals Research and Care Facility. 20 animals were injected with N-Nitroso-N-methylurea (NMU) (Figure 4.1). All of the animals that were injected weekly with 50 mg/kg NMU i.p. developed at least one palpable breast tumor after a period of 1-2 months. The photo of one of the developed mammary tumors is seen in Figure 4.2. The animal groups injected with NMU are summarized in Table 4.1.

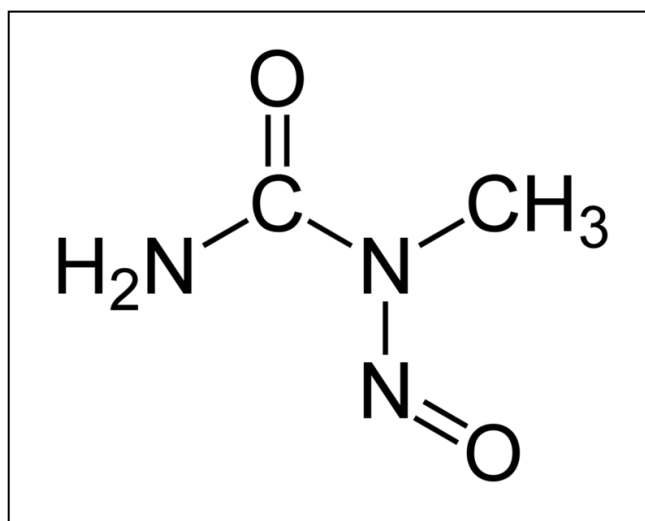


Figure 4.1. The molecular structure of N-Nitroso-N-methylurea (NMU).



Figure 4.2. NMU induced breast tumor.

Table 4.1. Dates of NMU injections and the average weights of the animals at the times of injections.

	1st Injection (Mean Weight)	2nd Injection (Mean Weight)	3rd Injection (Mean Weight)	4th Injection (Mean Weight)
1st Tumor Group	25.08.2010 36.9 gr n=3	01.09.2010 43.1 gr n=3	08.09.2010 53.2 gr n=3	15.09.2010 110.8 gr n=3
2nd Tumor Group	10.11.2010 41.5 gr n=3	17.11.2010 41.6 gr n=3	24.11.2010 52.8 gr n=2	01.12.2010 84.2 gr n=2
3rd Tumor Group	06.05.2011 33.4 gr n=3	13.05.2011 53.4 gr n=3	20.05.2011 76.3 gr n=3	30.05.2011 78.4 gr n=3
4th Tumor Group (Kobay A.S.)	07.06.2011 31.2 gr n=2	14.06.2011 31.4 gr n=2	22.06.2011 54.6 gr n=2	29.06.2011 72.7 gr n=2
5th Tumor Group	06.09.2011 32.9 gr n=3	13.09.2011 40.7 gr n=3	20.09.2011 61.1 gr n=3	27.09.2011 86.8 gr n=3
6th Tumor Group	03.01.2012 40.5 gr n=3	11.01.12 36,8 gr n=3	18.01.12 57,6 gr n=3	25.01.2012 86,2 gr n=3
7th Tumor Group	18.04.12 33,2 gr n=3	25.04.2012 49,5 gr n=3	02.05.12 69,7 gr n=3	09.05.12 92,5 gr n=3
	n= 20			n= 19

Table 4.2 shows the numbers of tumors, their sizes and their anatomical locations at the time of the sacrifices of the tumor bearing animals.

Table 4.2. The order of sacrifices, excised tissues, tumor locations & sizes at the time of sacrifices.

Sacrification	Tumor Sizes (cm²)	Mean Diameter $\sqrt[2]{A \times B}$
Control-1	-	-
Tumor-1	Right Axillary 2.2 cm ²	1.48 cm
Group-1	Right Inguinal 0.77 cm ²	0.87 cm
	Left Axillary 7.5 cm ² (Necrotic)	2.73 cm
Tumor-2	Right Inguinal 6.25 cm ²	2.5 cm
Group-1		
Control-2	-	-
Tumor-3	Right Axillary 1.5 cm ²	1.22 cm
Group-1	Right Inguinal 10.5 cm ²	3.24 cm
	Left Axillary 3 cm ²	1.73 cm
	Left Abdominal 10.5 cm ²	3.24 cm
	Left Inguinal 18 cm ² (Necrotic)	4.24 cm
Tumor-4	Left Axillary 3.4 cm ²	1.84 cm
Group-2	Right Abdominal 3 cm ²	1.73 cm

	Right Abdominal 13 cm ²	3.6 cm
Tumor-5	Left Inguinal 30 cm ²	5.47 cm
Group-2	Right Abdominal 13.75 cm ²	3.70 cm
Tumor-6	Left Inguinal 16 cm ²	4 cm
Group-3		
Tumor-7	Left Inguinal 3.75 cm ²	1.93 cm
Group-3	Right Axillary 11.25 cm ²	3.35 cm
	Right Inguinal 15.91 cm ²	3.98 cm
	Metastases to both of kidneys	
Control-3	-	-
Tumor-8	Total Abdominal Metastasis	
Group-4		
Control-4	-	-
Tumor-9	Left Inguinal 5 cm ²	2.23 cm
Group-3		
Tumor-10	Right Axillary 7.2 cm ²	2.68 cm
Group-4	Left Abdominal 20.14 cm ²	4.48 cm
Tumor-11	Inguinal 14 cm ²	3.74 cm
Group-5	Right Axillary 0.8 cm ²	0.89 cm
	Right Abdominal 0.8 cm ²	0.89 cm x 2
	Left Abdominal 1.6 cm ²	1.26 cm

Tumor-12 Group-5	Left Inguinal 11 cm ²	3.31 cm
Control-5	-	-
Tumor-13 Group-5	Left Inguinal 15,9 cm ² Right Axillary 2,7 cm ²	3,98 cm 1,64 cm
Tumor-14 Group-6	Left Axillary 5,4 cm ² Right Axillary 3,3 cm ² Right Inguinal 10 cm ²	2,32 cm 1,81 cm 3,16 cm
Tumor-15 Group-6	Right Axillary 3 cm ² Inguinal 18,9 cm ²	1,73 cm 4,34 cm
Control-6	-	-
Tumor-16 Group-6	Total Abdominal Metastasis	
Tumor-17 Group-7	Right Inguinal 2,24 cm ² Left Inguinal 0,88 cm ² Right Axillary 4,14 cm ²	1,49 cm 0,93 cm 2,03 cm
Tumor-18 Group-7	Right Axillary 5 cm ² Right Inguinal 1,44 cm ² Left Inguinal 12,5 cm ²	2,24 cm 1,2 cm 3,53 cm
Control-7	-	-
Tumor-19	Left Inguinal 1,8 cm ²	1,34 cm

Group-7	Left Inguinal 0,64 cm ²	0,8 cm
	Right Inguinal 0,8 cm ²	0,89 cm

Since it was reported that most of the tumors induced by NMU injections turn into adenocarcinomas at later stages; the tumor excisions were not performed until the tumors were ≥ 1 cm in diameter. As a general rule, animals were sacrificed before the tumor grows 4 cm in diameter, in order to prevent any problems with the general health conditions of the animals. The animals that develop lesions of necrosis over the skin covering the tumor area were sacrificed earlier and included in the experiments. Table 4.3 shows the statuses of tumors and ages of the animals at sacrifices.

Table 4.3. Statuses of tumors and ages of the animals at sacrifices.

No	Code	Age (Days)	Status
1	Tumor-1	127	Necrotic Tumor
2	Tumor-3	114	Necrotic Tumor
1	Tumor-2	154	
2	Tumor-4	196	
3	Tumor-5	233	
4	Tumor-6	278	
5	Tumor-9	267	
6	Tumor-10	117	

7	Tumor-11	126	
8	Tumor-12	182	
9	Tumor-13	155	
10	Tumor-14	168	
11	Tumor-15	184	
12	Tumor-17	157	
13	Tumor-18	161	
14	Tumor-19	169	
1	Tumor-7	204	Peritoneal Tumor (Metastases to both kidneys)
2	Tumor-8	212	Total Abdominal Metastasis
3	Tumor-16	266	Total Abdominal Metastasis

The general health conditions of all animals were closely monitored both before and after the injections. The only significant change observed was the decrease in motility of the tumor bearing animals. Weight losses were not observed in either the experiment or the control group rats. There were not any observations of health concerns in the control group animals, either. Tumor induction was shown to be successful in all of the animals injected with NMU (100 %). As seen in Table 4.1, one of the animals (member of the second tumor group) died after the second injection of NMU. As a result, a total of 1 rat was lost during the injection regimens.

7 animals obtained from Hacettepe University Laboratory Animals Research and Care Facility were injected with physiological saline solution for the control experiments (same protocol with the tumor group). The control animals were housed under the same conditions with the experiment group. Table 4.4 shows the ages of control animals at sacrifices.

Table 4.4. Ages of control animals at sacrifices.

No	Code	Age (Days)
1	Control-1	118
2	Control-2	164
3	Control-3	280
4	Control-4	300
5	Control-5	301
6	Control-6	180
7	Control-7	186

4.2. Tumor Excision and Mastectomy

The animals were sacrificed by the cervical dislocation technique. The rats were then sterilized by immersing in 70 % ethanol. The tumor masses were picked up carefully. The tumor tissues that were to be used for enzymatic digestion studies, were placed on a Petri dish.

For the control experiments, healthy rats that were injected with isotonic saline were sacrificed and the mastectomy protocol was performed

on their mammary tissues for further protocols of normal fibroblast cell isolation.

4.2.1. Normal and Cancer Associated Fibroblast Isolation

Normal fibroblasts were obtained from healthy mammary tissues of control female Sprague Dawley rats. Cancer Associated Fibroblasts (CAFs) were obtained from mammary carcinomas. As described in section 3.4.1, three different protocols were utilized for fibroblast and CAF isolations.

1. Enzymatic Digestion with Collagenase I and Hyaluronidase (Orimo et al.) (57)
2. Enzymatic Digestion with Collagenase II and DNase I
3. Enzymatic Digestion with Collagenase II and DNase I (different protocol) (220)

4.2.1.1. Enzymatic Digestion with Collagenase I and Hyaluronidase (Orimo et al.) (57)

The enzymatic digestion process was performed as described in section 3.4.1.1. The resulting digested tissue suspension was passed through a 70 μ m nylon cell strainer; the part passing through the strainer was collected. The collected fraction was centrifuged. The resulting pellet was resuspended in full DMEM medium and cultured in a flask.

All of the normal fibroblast isolation experiments with this technique from mammary tissues of healthy female rats, resulted in successful outcomes in our trials. These isolated fibroblast were cultured and successful primary cell cultures were obtained. Figure 4.3 shows one representative result of these normal tissue fibroblast isolations and primary cultures.

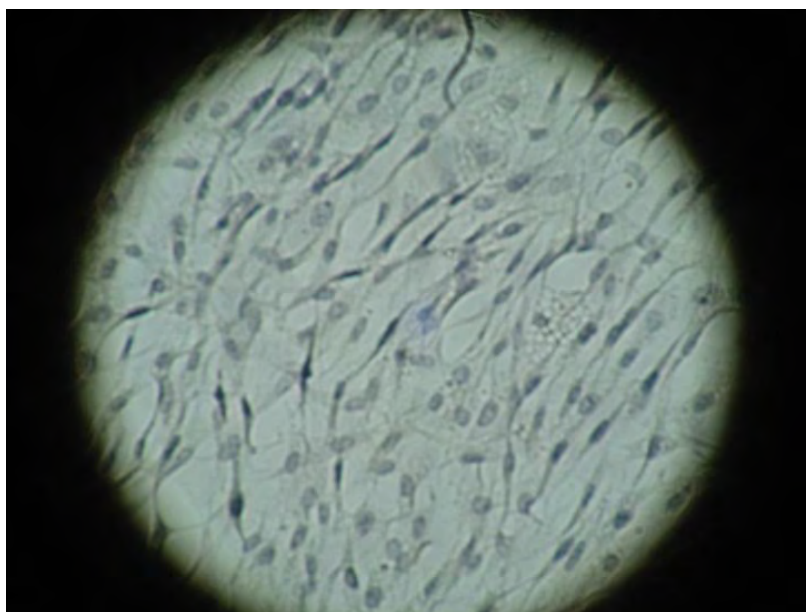


Figure 4.3. Normal fibroblasts (200X) obtained by enzymatic digestion with collagenase I and hyaluronidase.

Figure 4.4 shows one representative result of these CAF isolations and primary cultures.

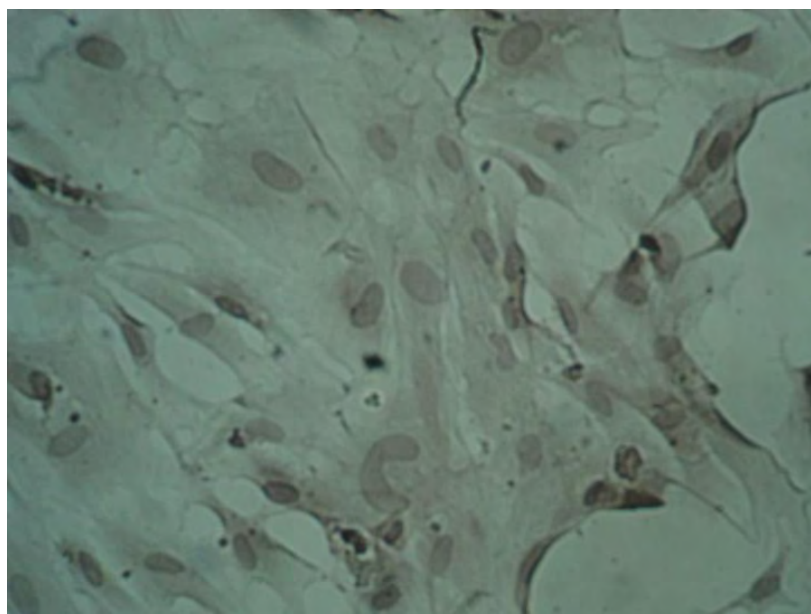


Figure 4.4. Carcinoma Associated Fibroblasts (200X) obtained by enzymatic digestion with collagenase I and hyaluronidase.

4.2.1.2. Enzymatic Digestion with Collagenase II and DNase-I

The enzymatic digestion process was performed as described in section 3.4.1.3. The resulting digested tissue suspension was passed through a 70 μ m nylon cell strainer; the part passing through the strainer was collected. The collected fraction was centrifuged. The resulting pellet was resuspended in full DMEM medium and cultured in a flask.

Isolation of normal fibroblasts from the mammary tissue of a healthy female rat was achieved with this technique. However, successful CAF isolation from mammary tumor tissue was not achieved when this technique was utilized.

Alternatives of various steps were also performed in efforts to isolate CAFs with this protocol. Various enzymatical digestion periods from 4 hours to 8 hours were tried. The same digestion process was also performed only with the Collagenase II and without utilizing the DNase-I enzyme (in order to eliminate any possible damage due to DNase-I). In spite of all these efforts, CAF isolation was not achieved. As mentioned above, normal fibroblasts could be obtained from a control animal with this technique. Such difficulties with CAF isolation are consistent with the literature in terms of problems in obtaining pure primary CAF populations.

4.2.1.3. Enzymatic Digestion with Collagenase II and DNase-I (different protocol) [2]

The enzymatic digestion process was performed as described in section 3.4.1.4. The resulting digested tissue suspension was differentially centrifuged. The resulting pellet was resuspended in full DMEM medium and cultured in a flask.

Normal fibroblast isolation from mammary tissue of a healthy female rat was also achieved with this technique. However, successful CAF isolation from mammary tumor tissue was not achieved when this technique was utilized, either.

Alternatives of various steps were also tried to optimize the protocol. Various enzymatical digestion periods from 2 hours to 12 hours were tried. The same digestion process was also performed only with the Collagenase II and without utilizing the DNase-I enzyme (in order to eliminate any possible damage due to DNase-I). In spite of all these efforts, CAF isolation was again not achieved. As mentioned above, normal fibroblasts could be obtained from a control animal with this technique. Such difficulties with CAF isolation were again thought to be consistent with the literature in terms of problems in obtaining pure primary CAF populations.

4.3. Morphological Analyses

The normal tissue fibroblasts that were obtained from healthy Sprague Dawley rats and the Cancer Associated Fibroblasts that were isolated from the tumors of NMU injected animals as described previously; were cultured in 8 chamber-well culture slides (BD).

Figure 4.3 shows normal fibroblasts and Figure 4.4 shows CAF cells.

4.3.1. Immunocytochemistry - Fibroblast Characterization

Characterizations of CAF cells were performed with immunocytochemistry stainings. For this reason, primary normal tissue fibroblasts and CAFs obtained from tumors were cultured in 8 chamber-well culture slides and stained as described in section 3.8.1.

Pancytokeratin and desmin specific antibodies were used for stainings in order to characterize the cells. The stained cells were examined with a light microscope. These stainings were performed both for fibroblasts obtained via the enzymatic protocol.

The stainings showed that both normal fibroblasts and CAFs were not stained at the "*negative control*", as expected. An epithelial cell marker, "*pancytokeratin*", did not stain either of these cell types, as expected. Furthermore, "*Desmin*", a muscle tissue marker did not stain either of these cell types, as expected.

4.4. Isolation of T Cells

CD4⁺ T cell and CD8⁺ T cell populations were obtained by fluorescence activated cell sorting with the use of proper fluorescent dye-tagged specific anti-rat CD3, CD4 and CD8 antibodies, as explained in section 3.5.3. Figure 4.5 demonstrates the gating strategy.

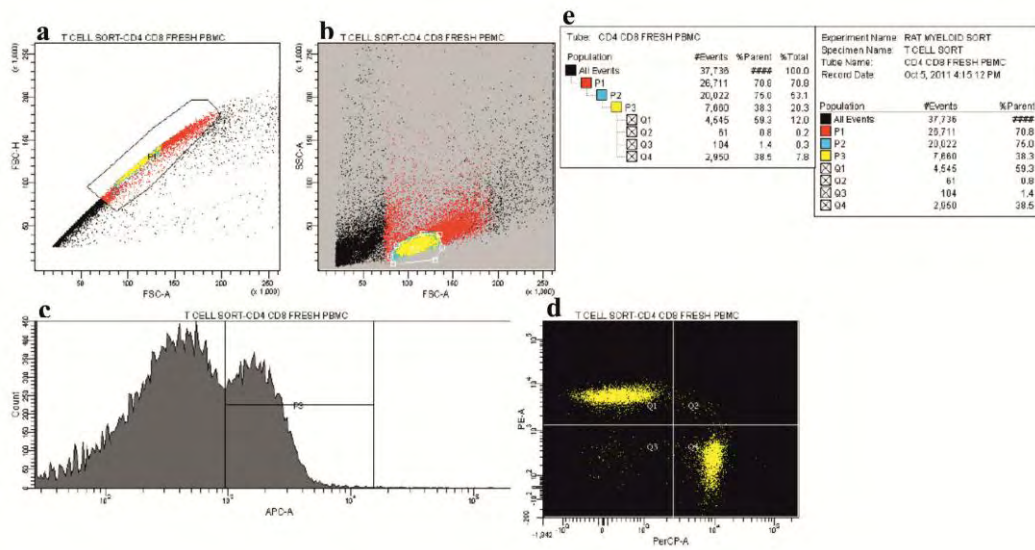


Figure 4.5. Gating strategy used in T cell sorting.

a. Discrimination of doublets

b. Selection of the lymphocyte gate

c. CD3 (APC) intensity histogram and selection of CD3⁺ cells

d. CD4 (PE) vs. CD8 (PerCP) signal dot-plot and selection of positively stained cells

e. Percentages of cells in specified gates

Figure 4.6 demonstrates the post-sort evaluations of these sorted T cells.

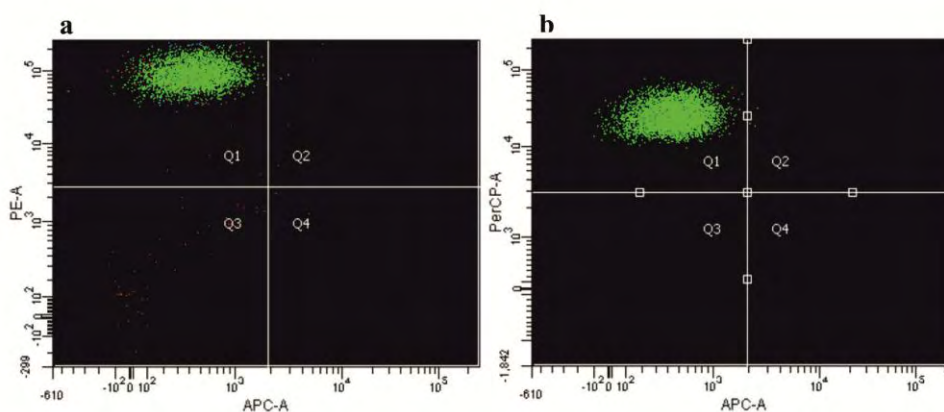


Figure 4.6. Post-sort evaluations.

a. CD4 (PE) staining of CD4⁺ cells

b. CD8 (PerCP) staining of CD8⁺ cells

4.5. Coculture Experiments

Settings for coculture experiments with either sorted CD4⁺ and CD8⁺ T cells or with splenocytes and PBMCs were explained in section 3.9.

4.6. Gene Expression Analyses (PCR)

DNA isolated from splenocytes cocultured with NFs and CAFs for 96 hours (at 37°C and 5 % CO₂ conditions) were used in order to investigate gene expression levels of CD25 and CD28 by real time RT-PCR technique.

Similarly, expression levels of TGF-β and IFN-γ genes in NF and CAF cells were assessed by real time RT-PCR. β-actin gene expression level was used as the internal standard for real time RT-PCR experiments. $2^{-\Delta\Delta Ct}$ method was used to analyze the results.

Real time RT-PCR results from splenocytes cocultured with NFs were used as the *baseline* and gene expression levels of splenocytes cocultured with CAFs were then compared to these values for the comparative calculations.

Expression levels of CD25 and CD28 genes in splenocytes cocultured with CAFs were shown to be not different. As the $2^{-\Delta\Delta C_t}$ values for CD25 and CD28 were calculated as 0.72 and 1.06, respectively; CAFs were concluded not to exert any significant effects on expressions of these genes in splenocytes.

Similarly, real time RT-PCR results from NF cells were used as the *baseline* and gene expression levels of CAF cells were then compared to these values for the comparative calculations.

CAFs were concluded not to significantly differ from NFs in respect to expressing TGF- β and IFN- γ , as the $2^{-\Delta\Delta C_t}$ values for these two genes were calculated as 1.3 and 1.1, respectively.

The gel electrophoresis images for CD25, CD28, TGF- β , IFN- γ and β -actin, which were investigated by the real time RT-PCR technique, are shown below (Figure 4.7-4.12).

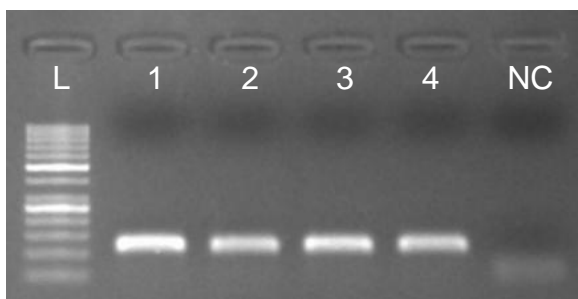


Figure 4.7. The gel electrophoresis image for the CD25 gene. (L: 50 bp DNA ladder (50-1000 bp), NC: Negative control, 1-4: Sample numbers)

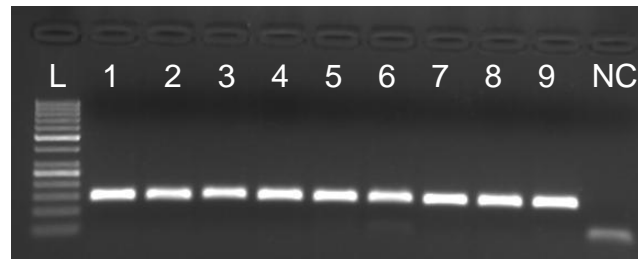


Figure 4.8. The gel electrophoresis image for the CD28 gene. (L: 50 bp DNA ladder (50-1000 bp), NC: Negative control, 1-9: Sample numbers)

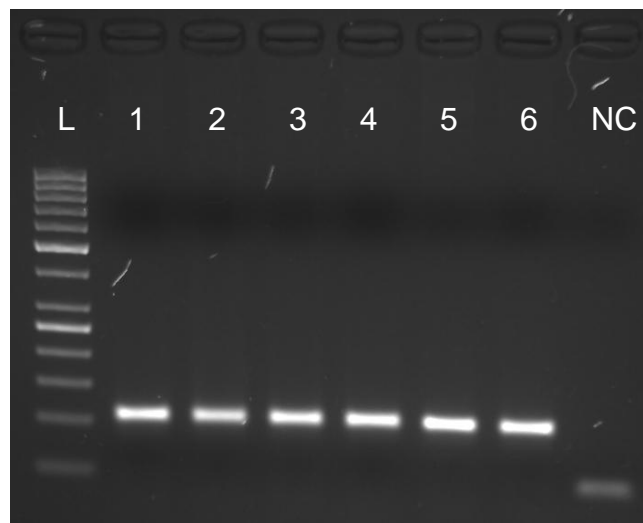


Figure 4.9. The gel electrophoresis image for the TGF- β gene. (L: 50 bp DNA ladder (50-1000 bp), NC: Negative control, 1-6: Sample numbers)

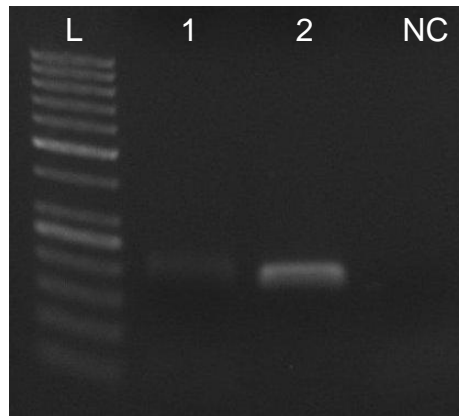


Figure 4.10. The gel electrophoresis image for the IFN- γ gene. (L: 50 bp DNA ladder (50-1000 bp), NC: Negative control, 1-2: Sample numbers)

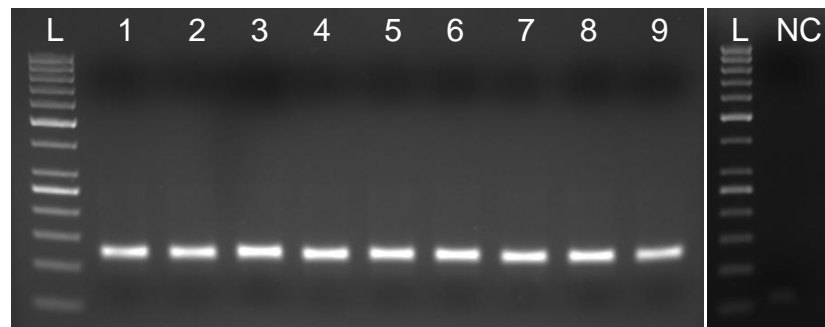


Figure 4.11. The gel electrophoresis image for the β -actin gene in splenocytes. (L: 50 bp DNA ladder (50-1000 bp), NC: Negative control, 1-9: Sample numbers)

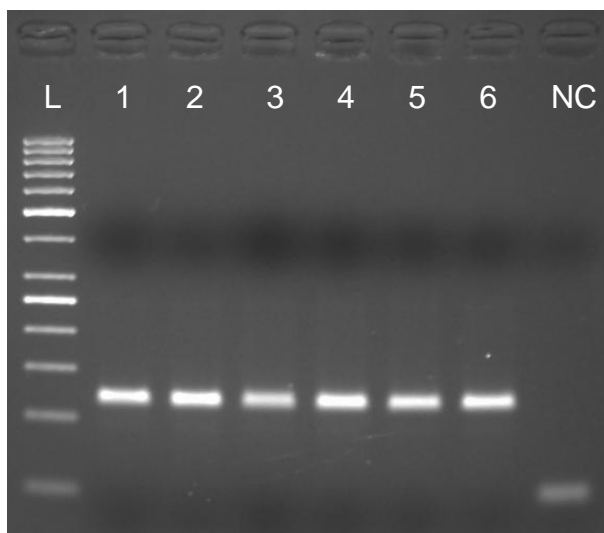


Figure 4.12. The gel electrophoresis image for the β -actin gene in CAFs and NFs. (L: 50 bp DNA ladder (50-1000 bp), NC: Negative control, 1-6: Sample numbers, CAF: Cancer Associated Fibroblast, NF: Normal Fibroblast)

4.7. Assessment of Cytokine Levels with Enzyme-Linked Immunosorbent Assays

Supernatants from two different coculture settings described in section 3.9 were collected and stored at -80°C for the cytokine assessments with ELISA. Supernatants of splenocyte-NF and splenocyte-CAF cocultures were collected at different time points and all these supernatants were later analyzed for IFN- γ and TGF- β levels.

According to the IFN- γ ELISA findings, there is not a statistically significant difference in terms of IFN- γ levels between supernatants from NF-splenocyte and CAF-splenocyte cocultures (Student's T Test, $p=0,15$) (Table 4.5, Figure 4.13).

IFN- γ	with 50.000 NF	with 50.000 CAF
Mean	157,309 pg/ml	158,478 pg/ml
Standard Error	0,47 pg/ml	0,624 pg/ml

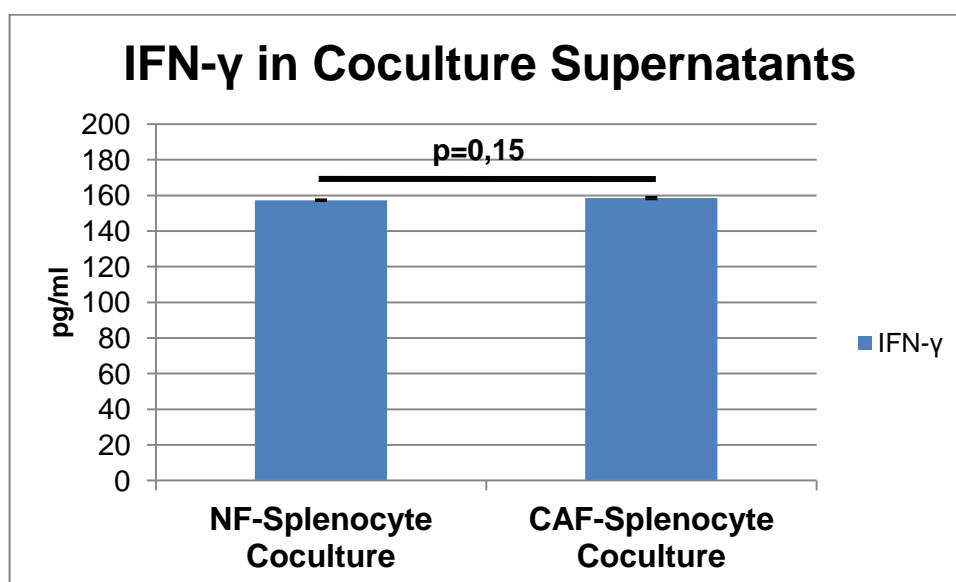


Table 4.5 and Figure 4.13. IFN- γ levels in supernatants from NF-splenocyte and CAF-splenocyte cocultures (mean and \pm standard error are shown). There is not a statistically significant difference between the two groups.

There is not a statistically significant difference in terms of TGF- β levels between supernatants from NF-splenocyte and CAF-splenocyte cocultures (Student's TTest, $p=0,99$) (Table 4.6, Figure 4.14).

TGF- β	with 50.000 NF	with 50.000 CAF
Mean	1291,64 pg/ml	1286,92 pg/ml
Standard Error	257,23 pg/ml	173,83 pg/ml

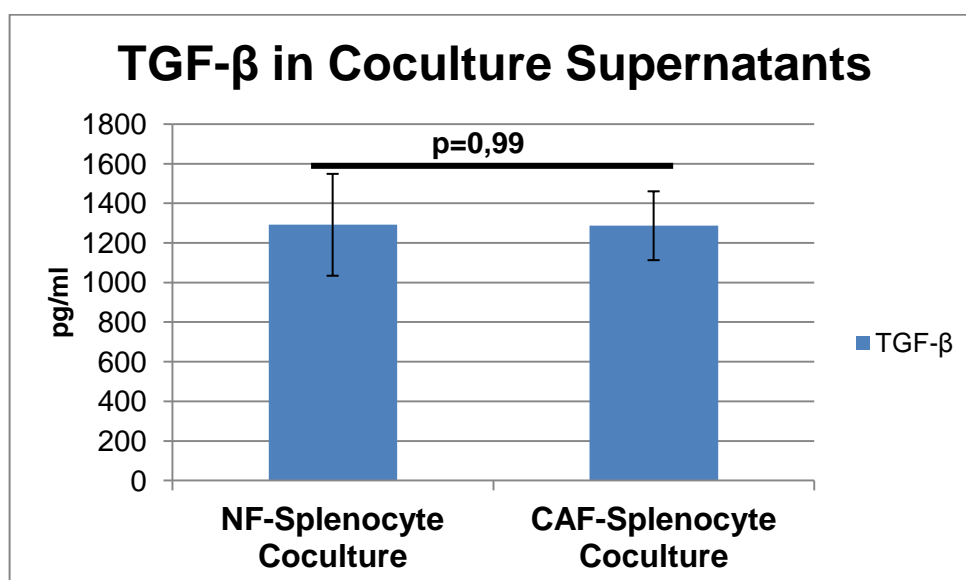


Table 4.6 and Figure 4.14. TGF- β levels in supernatants from NF-splenocyte and CAF-splenocyte cocultures (mean and \pm standard error are shown). There is not a statistically significant difference between the two groups.

4.8. Comet Assays

100 μ l of blood was drawn from the tail vein of each animal in four groups: 24 hours after the last one of 4-week of NMU injections (1) or 2 and 3 months after the last injection when the animals develop tumors (2, 3) and also the animals that were not injected with NMU (4). Standard assay procedure was followed.

According to the results, there were no significant differences in terms of DNA damage between the control group and the animals that had their last NMU injections 2 or 3 months before. On the other hand, the DNA damage was significantly high in the sample taken 24 hours after the NMU injection. Figure 4.15 shows the results of the negative control animal.

Figure 4.16 shows the results of the blood sample taken from an animal 24 hours after the last NMU injection. Figure 4.17 demonstrates the results of the blood sample taken from another animal 2 months after the last NMU injection

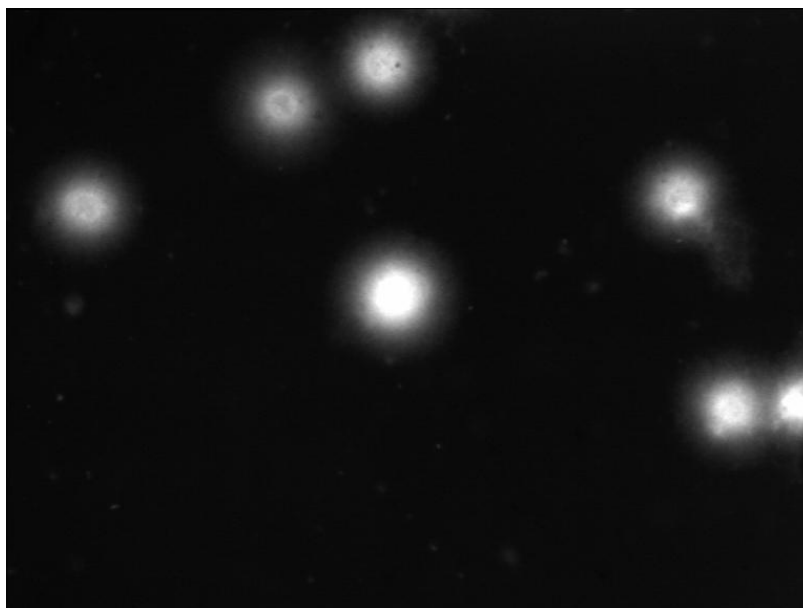


Figure 4.15. Results of the blood sample taken from the negative control animal.

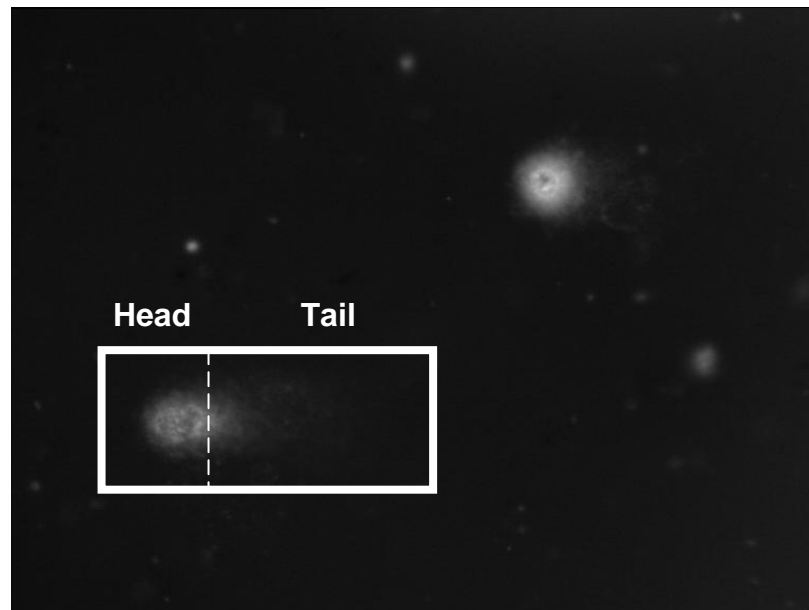


Figure 4.16. Results of the blood sample taken from an animal 24 hours after the last NMU injection.

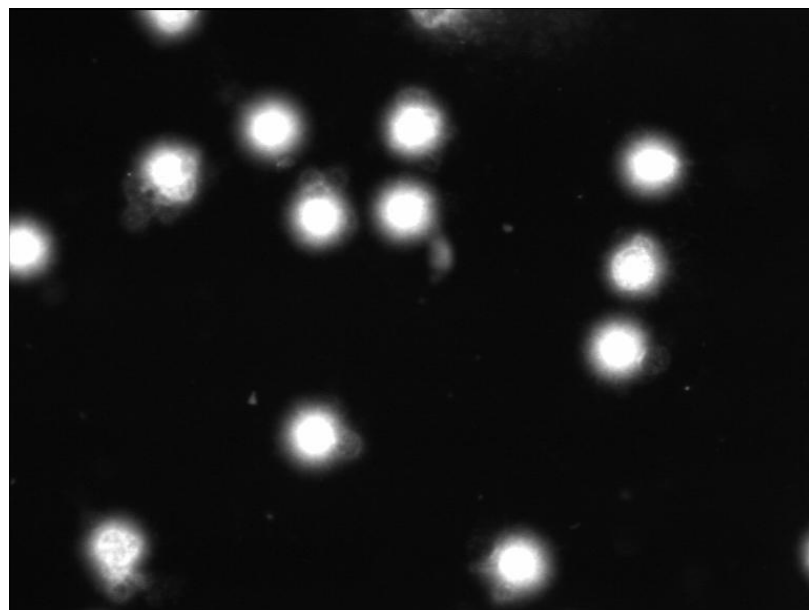


Figure 4.17. Results of the blood sample taken from another animal 2 months after the last NMU injection.

Tail lengths (Figure 4.18), tail migrations (Figure 4.19) and tail moments (Figure 4.20) were calculated for each of the four groups with the help of the software described in section 3.15.

According to the tail lengths in Figure 4.18, there were no significant differences in terms of tail length between the control group and the animals that had their last NMU injections 2 or 3 months before. However, the tail length was significantly higher in the sample taken 24 hours after the NMU injection than other groups. Similarly, tail migrations (demonstrated in Figure 4.19) and tail moments (demonstrated in Figure 4.20) were significantly high only in the sample taken 24 hours after the NMU injection, when compared to other groups.

When these findings were statistically evaluated, the control group and the animals that had their last NMU injections 2 or 3 months before were found to be similar in terms of DNA damage. As expected, DNA damage was found to be higher than other groups in the sample taken 24 hours after the NMU injection and this difference was statistically significant (Student's T test, $p < 0,05$). Figure 4.21 comparatively demonstrates all the results of four groups in a single graph. As a result, the DNA damaging effects of NMU were stronger in the first days that followed the injection. However, NMU induced systemic effects seem to return to control animal's levels 2-3 months after the last injection.

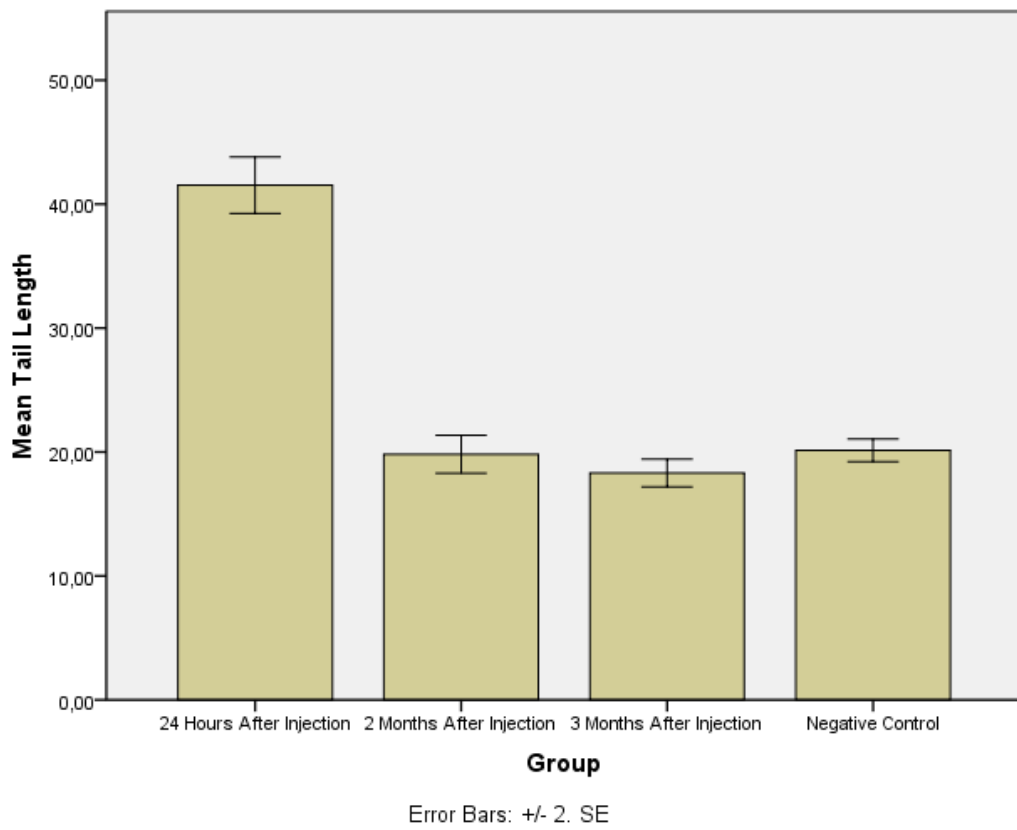


Figure 4.18. Tail length results of the blood samples taken from a control animal, from an animal 24 hours after the last NMU injection and from animals 2 and 3 months after the last NMU injections.

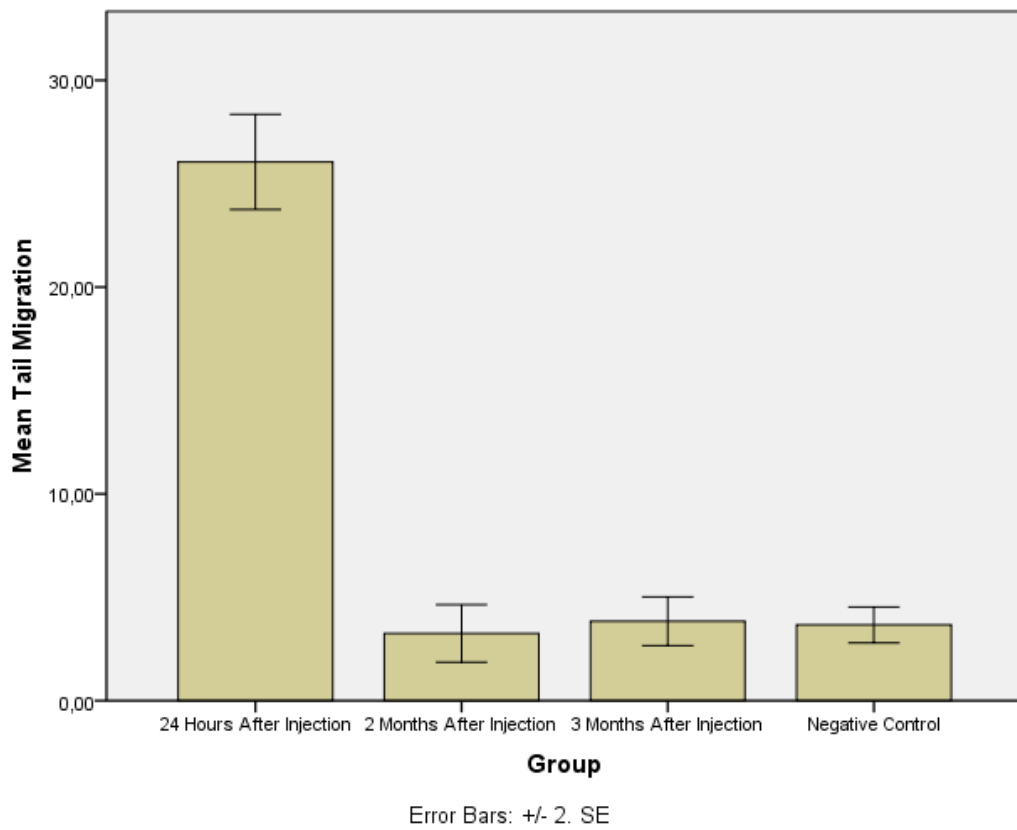


Figure 4.19. Tail migration results of the blood samples taken from a control animal, from an animal 24 hours after the last NMU injection and from animals 2 and 3 months after the last NMU injections.

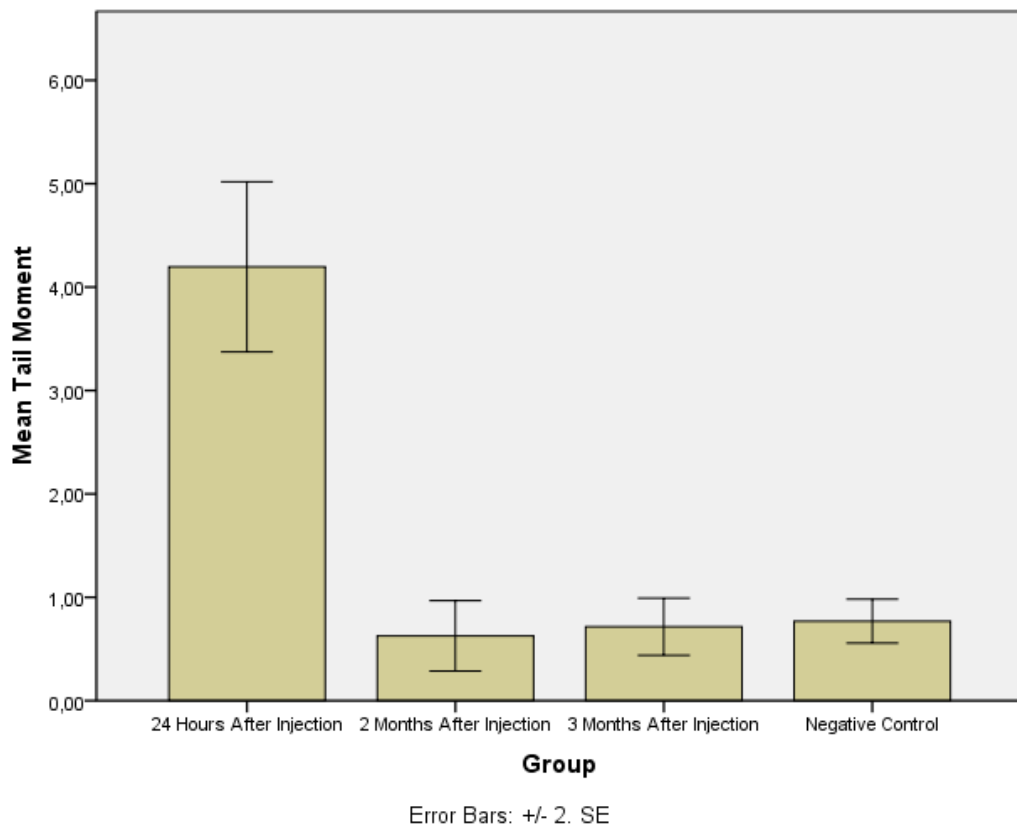


Figure 4.20. Tail moment results of the blood samples taken from a control animal, from an animal 24 hours after the last NMU injection and from animals 2 and 3 months after the last NMU injections.

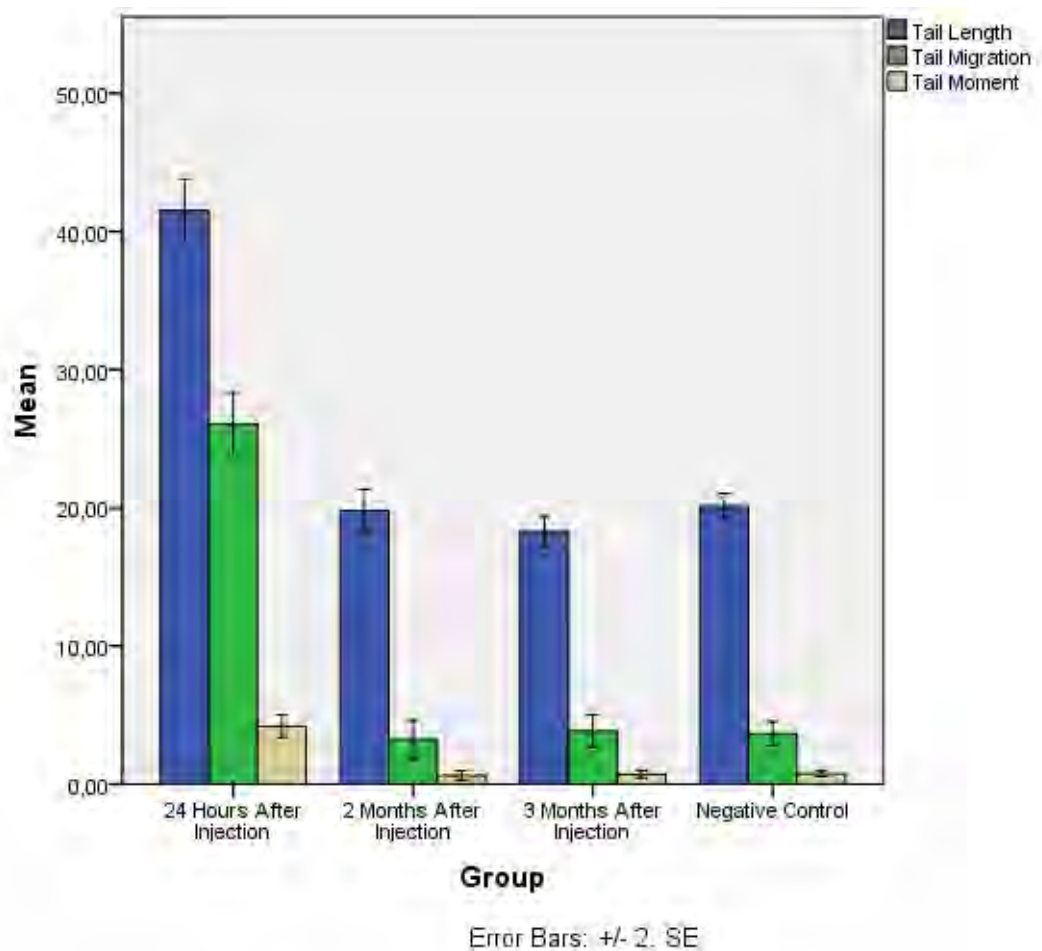


Figure 4.21. Comet Assay results of four animal groups.

4.9. Quality Control in Cell Cultures: Testing for Mycoplasma Contamination

3-monthly testing of all cell cultures for mycoplasma was introduced as a means of internal quality control program of the study. Mycoplasma presence was analyzed with Biological Industries EZ-PCR Mycoplasma Test Kit. The results of all of these experiments were negative and mycoplasma contamination was not detected. Figure 4.22 shows the result of one of these experiments.

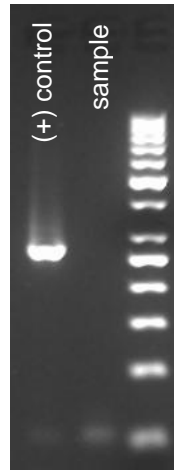


Figure 4.22. Mycoplasma contamination assessment.

5. DISCUSSION

The studies that have investigated the nature of the cells and molecules responsible for the functional insufficiency of the tumor infiltrating T cells usually focused on tumor cells themselves, tolerogenic dendritic cells and Tregs; however, the contribution of stromal cellular elements has not yet been well established. Fibroblasts are one of the most abundant cell types found in the stroma. Fibroblast cells turn into cancer associated fibroblasts (CAFs) and myofibroblasts in the tumor microenvironment. The scope of this study was to determine the role of cancer associated fibroblasts on the T cells.

For this reason, cancer associated fibroblasts were isolated from tumors generated by a rat chemical mammary carcinoma model. Then, these cells were cultured together with splenocytes.

The value of animal models in tumor immunology is priceless, since *in vivo* experiments simulate the diseases much better than *in vitro* counterparts. Many researchers are now abandoning the transplantation type tumor models, as they do not sufficiently represent the human tumors (184).

N-Nitroso-N-methylurea was reported to specifically and reproducibly induce a high incidence of breast carcinomas after a single intravenous or intraperitoneal dose (187). Periodical i.p. injections of NMU result in mammary adenocarcinomas with a high incidence in female Sprague-Dawley rats (189, 193, 194). In addition, NMU induced mammary tumors

have similar histopathological lesions with their human counterparts (189). Finally, NMU induced mammary adenocarcinomas simulate human breast cancer histopathology better than similar models utilized in mice (9-11). Since increasing the frequency and dose of carcinogen injections results in a decreased latent period for tumor formation (204), we utilized periodical four NMU injections for our experiments.

Immature Sprague Dawley rats are more sensitive to carcinogenic effects of NMU than multiparous ones, as the differentiation of mammary terminal end buds prevents cells from transformation (189, 207, 208). Therefore, we started the NMU injections when the animals were exactly 21 days old. Similar to the reports in the literature, NMU induced tumors reliably and organ site specific in our studies (189, 239).

As mentioned previously, only one animal out of a total of 20 NMU injected rats died due to the injections before it could be used in the experiments and other NMU injections for our rat chemical mammary carcinogenesis model resulted in tumor formations in rats in a consistent manner. Such a high tumor formation rate in the carcinogen injected animals seems to be satisfactory and demonstrated that our model proved to be successful. Previous studies in the literature also reported similar results that this NMU induced chemical carcinogenesis model induces mammary adenocarcinomas in female Sprague-Dawley rats at a high incidence (189, 193).

After the tumor bearing animals were sacrificed, their tumor tissues were isolated and used for CAF isolations. Even though normal fibroblast isolations from mammary tissues of healthy rats turned out to be successful, there have been difficulties in isolating CAFs from tumors.

In fact, such difficulties in isolating the CAFs were similar to previous findings in the literature that underline the problems in obtaining pure cell populations. CAF researches have usually been challenging; since CAF-specific markers are lacking and fibroblast cells can exhibit great heterogeneities (51). Sharon et al. used PDGFR- α as a surface marker to

isolate fibroblasts from tissues (240). However, this molecule is expressed by both NFs and CAFs (241, 242). Therefore, their approach results in isolation of both NFs and CAFs.

The difficulties in even specifically characterizing the CAFs make it much harder to isolate fibroblast cells from the tumor tissue. Due to the fact that these cells express varying amounts of different surface markers, Sugimoto et al. suggested that Cancer Associated Fibroblast definition actually describes a heterogeneous cell population (51).

The enzymatic method with collagenase I and hyaluronidase; described by Orimo et al. (57), was used in our experiments.

CAF definition indeed signifies a heterogeneous cell population. Therefore, immunocytochemistry studies were performed in order to characterize fibroblast and CAF cells. For this purpose, various studies in the literature suggest markers like collagen I; however, surface marker expression profiles of fibroblasts differ greatly. This phenomenon might actually be due to this vague CAF definition. Some researchers simply define CAFs as activated fibroblasts found specifically in the tumor microenvironment (4), whereas others accept the definition “cells that surround cancer epithelia”. On the other hand, Kalluri and Zeisberg suggested that CAFs are fibroblasts that have ability to promote tumorigenesis (43).

CAFs are similar to myofibroblasts in terms of expressing ED-A fibronectin, as “tumors are wounds that do not heal” (48).

Orimo et al. proposed a dissenting opinion that CAFs are stromal fibroblast populations that are present within tumors and these CAFs include populations of both myofibroblasts and fibroblasts (37).

Even normal fibroblasts from different locations in the body are considered distinct cell types based on their differential gene expression profiles (81). Anatomical location of the fibroblast cells can affect gene

expressions. There also exists a huge debate about the activation makers in stromal fibroblasts of solid tumors. Various reports suggested FSP and PDGF receptor- β as such markers (43, 50).

Sugimoto et al. also reported a unique FSP1 expressing CAF subpopulation (51). We think these FSP1 expressing CAF cells should be further investigated.

T cell sortings were performed successfully from healthy control animals. However, the stimulation of proliferation in such highly pure sorted T cell populations could not be achieved. Therefore, splenocytes isolated from healthy rats were utilized in coculture studies with NFs or CAFs. Furthermore, it was reported that autologous and allogeneic T lymphocytes are not activated in such cocultures (243). This finding paved the way for using these allogeneic coculture systems for our experiments. After the T and CAF cells were successfully isolated separately, the interactions of these two cell types could then be investigated in detail.

The results of real time RT-PCR experiments showed that there were not any changes in expression levels of CD25 and CD28 genes in splenocytes that were cocultured with CAFs. CAFs were concluded not to exert any significant effects on expressions of CD25 and CD28 genes in splenocytes (according to the real-time RT-PCR results).

Tumor associated fibroblasts were reported to secrete Interferon- γ (IFN- γ) and Transforming Growth Factor- β 1 (TGF- β 1). However, in our experiments CAFs were concluded not to significantly differ from NFs in respect to expressing TGF- β and IFN- γ (as the $2^{-\Delta\Delta Ct}$ values for these two genes were calculated as 1.3 and 1.1, respectively).

In order to investigate whether the gene expression levels are also represented in terms of protein levels, we assessed the coculture

supernatants for soluble IFN- γ and TGF- β . According to the results of ELISA studies, coculturing splenocytes with CAFs did not significantly affect IFN- γ levels in the supernatants ($p=0,155$).

A significant difference was not seen in soluble IFN- γ levels in the supernatants with ELISA studies. As a matter of fact, there was no significant difference in terms of IFN- γ gene expression levels between NF and CAF cells themselves according to the real time RT-PCR results. Briefly, 1-CAF were concluded not to significantly differ from NFs in respect to expressing TGF- β and IFN- γ . 2- There is not a statistically significant difference in terms of IFN- γ levels between supernatants from NF-splenocyte and CAF-splenocyte cocultures.

There is not a statistically significant difference in terms of TGF- β levels between supernatants from NF-splenocyte and CAF-splenocyte cocultures.

According to our TGF- β ELISA findings, there is not a statistically significant difference in terms of TGF- β levels between supernatants from NF-splenocyte and CAF-splenocyte cocultures. In fact, this finding was similar to our gene expression level results, where CAFs were found not to significantly differ from NFs in terms of TGF- β gene expression. Therefore, there is not a significant difference in both TGF- β gene and protein levels in either the cells or in the supernatants.

NMU shows suppressive effects on host immune system. NMU causes marked genotoxicity on proliferating lymphocytes, followed by increased apoptotic death (205). Furthermore, the toxic effects of NMU on spleen and bone marrow might continue about three more weeks after the injection (206). Therefore, making certain that the animals were not under such effects of NMU at the time of coculture experiments was a matter of utmost concern. For this reason, the residual effects of NMU were assessed by Comet Assays.

Comet assay was reported to be safer and more specific in terms of false positive results than other genotoxicity assays in the literature (244). Thus, probable DNA breaks due to NMU were assessed by the Comet assays. The results demonstrated that the effects of NMU injections are much more prominent at the short period of time following the injection. The systemic alterations in animals due to NMU normalize and return to the control animal state about 2-3 months after the last injection. Since the sacrifices and tumor excisions were performed 2-3 months after the last injection, it can be assumed that there were no confounding effects due to NMU at the time of experiments.

6. RESULTS AND RECOMMENDATIONS

- 21 days old female Sprague Dawley out-bred rats were used for the mammary carcinoma model experiments. All of the animals that were injected weekly with 50 mg/kg NMU i.p. developed at least one palpable breast tumor after a period of 1-2 months.
- NFs were obtained from healthy mammary tissues of control female Sprague Dawley rats. CAFs were obtained from mammary carcinomas.
- All of the NF isolation experiments with enzymatic digestion with Collagenase I and Hyaluronidase from mammary tissues of healthy female rats resulted in successful outcomes in our trials. These isolated NFs were cultured and successful primary cell cultures were obtained.
- Similar successful results could not be achieved when this technique was utilized on breast tumor tissues.
- Immunocytochemistry showed that both NFs and CAFs were not stained at the "*negative control*". An epithelial cell marker, "*pancytokeratin*", did not stain either of these cell types. Furthermore, "*desmin*", a muscle tissue marker did not stain either of these cell types.
- CD4⁺ T cell and CD8⁺ T cell populations were obtained by FACS with the use of proper fluorescent dye-tagged specific anti-rat CD3, CD4 and CD8 antibodies.
- Splenocytes were cocultured with CAFs and NFs.

- Expression levels of CD25 and CD28 genes in splenocytes cocultured with CAFs (compared to splenocytes cocultured with NFs) were shown not to change.
- There were no significant differences in terms of DNA damage between the control group and the animals that had their last NMU injections 2 or 3 months before. On the other hand, the DNA damage was significantly high in the sample taken 24 hours after the NMU injection.
- Cancer associated fibroblasts might be utilized as potential targets for cancer immunotherapy.

REFERENCES

1. American Cancer Society, *Cancer Facts & Figures 2012*.
2. American Cancer Society, *Breast Cancer Facts & Figures 2011-2012*.
3. Pietras, K. and A. Ostman, *Hallmarks of cancer: interactions with the tumor stroma*. *Exp Cell Res*, 2010. **316**(8): p. 1324-31.
4. Barsky, S.H., et al., *Desmoplastic breast carcinoma as a source of human myofibroblasts*. *Am J Pathol*, 1984. **115**(3): p. 329-33.
5. Ostman, A. and M. Augsten, *Cancer-associated fibroblasts and tumor growth--bystanders turning into key players*. *Curr Opin Genet Dev*, 2009. **19**(1): p. 67-73.
6. Gonda, T.A., et al., *Molecular biology of cancer-associated fibroblasts: can these cells be targeted in anti-cancer therapy?* *Semin Cell Dev Biol*, 2010. **21**(1): p. 2-10.
7. Rama, D., *Fibroblast-breast cancer cells' interaction and chemerin expression*, in *Department of Basic Oncology*. 2011, Hacettepe University Ankara. p. 156.
8. Esendagli, G., *The rat as a host to investigate tumor immunology*, in *The Rat in Cancer Research: A Crucial Tool for all Aspects of Translational Studies*, D.L. Pouliquen, Editor. 2012, Research Signpost: Kerala, India. p. 59-85.
9. Esendagli, G., et al., *Primary tumor cells obtained from MNU-induced mammary carcinomas show immune heterogeneity which can be*

- modulated by low-efficiency transfection of CD40L gene. Cancer Biol Ther, 2009. 8(2): p. 136-42.*
10. Esendagli, G., et al., *Coexistence of different tissue tumourigenesis in an N-methyl-N-nitrosourea-induced mammary carcinoma model: a histopathological report in Sprague-Dawley rats. Lab Anim, 2009. 43(1): p. 60-4.*
 11. Fahmi, T., et al., *Immune compartmentalization of T cell subsets in chemically-induced breast cancer. Scand J Immunol, 2010. 72(4): p. 339-48.*
 12. Wiseman, B.S. and Z. Werb, *Stromal effects on mammary gland development and breast cancer. Science, 2002. 296(5570): p. 1046-9.*
 13. Ross, M.H. and W. Pawlina, *Histology: A Text and Atlas (Histology. Sixth, North American Edition, With Correlated Cell and Molecular Biology ed. 2010: Lippincott Williams & Wilkins. 928.*
 14. Arendt, L.M., et al., *Stroma in breast development and disease. Semin Cell Dev Biol, 2010. 21(1): p. 11-8.*
 15. Watson, C.J. and W.T. Khaled, *Mammary development in the embryo and adult: a journey of morphogenesis and commitment. Development, 2008. 135(6): p. 995-1003.*
 16. Kimata, K., et al., *Participation of two different mesenchymes in the developing mouse mammary gland: synthesis of basement membrane components by fat pad precursor cells. J Embryol Exp Morphol, 1985. 89: p. 243-57.*
 17. Dienstmann, R. and J. Bines, *Evidence-based neoadjuvant endocrine therapy for breast cancer. Clin Breast Cancer, 2006. 7(4): p. 315-20.*

18. Longo, R., F. Torino, and G. Gasparini, *Targeted therapy of breast cancer*. *Curr Pharm Des*, 2007. **13**(5): p. 497-517.
19. Kumar, V., R.S. Cotran, and S.L. Robbins, *Robbins basic pathology*. 7th ed. 2003, Philadelphia, PA: Saunders. xii, 873 p.
20. Kumar, V., et al., *Robbins and Cotran pathologic basis of disease*. 7th ed. 2005, Philadelphia: Elsevier/Saunders. xv, 1525 p.
21. Hanahan, D. and R.A. Weinberg, *The hallmarks of cancer*. *Cell*, 2000. **100**(1): p. 57-70.
22. Mueller, M.M. and N.E. Fusenig, *Friends or foes - bipolar effects of the tumour stroma in cancer*. *Nat Rev Cancer*, 2004. **4**(11): p. 839-49.
23. Stephen, P., *THE DISTRIBUTION OF SECONDARY GROWTHS IN CANCER OF THE BREAST*. *The Lancet*, 1889. **133**(3421): p. 571-573.
24. Liotta, L.A. and E.C. Kohn, *The microenvironment of the tumour-host interface*. *Nature*, 2001. **411**(6835): p. 375-9.
25. Schauer, I.G., et al., *Cancer-associated fibroblasts and their putative role in potentiating the initiation and development of epithelial ovarian cancer*. *Neoplasia*, 2011. **13**(5): p. 393-405.
26. Folkman, J., *Angiogenesis in cancer, vascular, rheumatoid and other disease*. *Nat Med*, 1995. **1**(1): p. 27-31.
27. Bergers, G. and L.E. Benjamin, *Tumorigenesis and the angiogenic switch*. *Nat Rev Cancer*, 2003. **3**(6): p. 401-10.
28. Coussens, L.M. and Z. Werb, *Inflammation and cancer*. *Nature*, 2002. **420**(6917): p. 860-7.

29. Theret, N., et al., *Increased extracellular matrix remodeling is associated with tumor progression in human hepatocellular carcinomas*. Hepatology, 2001. **34**(1): p. 82-8.
30. DeCosse, J.J., et al., *Breast cancer: induction of differentiation by embryonic tissue*. Science, 1973. **181**(4104): p. 1057-8.
31. DeCosse, J.J., et al., *Embryonic inductive tissues that cause histologic differentiation of murine mammary carcinoma in vitro*. J Natl Cancer Inst, 1975. **54**(4): p. 913-22.
32. Polyak, K. and R. Kalluri, *The role of the microenvironment in mammary gland development and cancer*. Cold Spring Harb Perspect Biol, 2010. **2**(11): p. a003244.
33. Allinen, M., et al., *Molecular characterization of the tumor microenvironment in breast cancer*. Cancer Cell, 2004. **6**(1): p. 17-32.
34. Ma, X.J., et al., *Gene expression profiling of the tumor microenvironment during breast cancer progression*. Breast Cancer Res, 2009. **11**(1): p. R7.
35. Joyce, J.A. and J.W. Pollard, *Microenvironmental regulation of metastasis*. Nat Rev Cancer, 2009. **9**(4): p. 239-52.
36. Strutz, F., et al., *Identification and characterization of a fibroblast marker: FSP1*. J Cell Biol, 1995. **130**(2): p. 393-405.
37. Orimo, A. and R.A. Weinberg, *Heterogeneity of stromal fibroblasts in tumors*. Cancer Biol Ther, 2007. **6**(4): p. 618-9.
38. Rodemann, H.P. and G.A. Muller, *Characterization of human renal fibroblasts in health and disease: II. In vitro growth, differentiation, and collagen synthesis of fibroblasts from kidneys with interstitial fibrosis*. Am J Kidney Dis, 1991. **17**(6): p. 684-6.

39. Parsonage, G., et al., *A stromal address code defined by fibroblasts*. Trends Immunol, 2005. **26**(3): p. 150-6.
40. Simian, M., et al., *The interplay of matrix metalloproteinases, morphogens and growth factors is necessary for branching of mammary epithelial cells*. Development, 2001. **128**(16): p. 3117-31.
41. U.S. National Library of Medicine. *Fibroblast*. 2013 2013/04/29/ 2013/05/07/11:14:00; Available from:
<http://ghr.nlm.nih.gov/glossary=fibroblast>.
42. Castor, C.W., et al., *Activation of lung connective tissue cells in vitro*. Am Rev Respir Dis, 1979. **120**(1): p. 101-6.
43. Kalluri, R. and M. Zeisberg, *Fibroblasts in cancer*. Nat Rev Cancer, 2006. **6**(5): p. 392-401.
44. Sappino, A.P., et al., *Smooth-muscle differentiation in stromal cells of malignant and non-malignant breast tissues*. Int J Cancer, 1988. **41**(5): p. 707-12.
45. Gabbiani, G., G.B. Ryan, and G. Majne, *Presence of modified fibroblasts in granulation tissue and their possible role in wound contraction*. Experientia, 1971. **27**(5): p. 549-50.
46. Desmouliere, A., et al., *Apoptosis mediates the decrease in cellularity during the transition between granulation tissue and scar*. Am J Pathol, 1995. **146**(1): p. 56-66.
47. Rasanen, K. and A. Vaheri, *Activation of fibroblasts in cancer stroma*. Exp Cell Res, 2010. **316**(17): p. 2713-22.
48. Dvorak, H.F., *Tumors: wounds that do not heal. Similarities between tumor stroma generation and wound healing*. N Engl J Med, 1986. **315**(26): p. 1650-9.

49. Cirri, P. and P. Chiarugi, *Cancer associated fibroblasts: the dark side of the coin*. Am J Cancer Res, 2011. **1**(4): p. 482-97.
50. Micke, P. and A. Ostman, *Tumour-stroma interaction: cancer-associated fibroblasts as novel targets in anti-cancer therapy?* Lung Cancer, 2004. **45 Suppl 2**: p. S163-75.
51. Sugimoto, H., et al., *Identification of fibroblast heterogeneity in the tumor microenvironment*. Cancer Biol Ther, 2006. **5**(12): p. 1640-6.
52. Giannoni, E., et al., *Reciprocal activation of prostate cancer cells and cancer-associated fibroblasts stimulates epithelial-mesenchymal transition and cancer stemness*. Cancer Res, 2010. **70**(17): p. 6945-56.
53. De Wever, O. and M. Mareel, *Role of tissue stroma in cancer cell invasion*. J Pathol, 2003. **200**(4): p. 429-47.
54. Lohr, M., et al., *Transforming growth factor-beta1 induces desmoplasia in an experimental model of human pancreatic carcinoma*. Cancer Res, 2001. **61**(2): p. 550-5.
55. Dimanche-Boitrel, M.T., et al., *In vivo and in vitro invasiveness of a rat colon-cancer cell line maintaining E-cadherin expression: an enhancing role of tumor-associated myofibroblasts*. Int J Cancer, 1994. **56**(4): p. 512-21.
56. Gaggioli, C., et al., *Fibroblast-led collective invasion of carcinoma cells with differing roles for RhoGTPases in leading and following cells*. Nat Cell Biol, 2007. **9**(12): p. 1392-400.
57. Orimo, A., et al., *Stromal fibroblasts present in invasive human breast carcinomas promote tumor growth and angiogenesis through elevated SDF-1/CXCL12 secretion*. Cell, 2005. **121**(3): p. 335-48.

58. Ambrosino, E., J.A. Berzofsky, and M. Terabe, *Regulation of tumor immunity: the role of NKT cells*. *Expert Opin Biol Ther*, 2008. **8**(6): p. 725-34.
59. Berezhnaya, N.M., *Interaction between tumor and immune system: the role of tumor cell biology*. *Exp Oncol*, 2010. **32**(3): p. 159-66.
60. Singer, K., et al., *Suppression of T-cell responses by tumor metabolites*. *Cancer Immunol Immunother*, 2011. **60**(3): p. 425-31.
61. Kandulski, A., P. Malfertheiner, and T. Wex, *Role of regulatory T-cells in H. pylori-induced gastritis and gastric cancer*. *Anticancer Res*, 2010. **30**(4): p. 1093-103.
62. Hamai, A., et al., *Immune surveillance of human cancer: if the cytotoxic T-lymphocytes play the music, does the tumoral system call the tune?* *Tissue Antigens*, 2010. **75**(1): p. 1-8.
63. Barnas, J.L., et al., *T cells and stromal fibroblasts in human tumor microenvironments represent potential therapeutic targets*. *Cancer Microenviron*, 2010. **3**(1): p. 29-47.
64. Bagloli, C.J., et al., *More than structural cells, fibroblasts create and orchestrate the tumor microenvironment*. *Immunol Invest*, 2006. **35**(3-4): p. 297-325.
65. Hinz, B., et al., *The myofibroblast: one function, multiple origins*. *Am J Pathol*, 2007. **170**(6): p. 1807-16.
66. Sturm, A., et al., *Dual function of the extracellular matrix: stimulatory for cell cycle progression of naive T cells and antiapoptotic for tissue-derived memory T cells*. *J Immunol*, 2004. **173**(6): p. 3889-900.
67. Davis, L.S., et al., *Fibronectin promotes proliferation of naive and memory T cells by signaling through both the VLA-4 and VLA-5 integrin molecules*. *J Immunol*, 1990. **145**(3): p. 785-93.

68. Gallagher, P.G., et al., *Gene expression profiling reveals cross-talk between melanoma and fibroblasts: implications for host-tumor interactions in metastasis*. *Cancer Res*, 2005. **65**(10): p. 4134-46.
69. Buess, M., et al., *Characterization of heterotypic interaction effects in vitro to deconvolute global gene expression profiles in cancer*. *Genome Biol*, 2007. **8**(9): p. R191.
70. Denk, P.O., et al., *Effect of growth factors on the activation of human Tenon's capsule fibroblasts*. *Curr Eye Res*, 2003. **27**(1): p. 35-44.
71. Ronnov-Jessen, L. and O.W. Petersen, *Induction of alpha-smooth muscle actin by transforming growth factor-beta 1 in quiescent human breast gland fibroblasts. Implications for myofibroblast generation in breast neoplasia*. *Lab Invest*, 1993. **68**(6): p. 696-707.
72. Toullec, A., et al., *Oxidative stress promotes myofibroblast differentiation and tumour spreading*. *EMBO Mol Med*, 2010. **2**(6): p. 211-30.
73. Bergfeld, S.A. and Y.A. DeClerck, *Bone marrow-derived mesenchymal stem cells and the tumor microenvironment*. *Cancer Metastasis Rev*, 2010. **29**(2): p. 249-61.
74. Dominici, M., et al., *Minimal criteria for defining multipotent mesenchymal stromal cells. The International Society for Cellular Therapy position statement*. *Cytotherapy*, 2006. **8**(4): p. 315-7.
75. Radisky, D.C., P.A. Kenny, and M.J. Bissell, *Fibrosis and cancer: do myofibroblasts come also from epithelial cells via EMT?* *J Cell Biochem*, 2007. **101**(4): p. 830-9.
76. Radisky, D.C., et al., *Rac1b and reactive oxygen species mediate MMP-3-induced EMT and genomic instability*. *Nature*, 2005. **436**(7047): p. 123-7.

77. Kalluri, R. and R.A. Weinberg, *The basics of epithelial-mesenchymal transition*. J Clin Invest, 2009. **119**(6): p. 1420-8.
78. Medici, D., E.D. Hay, and B.R. Olsen, *Snail and Slug promote epithelial-mesenchymal transition through beta-catenin-T-cell factor-4-dependent expression of transforming growth factor-beta3*. Mol Biol Cell, 2008. **19**(11): p. 4875-87.
79. Stockinger, A., et al., *E-cadherin regulates cell growth by modulating proliferation-dependent beta-catenin transcriptional activity*. J Cell Biol, 2001. **154**(6): p. 1185-96.
80. Zeisberg, E.M., et al., *Discovery of endothelial to mesenchymal transition as a source for carcinoma-associated fibroblasts*. Cancer Res, 2007. **67**(21): p. 10123-8.
81. Chang, H.Y., et al., *Diversity, topographic differentiation, and positional memory in human fibroblasts*. Proc Natl Acad Sci U S A, 2002. **99**(20): p. 12877-82.
82. McNulty, R.J., *Fibroblasts and myofibroblasts: their source, function and role in disease*. Int J Biochem Cell Biol, 2007. **39**(4): p. 666-71.
83. Anderberg, C. and K. Pietras, *On the origin of cancer-associated fibroblasts*. Cell Cycle, 2009. **8**(10): p. 1461-2.
84. Moser, M. and O. Leo, *Key concepts in immunology*. Vaccine, 2010. **28 Suppl 3**: p. C2-13.
85. Murphy, K.P., et al., *Janeway's immunobiology*. 7th ed. 2008, New York: Garland Science. xxi, 887 p.
86. Hoebe, K., E. Janssen, and B. Beutler, *The interface between innate and adaptive immunity*. Nat Immunol, 2004. **5**(10): p. 971-4.

87. Pluddemann, A., S. Mukhopadhyay, and S. Gordon, *Innate immunity to intracellular pathogens: macrophage receptors and responses to microbial entry*. Immunol Rev, 2011. **240**(1): p. 11-24.
88. Abbas, A.K., A.H. Lichtman, and S. Pillai, *Cellular and molecular immunology*. Updated 6th ed. 2010, Philadelphia: Saunders/Elsevier. viii, 566 p.
89. Bonilla, F.A. and H.C. Oettgen, *Adaptive immunity*. J Allergy Clin Immunol, 2010. **125**(2 Suppl 2): p. S33-40.
90. Ueno, H., et al., *Dendritic cells and humoral immunity in humans*. Immunol Cell Biol, 2010. **88**(4): p. 376-80.
91. Amanna, I.J. and M.K. Slifka, *Contributions of humoral and cellular immunity to vaccine-induced protection in humans*. Virology, 2011. **411**(2): p. 206-15.
92. Boehm, T., *Design principles of adaptive immune systems*. Nat Rev Immunol, 2011. **11**(5): p. 307-17.
93. Kindt, T.J., et al., *Kuby immunology*. 2007: W.H. Freeman.
94. Rocha, N. and J. Neefjes, *MHC class II molecules on the move for successful antigen presentation*. EMBO J, 2008. **27**(1): p. 1-5.
95. Wucherpfennig, K.W., et al., *Structural biology of the T-cell receptor: insights into receptor assembly, ligand recognition, and initiation of signaling*. Cold Spring Harb Perspect Biol, 2010. **2**(4): p. a005140.
96. van der Merwe, P.A. and O. Dushek, *Mechanisms for T cell receptor triggering*. Nat Rev Immunol, 2011. **11**(1): p. 47-55.
97. Jensen, P.E., *Recent advances in antigen processing and presentation*. Nat Immunol, 2007. **8**(10): p. 1041-8.

98. Hansen, T.H. and M. Bouvier, *MHC class I antigen presentation: learning from viral evasion strategies*. Nat Rev Immunol, 2009. **9**(7): p. 503-13.
99. Bluestone, J.A., et al., *The functional plasticity of T cell subsets*. Nat Rev Immunol, 2009. **9**(11): p. 811-6.
100. Hirota, K., et al., *Fate mapping of IL-17-producing T cells in inflammatory responses*. Nat Immunol, 2011. **12**(3): p. 255-63.
101. Eyerich, S., et al., *Th22 cells represent a distinct human T cell subset involved in epidermal immunity and remodeling*. J Clin Invest, 2009. **119**(12): p. 3573-85.
102. Chang, H.C., et al., *The transcription factor PU.1 is required for the development of IL-9-producing T cells and allergic inflammation*. Nat Immunol, 2010. **11**(6): p. 527-34.
103. Akdis, M., et al., *Interleukins, from 1 to 37, and interferon-gamma: receptors, functions, and roles in diseases*. J Allergy Clin Immunol, 2011. **127**(3): p. 701-21 e1-70.
104. Vesely, M.D., et al., *Natural innate and adaptive immunity to cancer*. Annu Rev Immunol, 2011. **29**: p. 235-71.
105. Whiteside, T.L., *Immune responses to malignancies*. J Allergy Clin Immunol, 2010. **125**(2 Suppl 2): p. S272-83.
106. Yaneva, R., et al., *Peptide binding to MHC class I and II proteins: new avenues from new methods*. Mol Immunol, 2010. **47**(4): p. 649-57.
107. Finn, O.J., *Cancer immunology*. N Engl J Med, 2008. **358**(25): p. 2704-15.

108. de Visser, K.E., A. Eichten, and L.M. Coussens, *Paradoxical roles of the immune system during cancer development*. Nat Rev Cancer, 2006. **6**(1): p. 24-37.
109. Higgins, J.P., M.B. Bernstein, and J.W. Hodge, *Enhancing immune responses to tumor-associated antigens*. Cancer Biol Ther, 2009. **8**(15): p. 1440-9.
110. Buonaguro, L., et al., *Translating tumor antigens into cancer vaccines*. Clin Vaccine Immunol, 2011. **18**(1): p. 23-34.
111. Schreiber, R.D., L.J. Old, and M.J. Smyth, *Cancer immunoediting: integrating immunity's roles in cancer suppression and promotion*. Science, 2011. **331**(6024): p. 1565-70.
112. Dunn, G.P., L.J. Old, and R.D. Schreiber, *The three Es of cancer immunoediting*. Annu Rev Immunol, 2004. **22**: p. 329-60.
113. Rabinovich, G.A., D. Gabrilovich, and E.M. Sotomayor, *Immunosuppressive strategies that are mediated by tumor cells*. Annu Rev Immunol, 2007. **25**: p. 267-96.
114. Stagg, J. and M.J. Smyth, *NK cell-based cancer immunotherapy*. Drug News Perspect, 2007. **20**(3): p. 155-63.
115. Srivastava, S., A. Lundqvist, and R.W. Childs, *Natural killer cell immunotherapy for cancer: a new hope*. Cytotherapy, 2008. **10**(8): p. 775-83.
116. Sica, A., *Role of tumour-associated macrophages in cancer-related inflammation*. Exp Oncol, 2010. **32**(3): p. 153-8.
117. Mantovani, A. and A. Sica, *Macrophages, innate immunity and cancer: balance, tolerance, and diversity*. Curr Opin Immunol, 2010. **22**(2): p. 231-7.

118. Agrawal, S., et al., *CD3 hyporesponsiveness and in vitro apoptosis are features of T cells from both malignant and nonmalignant secondary lymphoid organs*. J Clin Invest, 1998. **102**(9): p. 1715-23.
119. Radoja, S., et al., *CD8(+) tumor-infiltrating T cells are deficient in perforin-mediated cytolytic activity due to defective microtubule-organizing center mobilization and lytic granule exocytosis*. J Immunol, 2001. **167**(9): p. 5042-51.
120. Boon, T., et al., *Human T cell responses against melanoma*. Annu Rev Immunol, 2006. **24**: p. 175-208.
121. Whiteside, T.L., *Immune cells in the tumor microenvironment. Mechanisms responsible for functional and signaling defects*. Adv Exp Med Biol, 1998. **451**: p. 167-71.
122. Prevost-Blondel, A., et al., *Tumor-infiltrating lymphocytes exhibiting high ex vivo cytolytic activity fail to prevent murine melanoma tumor growth in vivo*. J Immunol, 1998. **161**(5): p. 2187-94.
123. Sotomayor, E.M., et al., *Conversion of tumor-specific CD4+ T-cell tolerance to T-cell priming through in vivo ligation of CD40*. Nat Med, 1999. **5**(7): p. 780-7.
124. Piersma, S.J., et al., *High number of intraepithelial CD8+ tumor-infiltrating lymphocytes is associated with the absence of lymph node metastases in patients with large early-stage cervical cancer*. Cancer Res, 2007. **67**(1): p. 354-61.
125. Kryczek, I., et al., *Phenotype, distribution, generation, and functional and clinical relevance of Th17 cells in the human tumor environments*. Blood, 2009. **114**(6): p. 1141-9.

126. Weaver, C.T., et al., *IL-17 family cytokines and the expanding diversity of effector T cell lineages*. *Annu Rev Immunol*, 2007. **25**: p. 821-52.
127. Ikehara, Y., M. Yamanaka, and T. Yamaguchi, *Recent advancements in cytotoxic T lymphocyte generation methods using carbohydrate-coated liposomes*. *J Biomed Biotechnol*, 2010. **2010**: p. 242539.
128. Petersen, T.R., N. Dickgreber, and I.F. Hermans, *Tumor antigen presentation by dendritic cells*. *Crit Rev Immunol*, 2010. **30**(4): p. 345-86.
129. Gilboa, E., *DC-based cancer vaccines*. *J Clin Invest*, 2007. **117**(5): p. 1195-203.
130. Reslan, L., S. Dalle, and C. Dumontet, *Understanding and circumventing resistance to anticancer monoclonal antibodies*. *MAbs*, 2009. **1**(3): p. 222-9.
131. Karyampudi, L. and K.L. Knutson, *Antibodies in cancer immunotherapy*. *Cancer Biomark*, 2010. **6**(5-6): p. 291-305.
132. van der Burg, S.H. and C.J. Melief, *Therapeutic vaccination against human papilloma virus induced malignancies*. *Curr Opin Immunol*, 2011. **23**(2): p. 252-7.
133. Allan, C.P., et al., *The immune response to breast cancer, and the case for DC immunotherapy*. *Cytotherapy*, 2004. **6**(2): p. 154-63.
134. Wong, P.Y., et al., *Functional analysis of tumor-infiltrating leukocytes in breast cancer patients*. *J Surg Res*, 1998. **76**(1): p. 95-103.
135. Venetsanakos, E., et al., *High incidence of interleukin 10 mRNA but not interleukin 2 mRNA detected in human breast tumours*. *Br J Cancer*, 1997. **75**(12): p. 1826-30.

136. Camp, B.J., et al., *In situ cytokine production by breast cancer tumor-infiltrating lymphocytes*. *Ann Surg Oncol*, 1996. **3**(2): p. 176-84.
137. DeNardo, D.G. and L.M. Coussens, *Inflammation and breast cancer. Balancing immune response: crosstalk between adaptive and innate immune cells during breast cancer progression*. *Breast Cancer Res*, 2007. **9**(4): p. 212.
138. Munk, M.E. and M. Emoto, *Functions of T-cell subsets and cytokines in mycobacterial infections*. *Eur Respir J Suppl*, 1995. **20**: p. 668s-675s.
139. Romagnani, S., *The Th1/Th2 paradigm*. *Immunol Today*, 1997. **18**(6): p. 263-6.
140. Stout, R.D. and K. Bottomly, *Antigen-specific activation of effector macrophages by IFN-gamma producing (TH1) T cell clones. Failure of IL-4-producing (TH2) T cell clones to activate effector function in macrophages*. *J Immunol*, 1989. **142**(3): p. 760-5.
141. Parker, D.C., *T cell-dependent B cell activation*. *Annu Rev Immunol*, 1993. **11**: p. 331-60.
142. Tsung, K., et al., *IL-12 induces T helper 1-directed antitumor response*. *J Immunol*, 1997. **158**(7): p. 3359-65.
143. Kidd, P., *Th1/Th2 balance: the hypothesis, its limitations, and implications for health and disease*. *Altern Med Rev*, 2003. **8**(3): p. 223-46.
144. Shevach, E.M., *CD4+ CD25+ suppressor T cells: more questions than answers*. *Nat Rev Immunol*, 2002. **2**(6): p. 389-400.
145. Liyanage, U.K., et al., *Prevalence of regulatory T cells is increased in peripheral blood and tumor microenvironment of patients with*

- pancreas or breast adenocarcinoma*. J Immunol, 2002. **169**(5): p. 2756-61.
146. Zitvogel, L., A. Tesniere, and G. Kroemer, *Cancer despite immunosurveillance: immunoselection and immunosubversion*. Nat Rev Immunol, 2006. **6**(10): p. 715-27.
147. Cabrera, T., et al., *High frequency of altered HLA class I phenotypes in invasive breast carcinomas*. Hum Immunol, 1996. **50**(2): p. 127-34.
148. Vitale, M., et al., *HLA class I antigen and transporter associated with antigen processing (TAP1 and TAP2) down-regulation in high-grade primary breast carcinoma lesions*. Cancer Res, 1998. **58**(4): p. 737-42.
149. Broderick, L. and R.B. Bankert, *Membrane-associated TGF-beta1 inhibits human memory T cell signaling in malignant and nonmalignant inflammatory microenvironments*. J Immunol, 2006. **177**(5): p. 3082-8.
150. Broderick, L., et al., *IL-12 reverses anergy to T cell receptor triggering in human lung tumor-associated memory T cells*. Clin Immunol, 2006. **118**(2-3): p. 159-69.
151. Simpson-Abelson, M. and R.B. Bankert, *Targeting the TCR signaling checkpoint: a therapeutic strategy to reactivate memory T cells in the tumor microenvironment*. Expert Opin Ther Targets, 2008. **12**(4): p. 477-90.
152. Kim, R., M. Emi, and K. Tanabe, *Cancer immunoediting from immune surveillance to immune escape*. Immunology, 2007. **121**(1): p. 1-14.
153. Wilczynski, J.R. and M. Duechler, *How do tumors actively escape from host immunosurveillance?* Arch Immunol Ther Exp (Warsz), 2010. **58**(6): p. 435-48.

154. Bronte, V. and S. Mocellin, *Suppressive influences in the immune response to cancer*. J Immunother, 2009. **32**(1): p. 1-11.
155. Whiteside, T.L., *Signaling defects in T lymphocytes of patients with malignancy*. Cancer Immunol Immunother, 1999. **48**(7): p. 346-52.
156. Riches, J.C., A.G. Ramsay, and J.G. Gribben, *T-cell function in chronic lymphocytic leukaemia*. Semin Cancer Biol, 2010. **20**(6): p. 431-8.
157. Fayad, L., et al., *Interleukin-6 and interleukin-10 levels in chronic lymphocytic leukemia: correlation with phenotypic characteristics and outcome*. Blood, 2001. **97**(1): p. 256-63.
158. Steinman, R.M. and I. Mellman, *Immunotherapy: bewitched, bothered, and bewildered no more*. Science, 2004. **305**(5681): p. 197-200.
159. Melief, C.J., *Cancer immunotherapy by dendritic cells*. Immunity, 2008. **29**(3): p. 372-83.
160. Borghaei, H., M.R. Smith, and K.S. Campbell, *Immunotherapy of cancer*. Eur J Pharmacol, 2009. **625**(1-3): p. 41-54.
161. Sabado, R.L. and N. Bhardwaj, *Directing dendritic cell immunotherapy towards successful cancer treatment*. Immunotherapy, 2010. **2**(1): p. 37-56.
162. Westwood, J.A., et al., *Enhancing adoptive immunotherapy of cancer*. Expert Opin Biol Ther, 2010. **10**(4): p. 531-45.
163. Khan, A.R., et al., *Tumor infiltrating regulatory T cells: tractable targets for immunotherapy*. Int Rev Immunol, 2010. **29**(5): p. 461-84.
164. Huye, L.E. and G. Dotti, *Designing T cells for cancer immunotherapy*. Discov Med, 2010. **9**(47): p. 297-303.

165. Mathew, M. and R.S. Verma, *Humanized immunotoxins: a new generation of immunotoxins for targeted cancer therapy*. *Cancer Sci*, 2009. **100**(8): p. 1359-65.
166. Chouaib, S., et al., *Endothelial cells as key determinants of the tumor microenvironment: interaction with tumor cells, extracellular matrix and immune killer cells*. *Crit Rev Immunol*, 2010. **30**(6): p. 529-45.
167. Carmeliet, P., *Mechanisms of angiogenesis and arteriogenesis*. *Nat Med*, 2000. **6**(4): p. 389-95.
168. Lorusso, G. and C. Ruegg, *The tumor microenvironment and its contribution to tumor evolution toward metastasis*. *Histochem Cell Biol*, 2008. **130**(6): p. 1091-103.
169. Carmeliet, P. and R.K. Jain, *Angiogenesis in cancer and other diseases*. *Nature*, 2000. **407**(6801): p. 249-57.
170. Kerbel, R.S., *Tumor angiogenesis*. *N Engl J Med*, 2008. **358**(19): p. 2039-49.
171. Hanahan, D. and J. Folkman, *Patterns and emerging mechanisms of the angiogenic switch during tumorigenesis*. *Cell*, 1996. **86**(3): p. 353-64.
172. Whittaker, C.A., et al., *The echinoderm adhesome*. *Dev Biol*, 2006. **300**(1): p. 252-66.
173. Ozbek, S., et al., *The evolution of extracellular matrix*. *Mol Biol Cell*, 2010. **21**(24): p. 4300-5.
174. Sternlicht, M.D., et al., *The stromal proteinase MMP3/stromelysin-1 promotes mammary carcinogenesis*. *Cell*, 1999. **98**(2): p. 137-46.
175. Levental, K.R., et al., *Matrix crosslinking forces tumor progression by enhancing integrin signaling*. *Cell*, 2009. **139**(5): p. 891-906.

176. Erler, J.T., et al., *Lysyl oxidase is essential for hypoxia-induced metastasis*. *Nature*, 2006. **440**(7088): p. 1222-6.
177. Paszek, M.J., et al., *Tensional homeostasis and the malignant phenotype*. *Cancer Cell*, 2005. **8**(3): p. 241-54.
178. Erler, J.T., et al., *Hypoxia-induced lysyl oxidase is a critical mediator of bone marrow cell recruitment to form the premetastatic niche*. *Cancer Cell*, 2009. **15**(1): p. 35-44.
179. Hynes, R.O., *The extracellular matrix: not just pretty fibrils*. *Science*, 2009. **326**(5957): p. 1216-9.
180. Lu, P., V.M. Weaver, and Z. Werb, *The extracellular matrix: a dynamic niche in cancer progression*. *J Cell Biol*, 2012. **196**(4): p. 395-406.
181. Swartz, M.A., et al., *Tumor microenvironment complexity: emerging roles in cancer therapy*. *Cancer Res*, 2012. **72**(10): p. 2473-80.
182. Rotllant, J., et al., *Sparc (Osteonectin) functions in morphogenesis of the pharyngeal skeleton and inner ear*. *Matrix Biol*, 2008. **27**(6): p. 561-72.
183. Sangaletti, S., et al., *SPARC oppositely regulates inflammation and fibrosis in bleomycin-induced lung damage*. *Am J Pathol*, 2011. **179**(6): p. 3000-10.
184. Ostrand-Rosenberg, S., *Animal models of tumor immunity, immunotherapy and cancer vaccines*. *Curr Opin Immunol*, 2004. **16**(2): p. 143-50.
185. Huggins, C., L.C. Grand, and F.P. Brillantes, *Mammary cancer induced by a single feeding of polymucular hydrocarbons, and its suppression*. *Nature*, 1961. **189**: p. 204-7.

186. Chow, L.W., et al., *A rat cell line derived from DMBA-induced mammary carcinoma*. Life Sci, 2003. **73**(1): p. 27-40.
187. Thompson, H.J. and H. Adlakha, *Dose-responsive induction of mammary gland carcinomas by the intraperitoneal injection of 1-methyl-1-nitrosourea*. Cancer Res, 1991. **51**(13): p. 3411-5.
188. Welsch, C.W., *Host factors affecting the growth of carcinogen-induced rat mammary carcinomas: a review and tribute to Charles Brenton Huggins*. Cancer Res, 1985. **45**(8): p. 3415-43.
189. Thompson, H.J. and M. Singh, *Rat models of premalignant breast disease*. J Mammary Gland Biol Neoplasia, 2000. **5**(4): p. 409-20.
190. Kubatka, P., et al., *Chemoprevention of mammary carcinogenesis in female rats by rofecoxib*. Cancer Lett, 2003. **202**(2): p. 131-6.
191. Hill, M., et al., *Immunobiological characterization of N-nitrosomethylurea-induced rat breast carcinomas: tumoral IL-10 expression as a possible immune escape mechanism*. Breast Cancer Res Treat, 2004. **84**(2): p. 107-16.
192. Mostbock, S., et al., *Reduction of 1-methyl-1-nitrosourea-induced tumor burden with DNA vaccines encoding mutated ras epitopes and the costimulatory molecule B7.1*. Gen Physiol Biophys, 2003. **22**(4): p. 561-5.
193. Isaacs, J.T., *Genetic control of resistance to chemically induced mammary adenocarcinogenesis in the rat*. Cancer Res, 1986. **46**(8): p. 3958-63.
194. Esendagli, G., *Genetic modification of mammary tumor cells generated by chemical carcinogenesis with CD40 ligand and evaluation as an allogeneic vaccine preparation, in Department of Basic Oncology*. 2007, Hacettepe University: Ankara. p. 154.

195. National Center for Biotechnology Information. *PubChem Compound Database*; CID=12699. 2013 2013/05/07/20:47:23; Available from: http://pubchem.ncbi.nlm.nih.gov/summary/summary.cgi?cid=12699&oc=ec_rcs.
196. Nagao, T., et al., *Induction of fetal malformations after treatment of mouse embryos with methylnitrosourea at the preimplantation stages*. *Teratog Carcinog Mutagen*, 1991. **11**(1): p. 1-10.
197. Faustman, E.M., et al., *In vitro developmental toxicity of five direct-acting alkylating agents in rodent embryos: structure-activity patterns*. *Teratology*, 1989. **40**(3): p. 199-210.
198. Cox, R. and C.C. Irving, *O6-methylguanine accumulates in DNA of mammary glands after administration of N-methyl-N-nitrosourea to rats*. *Cancer Lett*, 1979. **6**(4-5): p. 273-8.
199. da Silva Franchi, C.A., et al., *Thymic lymphomas in Wistar rats exposed to N-methyl-N-nitrosourea (MNU)*. *Cancer Sci*, 2003. **94**(3): p. 240-3.
200. Brown, K., A. Buchmann, and A. Balmain, *Carcinogen-induced mutations in the mouse c-Ha-ras gene provide evidence of multiple pathways for tumor progression*. *Proc Natl Acad Sci U S A*, 1990. **87**(2): p. 538-42.
201. Niwa, K., et al., *Rapid induction of endometrial carcinoma in ICR mice treated with N-methyl-N-nitrosourea and 17 beta-estradiol*. *Jpn J Cancer Res*, 1991. **82**(12): p. 1391-6.
202. Ting, A.Y., et al., *Characterization of a preclinical model of simultaneous breast and ovarian cancer progression*. *Carcinogenesis*, 2007. **28**(1): p. 130-5.

203. Zhou, S., et al., *Effect of dietary fatty acids on tumorigenesis of colon cancer induced by methyl nitrosourea in rats*. J Environ Pathol Toxicol Oncol, 2000. **19**(1-2): p. 81-6.
204. Macejova, D. and J. Brtko, *Chemically induced carcinogenesis: a comparison of 1-methyl-1-nitrosourea, 7,12-dimethylbenzanthracene, diethylnitroso-amine and azoxymethan models (minireview)*. Endocr Regul, 2001. **35**(1): p. 53-9.
205. Tronov, V.A., et al., *Sensitivity of human lymphocytes to genotoxic effect of n-methyl-n-nitrosourea: possible relation to gynecological cancers*. Exp Oncol, 2006. **28**(4): p. 314-8.
206. Inoue, T., et al., *Residual toxicity in hematopoietic cells following a single dose of methylnitrosourea*. Leuk Res, 1984. **8**(1): p. 105-16.
207. Thompson, T.A., J.D. Haag, and M.N. Gould, *ras gene mutations are absent in NMU-induced mammary carcinomas from aging rats*. Carcinogenesis, 2000. **21**(10): p. 1917-22.
208. Thordarson, G., et al., *Growth and characterization of N-methyl-N-nitrosourea-induced mammary tumors in intact and ovariectomized rats*. Carcinogenesis, 2001. **22**(12): p. 2039-47.
209. Singh, M., J.N. McGinley, and H.J. Thompson, *A comparison of the histopathology of premalignant and malignant mammary gland lesions induced in sexually immature rats with those occurring in the human*. Lab Invest, 2000. **80**(2): p. 221-31.
210. Russo, J., et al., *Comparative study of human and rat mammary tumorigenesis*. Lab Invest, 1990. **62**(3): p. 244-78.
211. Medina, D., *The preneoplastic phenotype in murine mammary tumorigenesis*. J Mammary Gland Biol Neoplasia, 2000. **5**(4): p. 393-407.

212. Thompson, H.J., et al., *Temporal sequence of mammary intraductal proliferations, ductal carcinomas in situ and adenocarcinomas induced by 1-methyl-1-nitrosourea in rats*. *Carcinogenesis*, 1998. **19**(12): p. 2181-5.
213. Sukumar, S. and M. Barbacid, *Specific patterns of oncogene activation in transplacentally induced tumors*. *Proc Natl Acad Sci U S A*, 1990. **87**(2): p. 718-22.
214. Zhang, R., J.D. Haag, and M.N. Gould, *Reduction in the frequency of activated ras oncogenes in rat mammary carcinomas with increasing N-methyl-N-nitrosourea doses or increasing prolactin levels*. *Cancer Res*, 1990. **50**(14): p. 4286-90.
215. Dincer, Y. and S. Kankaya, *Comet Assay for Determining of DNA Damage: Review*. *Turkiye Klinikleri Journal of Medical Sciences*, 2010. **30**(4): p. 1365-1373.
216. Hartmann, A., et al., *Recommendations for conducting the in vivo alkaline Comet assay. 4th International Comet Assay Workshop*. *Mutagenesis*, 2003. **18**(1): p. 45-51.
217. Tice, R.R., et al., *Single cell gel/comet assay: guidelines for in vitro and in vivo genetic toxicology testing*. *Environ Mol Mutagen*, 2000. **35**(3): p. 206-21.
218. Green, M.H., et al., *Comet assay to detect nitric oxide-dependent DNA damage in mammalian cells*. *Methods Enzymol*, 1996. **269**: p. 243-66.
219. Collins, A.R., *The comet assay for DNA damage and repair: principles, applications, and limitations*. *Mol Biotechnol*, 2004. **26**(3): p. 249-61.

220. Tsuyada, A., et al., *CCL2 Mediates Cross-talk between Cancer Cells and Stromal Fibroblasts That Regulates Breast Cancer Stem Cells*. *Cancer Res*, 2012. **72**(11): p. 2768-79.
221. Biochrom. *Separating solutions and lectins*. 2012 [cited 2012 14.06.2012]; Separating solutions are used for isolation of cells or cellular particles during density gradient centrifugation]. Available from: <http://www.biochrom.de/en/products/separating-solutions/>.
222. Sigma Aldrich. *Histopaque-1077 sterile-filtered, density: 1.077 g/mL*. 2013 2013/05/21/19:49:00; Available from: [http://www.sigmaaldrich.com/etc/medialib/docs/Sigma-Aldrich/Product Information Sheet/1/10771-research-use-pis.Par.0001.File.tmp/10771-research-use-pis.pdf](http://www.sigmaaldrich.com/etc/medialib/docs/Sigma-Aldrich/Product%20Information%20Sheet/1/10771-research-use-pis.Par.0001.File.tmp/10771-research-use-pis.pdf).
223. Assistance Publique – Hôpitaux de Paris. *Principe du Ficoll*. 2013 2013/05/22/21:28:02; Available from: <http://prbmondor.aphp.fr/Preparation-des-echantillons.html>.
224. World Health Organization. Dept. of Immunization Vaccines and Biologicals., *Polio laboratory manual*. 4th ed. 2004, Geneva: World Health Organization. 157 p.
225. Freshney, R.I., *Culture of animal cells : a manual of basic technique and specialized applications*. 6th ed. 2010, Hoboken, N.J.: Wiley-Blackwell. xxxi, 732 p., 28 p. of plates.
226. Perez, S. *Cell counts using Improved Neubauer haemocytometer*. 2006 [cited 2012 14.06.2012]; Available from: <http://people.oregonstate.edu/~weisv/Protocols/Symbiodinium/Cell%20Counts.pdf>.
227. Thermo Scientific. *Mr. Frosty Freezing Container | Thermo Scientific*. 2013 2013/05/22/21:29:19; Available from:

http://www.thermoscientific.com/ecom/servlet/productsdetail_11152_11964137_-1.

228. Biological Industries. *EZ-PCR Mycoplasma Test Kit*. 2013 2013/05/20/13:22:26; Available from: [http://www.bioind.com/Media/Uploads/ez_pcr_20-700-20\(1\).pdf](http://www.bioind.com/Media/Uploads/ez_pcr_20-700-20(1).pdf).
229. BD Biosciences. *BD Falcon 8-well CultureSlide*. 2012 [cited 2012 14.06.2012]; BD Falcon 8-well CultureSlide, glass slide with polystyrene vessel, lid, and safety removal tool]. Available from: <http://catalog.bd.com/bdCat/viewProduct.doCustomer?productNumber=354108>.
230. Abcam. *Immunocytochemistry and immuofluorescence protocol*. 2012 [cited 2012 14.06.2012]; Guideline procedure for staining of cell cultures using immunofluoresence]. Available from: <http://www.abcam.com/index.html?pageconfig=resource&rid=11417>.
231. Bender MedSystems. *Rat TGF-beta1 Platinum ELISA*. 2013 2013/05/09/09:25:38; Available from: <http://www.bendermedsystems.org/products.php?nr=BMS623/2&search=BMS623/2&no=2>.
232. eBioscience. *Rat IFN-gamma Platinum ELISA*. 2013 2013/05/09/09:22:32; Available from: <http://www.ebioscience.com/rat-ifn-gamma-platinum-elisa-kit.htm>.
233. Qiagen. *QIAamp DNA Blood Mini Kit*. 2013 2013/05/09/09:20:11; Available from: <http://www.qiagen.com/Products/Catalog/Sample-Technologies/DNA-Sample-Technologies/Genomic-DNA/QIAamp-DNA-Blood-Mini-Kit#resources>.
234. Ambion. *Ambion DNA-free (Life Technologies)*. 2013 2013/05/09/09:42:32; Available from: <http://products.invitrogen.com/ivgn/product/AM1906>.

235. Thermo Scientific. *RevertAid First Strand cDNA Synthesis Kit* | Thermo Scientific. 2013 2013/05/09/10:44:16; Available from: <http://www.thermoscientificbio.com/reverse-transcription-rtqpcr/rtqpcr/revertaid-first-strand-cdna-synthesis-kit/>.
236. Roche Applied Science. *LightCycler DNA Master SYBR Green I*. 2013 2013/05/09/12:25:42; Available from: <http://www.roche-applied-science.com/shop/en/us/products/lightcycler-dna-master-sybr-green-i>.
237. Pfaffl, M.W., *A new mathematical model for relative quantification in real-time RT-PCR*. Nucleic Acids Res, 2001. **29**(9): p. e45.
238. Thermo Scientific. *GeneRuler 50 bp DNA Ladder, 50-1000 bp (Fermentas)*. 2013 2013/05/09/14:52:41; Available from: <http://www.thermoscientificbio.com/nucleic-acid-electrophoresis/generuler-50-bp-dna-ladder/>.
239. Perse, M., et al., *N-methylnitrosourea induced breast cancer in rat, the histopathology of the resulting tumours and its drawbacks as a model*. Pathol Oncol Res, 2009. **15**(1): p. 115-21.
240. Sharon, Y., et al., *Isolation of normal and cancer-associated fibroblasts from fresh tissues by Fluorescence Activated Cell Sorting (FACS)*. J Vis Exp, 2013(71): p. e4425.
241. Erez, N., et al., *Cancer-Associated Fibroblasts Are Activated in Incipient Neoplasia to Orchestrate Tumor-Promoting Inflammation in an NF-kappaB-Dependent Manner*. Cancer Cell, 2010. **17**(2): p. 135-47.
242. Pietras, K., et al., *Functions of paracrine PDGF signaling in the proangiogenic tumor stroma revealed by pharmacological targeting*. PLoS Med, 2008. **5**(1): p. e19.

243. Young, E. and W.J. Stark, *In vitro immunological function of human corneal fibroblasts*. Invest Ophthalmol Vis Sci, 1988. **29**(9): p. 1402-6.
244. Burlinson, B., *The in vitro and in vivo comet assays*. Methods Mol Biol, 2012. **817**: p. 143-63.

APPENDICES

Appendix 1. Research ethics approval for animal experimentation received from "Hacettepe University Institutional Animal Care and Use Ethics Committee, Ankara"

Appendix 2. Award received

- **2013 Prof. Dr. Ali Haydar Taşpınar Award** received from “*Türkiye Kanserle Savaş Vakfı*”.

Appendix 3. Scientific meetings where the data of the thesis was presented

International Presentations

- Gunaydin G, Dolen Y, Unver N, Kesikli SA, Guc D. (2013, August). The effects of Cancer Associated Fibroblasts on mechanisms of immune evasion in a rat chemical mammary carcinoma model. Poster session presented at **15th International Congress of Immunology**, Milan, Italy.
- Gunaydin G, Dolen Y, Kesikli SA, Guc D. (2012, September). The identification of the Cancer Associated Fibroblasts and functional analyses for mechanisms of immune evasion in a rat chemical

mammary carcinoma model. Poster session presented at **3rd European Congress of Immunology**, Glasgow, Scotland.

- Gunaydin G, Dolen Y, Kesikli SA, Guc D. (2012, May). The identification of the tumor microenvironment members, specifically cancer associated fibroblasts, for functional analyses in a rat chemical mammary carcinoma model. Poster session presented at **Global Academic Programs (GAP) Conference**, Oslo, Norway.
- Gunaydin G, Dolen Y, Kesikli SA, Guc D. (2012, April). The Identification of the Cancer Associated Fibroblasts. Lecture presented at **Molecular Immunology & Immunogenetics Congress 2012**, Antalya, Turkey.

National Presentations

- Gunaydin G, Dolen Y, Unver N, Kesikli SA, Guc D. (2013, April). Kanslerle İlişkili Fibroblastların tümörün immün kaçış mekanizmalarındaki fonksiyonel rollerinin, sıçan kimyasal meme kanseri modelinde araştırılması. Lecture presented at **22nd National Congress of Immunology**, Cesme, Turkey.
- Gunaydin G, Dolen Y, Unver N, Kesikli SA, Guc D. (2013, April). Sıçan kimyasal meme kanseri modelinde Kanslerle İlişkili Fibroblastların tanımlanması ve bu hücrelerin tümörün immün kaçış mekanizmalarındaki fonksiyonel rollerinin araştırılması. Poster session presented at **20th National Congress of Cancer**, Antalya, Turkey.



Sayı: B.30.2.HAC.0.05.06.00/

40

26 Mayıs 2011

427

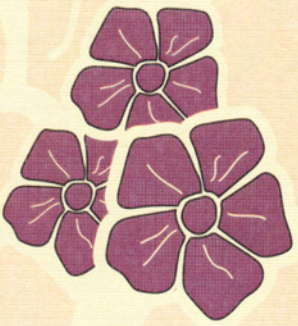
HAYVAN DENEYLERİ YEREL ETİK KURUL KARARI

TOPLANTI TARİHİ : 24.05.2011 (SALI)
TOPLANTI SAYISI : 2011/3
DOSYA KAYIT NUMARASI : 2011/28
KARAR NUMARASI : 2011/28-3
ARAŞTIRMA YÜRÜTÜCÜSÜ : Prof. Dr. Dicle Güç
HAYVAN DENEYLERİNDEN : Dr. Gürcan Günaydın
SORUMLU ARAŞTIRMACI :
YARDIMCI ARAŞTIRMACILAR : -
ONAYLANAN HAYVAN TÜRÜ ve SAYISI : 27 adet Sprague-Dawley sıçan
ONAY GEÇERLİLİK SÜRESİ : 12 ay

Üniversitemiz Onkoloji Enstitüsü Temel Onkoloji Anabilim Dalı öğretim üyelerinden Prof. Dr. Dicle Güç'ün yürütücüsü olduğu 2011/28 dosya numaralı ve "*Sıçan Kimyasal Meme Kanseri Modelinde Tümör Mikroçevresinin T Hücre Yanıtları Üzerine Etkisi*" isimli çalışma Hayvan Deneyleri Yerel Etik Kurulu Yönergesi'ne göre uygun bulunarak oy birliği ile onaylanmasına karar verilmiştir

Sorumlu araştırmacı deneylere başlangıç tarihini Etik Kurula bildirmekle yükümlüdür

Prof. Dr. Hakan S. ORER
Etik Kurul Başkanı



Türkiye Kanserle Savaş Vakfı

Gürcan Günaydın, Yusuf Dölen, Neşe Ünver, Sacit Altuğ Kesikli, Dicle Güç Hacettepe Üniversitesi Kanser Enstitüsü, Temel Onkoloji Anabilim Dalı, Ankara

20. Ulusal Kanser Kongresinde yapmış olduğunuz “**Sıçan Kimyasal Meme Kanseri Modelinde Kanserle İlişkili Fibroblastların Tanımlanması ve Bu Hücrelerin Tümörün İmmün Kaçış Mekanizmalarındaki Fonksiyonel Rollerinin Araştırılması**” başlıklı çalışmanız 2013 Prof. Dr. Ali Haydar Taşpınar ödülüne uygun görülmüştür.

Başarılarınızın devamını dileriz.

Dr. Y. Etey

Türkiye Kanserle Savaş Vakfı Yönetim Kurulu

Prof. Dr. Metin Ertem
Başkan



TÜRKİYE
KANSERLE
SAVAŞ VAKFI
1977

145

BOOK OF ABSTRACTS

Co-Editors: Luciano Adorini, Massimo Locati



P5.20.032**Panobinostat in combination with azacitidine reduces the frequency of TNFR2+ Tregs in newly diagnosed acute myeloid leukemia patients.**

C. Govindaraj¹, P. Tan², P. Walker², A. We², A. Spencer², M. Plebanski¹;

¹Monash University, Melbourne, Australia, ²Alfred hospital, Melbourne, Australia.

Acute Myeloid Leukemia provides an environment that enables immune suppression, resulting in functionally defective effector T cells. Regulatory T cells (Tregs) are significant contributors to the impaired anti-tumor immunity. Expression of the TNF receptor TNFR2 on Tregs identifies a potent regulatory subset, and since TNF is present at high levels within AML patients, we hypothesized TNFR2+ Tregs may be a functionally relevant Treg subset in AML. Furthermore, the effect of the emerging epigenetic treatment drug combination, panobinostat and azacitidine on T cells and Tregs, particularly TNFR2+ Tregs has not been previously investigated in AML or other blood diseases. Here, we demonstrate that TNFR2+ Tregs are the dominant highly functionally relevant Treg population within AML patients. Treatment with azacitidine and panobinostat resulted in a decrease in TNFR2+ Tregs, but not TNFR2- Tregs in AML patients. Moreover, patients who had a reduction in their TNFR2+ Tregs in both the bone marrow and peripheral blood responded positively to treatment. These patients consequently also showed increased IFN γ and IL-2 production by effector T cells isolated from the bone marrow. In vitro mechanistic studies suggested that panobinostat and not azacitidine, primarily and dominantly drives the reduction in Tregs. AML patients who responded clinically to panobinostat and azacitidine therapy had an immune profile associated with decreased TNFR2+ Tregs and increased effector T cells.

P5.20.033**The effects of Cancer Associated Fibroblasts on mechanisms of immune evasion in a rat chemical mammary carcinoma model**

G. Gunaydin, Y. Dolen, N. Unver, S. Kesikli, D. Guc;
Hacettepe University Cancer Institute Department of Basic Oncology, Ankara, Turkey.

Objective: Fibroblast cells turn into cancer associated fibroblasts(CAFs) in tumor microenvironment. Tissue fibroblasts have previously been shown to affect T-cell functions. However, studies investigating the effects of CAFs on T-cells are limited in the literature.

Methods: N-Nitroso N-Methyl Urea(NMU) induced experimental mammary carcinogenesis model was utilized. Tumors were harvested surgically under sterile conditions for CAF isolation. CAFs and healthy tissue fibroblasts were immunostained to evaluate expression differences of markers like α -Smooth-Muscle-Actin(α SMA) and Vimentin. DNA damage of peripheral blood cells due to NMU were analyzed by Comet Assays. Cocultures of CAFs with lymphocytes employing Carboxyfluorescein-succinimidyl-ester(CFSE) proliferation assays were performed. Surface and intracellular expressions of immune activation markers (CD25, IFN- γ) of T-cells cocultured with CAFs were analyzed. Levels of IL-4 were analyzed in CAF-splenocyte cocultures. Gene expression levels of several immune activation markers like CD25 and costimulatory molecules like CD28 in splenocytes were investigated.

Results: The immunostainings showed that CAFs had significantly higher levels of α SMA expression. Comet Assays showed that levels of DNA damage in tumor-bearing animals were similar to control levels. CAFs decreased proliferations of splenocytes in cocultures. Flow cytometry experiments showed that CAFs decreased intracellular expressions of immune activation markers like IFN- γ in T-cells. Supernatants of CAF-splenocyte cocultures were shown to have increased levels of IL-4. Splenocytes cocultured with CAFs were found to have decreased gene expression levels of costimulatory molecules.

Conclusions: A rat chemical breast carcinogenesis model was successfully employed and CAFs were stably propagated. Coculture experiments suggested an immunomodulatory role for CAFs on immunity against breast cancer.

P5.20.034**Effects of Silymarin on frequency and function of Myeloid-derived suppressor cells in animal model of tumor**

M. Hafezi¹, A. Namdar², N. Khosravianfar³, A. Razavi⁴, J. Hadjati⁵;
¹Department of Immunology, School of Pathobiology, Tehran University of Medical sciences, Tehran, Iran, ²Department of Immunology, School of Medicine, Isfahan University of Medical Sciences, Isfahan, Iran, ³Department of Pathobiology, School of Public Health, Tehran University of Medical Sciences, Tehran, Iran, ⁴Department of Immunology, School of Pathobiology, Tehran University of Medical Sciences, Tehran, Iran, ⁵Department of Immunology, School of Medicine, Tehran University of Medical Sciences, Tehran, Iran.

Background: Myeloid-derived suppressor cells (MDSC) are identified as heterogeneous population of immature myeloid cells (IMCs) including precursors of macrophages, granulocytes, and dendritic cells (DC). These cells accumulate during tumor formation; facilitate immune escape, and therefore promote tumor progression. Silymarin, a plant flavonoid isolated from the seeds of milk thistle (*Silybum marianum*), has been indicated to possess antioxidant, anti-inflammatory and immunomodulatory properties. We sought to determine silymarin's effects on the frequency and function of MDSC population accumulated during tumor progression.

Methods: We isolated MDSCs from spleen of tumor bearing mice treated with silymarin by MACS method. Then, the number of MDSCs and also their ROS production were evaluated using flow cytometry and compared with untreated group. Moreover, the silymarin's effect on NO production was analyzed using ELISA.

Results: Our results showed that silymarin had some positive effects on number and function of MDSCs.

Conclusion: Silymarin, as an anti-inflammatory drug, may exert beneficial effects on T cell responses against tumors and should be considered as an agent that affects the number and function of MDSCs. Further studies are needed to shed light on adjuvant anti-cancer effects of this compound which potentially could be used as combination therapy of cancer.

Key words: MDSC, Silymarin, Anti-inflammatory, ROS, NO

P5.20.035**Formation of vascular mimicry in human gastric cancer and the correlation with LOX and MMP-9**

M. Han, Y. Cao, H. Sun, R. Bai;
Ningxia Medical University, Yinchuan, China.

To explore the correlations of lysyl oxidase (LOX) and matrix metalloproteinases-9 (MMP-9) with formation of VM in gastric carcinoma tissue. Gastric cancer tissues were collected from 49 patients with diagnosis of gastric cancer. According to metastasis (include lymph node and distant metastasis), gastric cancer tissues were divided into the group of metastasis and the group of non-metastasis. According to the invasion, gastric cancer tissues were divided into the group of T1 + T2 and the group of T3 + T4. The formations of VM were measured through CD34 and PAS double staining on gastric cancer tissue slices. The distributions of LOX and MMP-9 were observed using immunohistochemistry. Relative levels of LOX and MMP-9 were surveyed by Western-blot and immunohistochemistry. The locations of LOX and MMP-9 were detected by Immunofluorescence. Results showed, in gastric carcinoma tissues, the VM formation in group with metastasis were more than that in group without metastasis ($P < 0.05$), the level of LOX and MMP-9 protein were higher in group with metastasis than that in group without metastasis ($P < 0.05$); the expression of LOX in group of T3 + T4 were more abundant than in T1 + T2 group ($P < 0.05$). The levels of LOX was positively correlated with VM formation in gastric carcinoma tissues, the levels of MMP-9 was positively correlated with VM formation. The immunofluorescence results suggested that LOX often located in the area that MMP-9 expressed. The results suggest that VM promotes the invasion and metastasis of gastric cancer, LOX and MMP-9 may be facilitative factors in VM formation.

A Healthier Future Through Research, Education & Innovation



#ECI2012



2012
GLASGOW

FINAL
PROGRAMME

3rd European Congress of Immunology
5-8 September, 2012
Glasgow, Scotland

www.eci-glasgow2012.com



European Federation of
Immunological Societies

British Society for
immunology

signaling specifically causes cell death in melanoma cells *in vitro*. We addressed the question whether ATRA pre treatment could enhance the efficacy of polyI:C and if so, would ATRA have any additional effects on this process.

Materials and methods: WM35 and WM983A human melanoma cells were obtained from ATCC and cultured according to the recommended protocol. Human dendritic cells (DCs) and macrophages were differentiated from blood derived monocytes. CD1a⁺ and CD1a⁺ DCs were sorted by FACS DiVa. Relative mRNA expressions were analyzed by real time Q PCR. Protein expressions were measured by Western blot, the levels of secreted chemokines/cytokines were detected by ELISA. Small interfering RNA (siRNA) was introduced by electroporation. Migration assays were performed in transwell chambers.

Results: We found that combined treatment of human melanoma cells with ATRA and pI:C strongly increased the expression of TLR3 and MDA5 in both WM35 and WM983A cells associated to significantly higher mRNA and secreted levels of IFN β , CXCL1, CXCL8/IL 8, CXCL9, and CXCL10 than cells treated with either ATRA or polyI:C. Silencing of MDA5 by siRNA moderately affected IFN β secretion, whereas TLR3 knock down interfered with both CXCL chemokine and IFN β production. Furthermore, supernatants of ATRA+polyI:C activated cultures increased the migration of both human monocyte derived macrophages and CD1a⁺ dendritic cells significantly as compared to the supernatants of cells treated with either ATRA or polyI:C, and this effect occurred in a TLR3 dependent manner.

Conclusions: In conclusion, consecutive treatment with ATRA and polyI:C results in strong, TLR3/MDA5 mediated chemokine and interferon responses in cultured human melanoma cells, which triggers a functional migratory response in professional antigen presenting cells. This novel mode of concomitant activation may offer a more efficient treatment option for future melanoma therapy.

P1391

The first encounter between tumor cells and immune system cells

M. G. Ruocco, T. Courau & D. Klatzmann

UMR7211, Department of Immunology, Paris, France

Purpose/Objective: Regulatory T cells (Tregs) play a key role in the immune response to tumors. In cancer patients, a high number of Tregs is indicative of a poor prognosis as their abundance is inversely correlated with survival. In contrast, tipping the balance in favor of effector T cells (Teffs) has been associated to favorable prognosis. The suppressive function of Tregs is considered one of the main obstacles to successful immunotherapy.

We have previously shown that at the time of tumor emergence, activated memory Tregs (amTregs) are the first to be involved in the immune response (Darrasse Jeze *et al.* JCI 2009). Prior to Teffs, amTregs mount a secondary memory response against self antigens expressed by the tumor that overpowers Teffs, suggesting that the activation status of Tregs and Teffs dictates the tumor outcome.

Here we characterized the first encounter between tumor cells, Tregs and Teffs.

Materials and methods: We used a combination of genetic tools, fluorescent markers and multiphoton intravital microscopy.

Results: We described the dynamics of immune system cells within the microenvironment of an emerging tumor. Furthermore, we analyzed different conditions aimed to perturb tumor growth in order to identify the spatio temporal mechanisms and the cellular dynamics that determine tumor growth or tumor rejection.

Conclusions: A better understanding of the dynamic behavior of immune system cells during the very early stages of tumor emergence will allow to identify new strategies for immunotherapy.

P1392

The HIF-1 α hypoxia response in tumor-infiltrating T lymphocytes induces functional CD137 (4-1BB) for immunotherapy

A. Palazon,* I. Martínez Forero,* A. Teijeira,* A. Morales Kastresana,* S. Hervás Stubbs,* M. O. Landázuri,[†] J. Aragonés,[‡] M. Jure Kunkel[‡] & I. Melero*

**CIMA, Gene therapy and Hepatology, Pamplona, Spain, [†]Hospital la Princesa, Immunology, Madrid, Spain, [‡]Bristol Myers Squibb, Research and Development, Princeton, NJ, USA*

Purpose/Objective: To study the effects of hypoxia in the tumor microenvironment, as sensed by the HIF 1 α system, on the expression of CD137 on tumor infiltrating lymphocytes (TILs). To take advantage of CD137 being expressed selectively on TILs and check the efficacy of immunotherapy with agonist anti CD137 mAb delivered intratumorally.

Materials and methods: Mice: OT 1, OT 2, CD45.1, Rag^{-/-} and MMTVneuT, Hif 1 α floxed UBC Cre ERT2 mice. Cell lines: CT26, B16 OVA and MC38. *In vivo* tumor growth: 0.5x10⁶ tumor cells were injected subcutaneously. Tumor hypoxia was measured by positron emission tomography (PET) with the radiotracer fluorine 18 fluoromisonidazole (18^F FMISO). Flow cytometry: FACSCantoII and FACSCalibur (BD Pharmingen) as indicated were used for cell acquisition and data analysis was carried out using FlowJo. Tissue immunofluorescence staining was performed on 10 μ m thick cryosections. Monoclonal antibodies for *in vivo* experiments: agonistic mouse anti CD137 (clone 2A) and blocking anti B7 H1 (PD L1) (clone 10B5).

Results: The tumor microenvironment of transplanted and spontaneous mouse tumors is profoundly deprived of oxygenation as confirmed by PET imaging. CD8 and CD4 tumor infiltrating T lymphocytes (TILs) of transplanted colon carcinomas, melanomas and spontaneous breast adenocarcinomas are CD137 (4 1BB) positive, as opposed to their counterparts in tumor draining lymph nodes and spleen. Expression of CD137 on activated T lymphocytes is markedly enhanced by hypoxia and the prolyl hydroxylase inhibitor DMOG. Importantly, hypoxia does not up regulate CD137 in inducible HIF 1 α knock out T cells, and such HIF 1 α deficient T cells remain CD137 negative even when becoming TILs, in clear contrast to co infiltrating and co transferred HIF 1 α sufficient T lymphocytes. The fact that CD137 is selectively expressed on TILs was exploited to confine the effects of immunotherapy with agonist anti CD137 monoclonal antibodies (mAb) to the tumor tissue. As a result, low dose intratumoral injections avoid liver inflammation, achieve antitumor systemic effects and permit synergistic therapeutic effects with PD L1/B7 H1 blockade.

Conclusions: CD137 (4 1BB) is an important molecular target to augment antitumor immunity. Hypoxia in the tumor microenvironment as sensed by the HIF 1 α system increases expression of CD137 on tumor infiltrating lymphocytes which thereby become selectively responsive to the immunotherapeutic effects of anti CD137 agonist monoclonal antibodies as those used in ongoing clinical trials.

P1393

The identification of the Cancer Associated Fibroblasts and functional analyses for mechanisms of immune evasion in a rat chemical mammary carcinoma model

G. Gunaydin, Y. Dolen, S. A. Kesikli & D. Guc

Basic Oncology, Institute of Oncology, Hacettepe University Ankara, Turkey

Purpose/Objective: Seed centric cancer models do not take into account the probable impact of the microenvironment, soil, that the tumor cells reside in. Fibroblasts are thought to be involved in a dynamic crosstalk with other cells of the tumor microenvironment. The

aim of this study is to characterize and effectively isolate cancer associated fibroblasts (CAFs) for further functional assays.

Materials and methods: N Nitroso N Methyl Urea (NMU) induced experimental mammary carcinogenesis model was utilized. Twenty one days old female Sprague Dawley rats were injected once a week for 4 weeks with NMU. When the animals are about 3 months old, developed tumors were harvested surgically under sterile conditions for CAF isolation. Fibroblasts were isolated from breast tumor tissues using a protocol which utilizes collagenase and hyaluronidase. Enzymatically digested tissues were then cultured in fibroblast selective medium. The same protocol was also used to isolate normal tissue fibroblasts from healthy mammary tissues. These CAFs and healthy tissue fibroblasts were immunostained to show their differential expressions of surface markers such as α Smooth Muscle Actin (α SMA) and Vimentin, in order to distinguish CAFs from their normal tissue counterparts. Probable DNA damage of peripheral blood cells due to the NMU injections were evaluated by Comet Assays at different time points. Coculture of CAFs with lymphocytes and Carboxyfluorescein succinimidyl ester (CFSE) proliferation assays were performed for functional analyses.

Results: The immunostainings clearly showed that CAFs had significantly higher levels of α SMA expression than normal fibroblasts. This finding of differential α SMA expression was shown to fade out with further passages of cultured CAFs. Histological examinations also revealed significant morphological differences between these cells. The Comet Assays showed that levels of DNA damage in peripheral blood cells of tumor bearing animals were similar to control levels after 2 months post injection. CFSE proliferation assays showed the immunosuppressive effects of CAFs on lymphocytes (see Fig. 1).

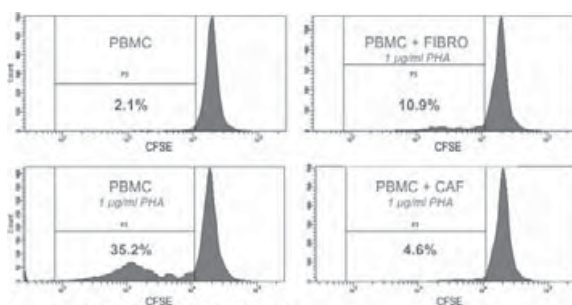


Fig. 1: CFSE Proliferation Assay Results

Conclusions: CAFs were successfully propagated using a rat chemical breast carcinogenesis model. Functional analyses with these CAFs were performed employing various coculture systems and showed their immunomodulatory roles on immunity against breast cancer.

P1394

The importance of epitope choice for adoptive T cell therapy

A. Jukica,* P. M. Kloetzel,† K. Schmidt,† B. Weißbrich,‡ C. Perez,* J. Charo,* K. Anders,* J. Sidney,§ A. Sette,§ C. Keller,† T. N. Schumacher,¶ D. Busch,‡ U. Seifert** & T. Blankenstein*
 *Max Delbrück Center for Molecular Medicine (MDC), Molecular Immunology and Gene Therapy, Berlin, Germany, †Charité Universitätsmedizin Berlin, Institute for Biochemistry, Berlin, Germany, ‡Technical University Munich, Institute for Medical Microbiology Immunology and Hygiene, Munich, Germany, §La Jolla Institute for Allergy and Immunology, Division of Vaccine Discovery, La Jolla, CA, USA, ¶The Division of Immunology, The Netherlands Cancer Institute, Amsterdam, The Netherlands, **Otto von Guericke Universität Magdeburg, Institute for Molecular and Clinical Immunology, Magdeburg, Germany

Purpose/Objective: Due to high genetic instability large established tumors contain different cell variants, where some can be therapy

resistant and lead to tumor escape. There are many factors contributing to the outgrowth of these escape variants that have to be taken into consideration for achieving optimal Results: . In this study we show the importance of epitope choice for a given target antigen by comparing rejection of large established SV40 Large T positive (T Ag⁺) tumors either by targeting subdominant epitope pI or immunodominant pIV.

Materials and methods: Retroviral transduction of mouse T cells, flow cytometry, cytokine release, MHC peptide binding, T cell avidity, tumor challenge and adoptive T cell therapy, *in vivo* kill, *in vivo* bioluminescent imaging, western blot, proteasomal cleavage, mass spectrometry.

Results: T cells engineered to express pI or pIV specific T cell receptors (TCRs) were potent enough to long term reject large established T Ag⁺ tumors. However, when tumors expressing low levels of MHC class I were treated, only TCR I T cells rejected these tumors, while TCR IV T cells selected IFN γ unresponsive escape variants. *Ex vivo* recognition of these escape variants was impaired for TCR IV, but not for TCR I T cells, indicating that in contrast to pI, pIV recognition was dependent on IFN γ stimulation. TCR I and TCR IV T cells had comparable avidity, and pI and pIV had similar affinity for the MHC class I molecule, therefore, the differential outcome of the two therapies could not be attributed to these factors. The difference was in the proteasomal cleavage of the two epitopes: pI was directly produced by the proteasome, while only N terminal precursors were generated for pIV. Due to IFN γ unresponsiveness of the escape variants, ERAAP could not be upregulated by IFN γ stimulation.

Conclusions: We speculate that the N terminal precursors could not be efficiently trimmed to generate the pIV epitope, allowing tumors to escape only TCR IV but not TCR I T cell therapy. We conclude that IFN γ independent epitopes might be better targets for adoptive T cell therapy of tumors expressing low levels of MHC class I.

P1395

The PD-1/PD-L1 axis contributes to T cell dysfunction in chronic lymphocytic leukemia

D. Brusa,* S. Serra,* M. Bianco,† M. Coscia,‡ D. Rossi,§ G. Gaidano,§ G. Fedele† & S. Deaglio*

*Hugef, Genetic biology and biochemistry, Turin, Italy, †Department of infectious parasitic and immuno mediated diseases, Istituto superiore sanità, Rome, Italy, ‡Division of Hematology, San Giovanni Battista Hospital, Turin, Italy, §Division of Hematology, Department of Clinical and Experimental Medicine & BRMA, University of Eastern Piedmont and AOU Maggiore della Carità, Novara, Italy

Purpose/Objective: Chronic Lymphocytic Leukemia (CLL) is characterized by the progressive accumulation of a population of mature B lymphocytes. It is marked by profound defects in T cell functions. Programmed death 1 (PD 1) is a cell surface molecule that inhibits T cell activation and is involved in tumor escape mechanisms through binding of the specific PD L1 ligand. The aim of this work is to evaluate expression and function of the PD 1/PD L1 axis in CLL.

Materials and methods: We compared T cell subpopulations of CLL patients ($n = 120$) to age and sex matched healthy donors (HD, $n = 30$) using multiparameter flow cytometry. Immunohistochemical analyses were used to study PD 1 and PD L1 expression in the lymph node microenvironment. Functional assays were used to determine the involvement of the PD 1/PD L1 axis in shaping T cell responses.

Results: The first finding of this work is that CD4⁺ T lymphocytes from CLL patients express significantly higher levels of the PD 1 receptor, as compared to the same cells purified from age and sex matched donors (52% versus 34%, $P < .001$). In keeping with the notion that PD 1 is a marker of cell exhaustion, we found that CD4⁺ T lymphocytes from CLL patients display increased numbers of effector

Meditasjon mot kognitiv svikt

GAP 2012: Nevrologiske komplikasjoner er vanlige komplikasjoner etter kjemoterapi. Forskere ved Hospital Israelita Albert Einstein sykehuset i São Paulo, Brasil, ser i en pågående studie på om

tibetansk meditasjon kan hjelpe mot behandlingsrelatert kognitiv svikt.

Pasientene mediterer to ganger i uken i åtte uker. Meditasjonsprogrammet er basert på gamle

tibetanske tekster. Det varer i én time og fokuserer på pust, tilstedeværelse, konsentrasjon samt teknikker for visualisering. Studien har 80 deltakere, som alle er kvinner behandlet for brystkreft.

Dårlige nyheter

GAP 2012: En onkolog kan gi dårlige nyheter til pasientene i gjennomsnitt 20.000 ganger i løpet av sin karriere. Av leger forventes det at de skal ta del i svært mange aspekter i pasientens behandling.

151

Lege Marvin Omar Delgado fra USA, kommenterte lege pasient kommunikasjon i sin presentasjon.

En lege som kommuniserer effektivt, hjelper pasienten å forstå egen sykdom, sier Delgado.

re satsingsområdet

forskjellen mellom mutasjon som en sjåfør eller passasjer. – Vi kan se at et legemiddel kan ha effekt hos over 40 prosent med en gitt genmutasjon, men bare hvis mutasjonen er en såkalt sjåfør. Er mutasjonen en passasjer, har ikke legemiddelet effekt.

Mills utdyper det komplekse bildet overfor Dagens Medisin:

– Blant annet kan det være ulike genmutasjoner i svulsten og i metastasene. Dette fordrer langt flere biopsier enn tidligere. Det er avgjørende for riktig behandling å kunne karakterisere hver enkelt tumor nøyaktig nok. Mange svulster har ulike genmutasjoner på flere områder i svulsten.

En liten andel av kreftpasienter som får persontilpasset behandling, viser et svært uvanlig sykdomsforløp. Mills oppfordrer forskere til å bruke enkeltcase som utgangspunkt for videre fors-

kning. Sykehuset i Texas har eget program for det de kaller «unusual responders», nettopp for å lære av hver enkelt pasient og kartlegge årsakene til uvanlig ekstraordinær respons.

Må være realistiske

Den amerikanske kreftforskeren sier det ennå er et stykke igjen før de nye legemidlene kan vise til helbredelse: – Vi har gjort store fremskritt og kan i dag behandle kreftformer hvor vi tidligere ikke hadde noen behandling. Vi har tatt et første skritt på veien innen persontilpasset kreftbehandling, og fremover blir det lettere. For ti år siden ville verden ha ledd av meg, for fem år siden ville folk trodd jeg var gal, men i dag kan vi gi individualisert behandling. Men selv med mer målrettet terapi er det uventet mange pasienter med biomarkører for en gitt be-



Vi må forstå sammenhengene, systembiologien, for å kunne behandle optimalt

Anne Lise Børresen Dale, professor og seksjonsleder ved OUS Radi umhospitalet

handling, som ikke har respons, eller bare har kortvarig effekt.

– Er det en fare for at vitenskapen går for raskt frem?

– Den største faren er at vi lover for mye. Vi må være realistiske. Pasientene tror at skreddersydd behandling kan helbrede – uten bivirkninger, svarer Mills.

Professor Øystein Fodstad, leder av Institutt for kreftforskning ved OUS Radiumhospitalet, var en av tilhørerne til Mills foredrag.

– Det blir mer og mer klart at kreft er resultatet av et høyst komplisert samspill av en rekke faktorer der pasientens normale vev og konstitusjon også spiller inn. Videre forskning på dette samspillet, slik som professor Mills gjør, er derfor særdeles viktig, sier Fodstad til Dagens Medisin.

Lisbeth Nilsen 482 76 048
lisbeth.nilsen@dagensmedisin.no

FAKTA

GAP2012

► Global Academic Programs (GAP) 2012 ble arrangert 14. 16. mai i Oslo av Norwegian Cancer Consortium i samarbeid med Oslo universitetssykehus, Kreftregisteret og Stavanger universitetssykehus.

► Konferansen er et kunnskaps og kompetanse utvekslings opplegg med MD Anderson Cancer Center i USA.
► Cirka 400 forskere deltok fra 24 ledende kreftsykehus over hele verden.

Kilde: Norwegian Cancer Consortium

Deltakere på GAP2012

Gurcan Gunaydin, Tyrkia

Stilling: Lege, Hacettepe University, Ankara, Department of Basic oncology
Forsker på: Brystkreft, immunreaksjoner og immunoverlevelse ved brystkreft.

Forventninger til konferansen: Samarbeid, løse problemer, få nye erfaringer og se Norge. Jeg har forsket på brystkreft i to år. Den største utfordringen innen mitt forskningsområde er kompleksiteten når det gjelder brystkreft.



Meenakshi Thakur, India

Stilling: Radiolog ved Tata Memorial Hospital, Mumbai
Forsker på: MR og mammografi
Forventninger: Snakke med andre forskere, høre hva de gjør. Forekomsten av brystkreft i India er økende ettersom vi får mer og mer velstand. For oss som ikke har så mange screeningprogrammer, er MR svært viktig for å oppdage tidlige tegn på kreft.



Marvin Omar Delgado Guay, USA

Stilling: Lege, Department of Palliative Care and Rehabilitation Medicine, MD Anderson Cancer Center
Forsker på: Palliativ omsorg.
Forventninger: Jeg ser på symp tomhåndtering hos pasienter med langtkommen kreft, og på hvordan jeg kan hjelpe dem med å kontrollere følelsesmessige symptomer. Palliativ omsorg er mye mer enn medisiner. Av konferansen forventer jeg å få ulik kunnskap for å forbedre behandlingskvaliteten for mine pasienter.



Mary Edgerton, USA

Stilling: Patolog ved MD Anderson Cancer Center
Forsker på: Jeg er her for å spre informasjon om vevsbanker.
Forventninger: Målet mitt er å gi søsternetter hjelp og råd når det gjelder vevsbanker. Området er komplekst og strengt regulert.



– En ære

Professor og onkolog Sigbjørn Smeland sier det er en ære at GAP konferansen ble lagt til Norge.

– At konferansen ble lagt til oss, viser betydningen det norske kreftmiljøet har. Dette er et unikt samarbeid mellom institusjonene og en strategisk allianse som dekker hele verden. Dette har innflytelse blant annet på politiske beslutningstakere, sier Sigbjørn Smeland til Dagens Medisin.

De over 400 deltakerne kom fra ledende kreftsykehus, såkalte «sister institutions» til MD Anderson, fra Asia, Midt-Østen, Sentral- og Sør-Amerika og Europa, opplyser Norwegian Cancer Consortium.

Anne Grete Stovrik 450 73 971
ags@dagensmedisin.no



Den største faren er at vi lover for mye. Persontilpasset behandling er ikke noe vi kan tilby alle kreftpasienter i dag

Gordon B. Mills, professor ved University of Texas MD Anderson Cancer Center



Global Academic Programs 2012 Conference
Oslo, Norway
May 14 – 16, 2012

Presenting Author Information

First Name: GURCAN
Last Name: GUNAYDIN
Title: MEDICAL DOCTOR

The identification of the tumor microenvironment members, specifically cancer associated fibroblasts, for functional analyses in a rat chemical mammary carcinoma model.

Department of Basic Oncology, Institute of Oncology, Hacettepe University, Ankara, Turkey

Constituents of the tumor microenvironment are among key players determining the cancer cell behavior. Seed-centric models do not take into account the probable impact of the microenvironment, soil, that the tumor cells reside in. Fibroblasts are among the most common types of cells found both in connective tissues and the tumor microenvironment. They are thought to be involved in a dynamic crosstalk with other cells of the tumor microenvironment. The aim of this study is to characterize and effectively isolate cancer associated fibroblasts (CAFs) for further functional assays. N-Nitroso-N-Methyl Urea (NMU) induced experimental mammary carcinogenesis model was utilized. 21 days old 20 female Spraque-Dawley rats were injected once-a-week for four weeks with i.p. 50mg/kg NMU. For the control experiments, seven rats were injected with isotonic saline using the same protocol. When the animals are about two months old, developed tumors were harvested surgically under sterile conditions for CAF isolation. Fibroblasts were isolated from breast tumor tissues using a protocol which utilizes collagenase I and hyaluronidase. Enzymatically digested tissues were then cultured in fibroblast-selective-medium. The same protocol was also used to isolate normal tissue fibroblasts from healthy mammary tissues. These CAFs and healthy tissue fibroblasts were immunostained to show their differential expressions of surface markers such as α -Smooth Muscle Actin (α -SMA) and Vimentin, in order to distinguish CAFs from their normal tissue counterparts. These immunostainings clearly showed that CAFs had significantly higher levels of α -SMA expression than normal fibroblasts. This finding of differential α -SMA expression was shown to fade out with further passages of cultured CAFs. Histological examinations also revealed significant morphological differences between these cells. In conclusion, CAFs were successfully propagated using a rat chemical breast carcinogenesis model. Further functional analyses with these CAFs will be performed employing various coculture systems to investigate their roles in immunity against breast cancer.



MOLECULAR IMMUNOLOGY & IMMUNOGENETICS CONGRESS 2012



TURKISH JOURNAL *of* IMMUNOLOGY

The Official Journal of the Turkish Society of Immunology



Türk İmmünoloji Dergisi – Volume: 1, Number: 17

Supplement (Molecular Immunology & Immunogenetics Congress – Abstract Book), 2012

TURKISH JOURNAL OF IMMUNOLOGY

**The Official Journal of the Turkish Society of Immunology
Volume: 1, Number: 17, Supplement**

**Molecular Immunology & Immunogenetics Congress –
Abstract Book, 2012**

Editors-in-Chief: Gunnur DENİZ, PhD, Professor

Managing Editor: H. Barbaros ORAL, MD PhD, Professor

Editorial Reviewer Board

Ahmet GÜL, Turkey
Aydan İKİNCİOĞULLARI, Turkey
Caner SUSAL, Germany
Cezmi AKDIŞ, Switzerland
Dicle GÜÇ, Turkey
Ender TERZİOĞLU, Turkey
Gaye ERTEN, Turkey
Güher SARUHAN DİRESKENELİ, Turkey
Gülderen YANIKKAYA DEMİREL, Turkey
Haner DİRESKENELİ, Turkey
İlhan TEZCAN, Turkey
Jagues PILOT, France
Jon D. LAMAN, the Netherlands
Mahmut ÇARİN, Turkey

Mübeccel AKDIŞ, Switzerland
Necil KÜTÜKÇÜLER, Turkey
Nerin BAHÇECİLER, Republic of Northern Cyprus
Özden SANAL, Turkey
Peter M. Johnson, UK
Pier L. MELONI, Italy
Şebnem KILIÇ, Turkey
Selim Badur, Turkey
Stanimir KYURKCHIEV, Bulgaria
Stefan KAUFMANN, Germany
Stephen E. CHRISTMAS, UK
Şefik Şanal ALKAN, Switzerland
Tevfik DORAK, USA
Yehuda SHOENFELD, Israel

OP-4

THE IDENTIFICATION OF THE TUMOR MICROENVIRONMENT MEMBERS, SPECIFICALLY CANCER ASSOCIATED FIBROBLASTS, FOR FUNCTIONAL ANALYSES IN A RAT CHEMICAL MAMMARY CARCINOM

Gurcan GUNAYDIN, Basic Oncology, Hacettepe University Institute of Oncology, Ankara
Yusuf DOLEN, Basic Oncology, Hacettepe University Institute of Oncology, Ankara
Sacit Altug KESIKLI, Basic Oncology, Hacettepe University Institute of Oncology, Ankara
Dicle GUC, Basic Oncology, Hacettepe University Institute of Oncology, Ankara

Constituents of the tumor microenvironment are among key players determining the cancer cell behavior. Seed-centric models do not take into account the probable impact of the microenvironment, soil, that the tumor cells reside in. Fibroblasts are among the most common types of cells found both in connective tissues and the tumor microenvironment. They are thought to be involved in a dynamic crosstalk with other cells of the tumor microenvironment. The aim of this study is to characterize and effectively isolate cancer associated fibroblasts (CAFs) for further functional assays. N-Nitroso-N-Methyl Urea (NMU) induced experimental mammary carcinogenesis model was utilized. 21 days old 20 female Sprague-Dawley rats were injected once-a-week for four weeks with i.p. 50mg/kg NMU. For the control experiments, seven rats were injected with isotonic saline using the same protocol. When the animals are about two months old, developed tumors were harvested surgically under sterile conditions for CAF isolation. Fibroblasts were isolated from breast tumor tissues using a protocol which utilizes collagenase I and hyaluronidase. Enzymatically digested tissues were then cultured in fibroblast-selective-medium. The same protocol was also used to isolate normal tissue fibroblasts from healthy mammary tissues. These CAFs and healthy tissue fibroblasts were immunostained to show their differential expressions of surface markers such as α -Smooth Muscle Actin (α -SMA) and Vimentin, in order to distinguish CAFs from their normal tissue counterparts. These immunostainings clearly showed that CAFs had significantly higher levels of α -SMA expression than normal fibroblasts. This finding of differential α -SMA expression was shown to fade out with further passages of cultured CAFs. Histological examinations also revealed significant morphological differences between these cells. In conclusion, CAFs were successfully propagated using a rat chemical breast carcinogenesis model. Further functional analyses with these CAFs will be performed employing various coculture systems to investigate their roles in immunity against breast cancer.

Keywords: cancer, associated fibroblast, breast cancer, tumor microenvironment, chemical carcinogenesis

Kanserle İlişkili Fibroblastların tümörün immün kaçış mekanizmalarındaki fonksiyonel rollerinin, sıçan kimyasal meme kanseri modelinde araştırılması

Gürçan Günaydın, Yusuf Dölen, Neşe Ünver, Sacit Altuğ Kesikli, Dicle Güç
Hacettepe Üniversitesi Kanser Enstitüsü, Temel Onkoloji Anabilim Dalı, Ankara

AMAÇ: Fibroblastlar, tümör mikroçevresinde KİF'lere (Kanserle-ilişkili-fibroblast) dönüşürler. Tümöre karşı gelişen yetersiz immün yanıtlarda KİF'lerin önemli rolü olduğu düşünülmektedir, ancak bu konuda çalışmalar kısıtlıdır. Bu çalışmayla, KİF'lerin efektör T-hücre yanıtları üzerindeki etkilerinin aydınlatılması; böylece tümör mikroçevresinin tümöre karşı immün yanıtlardaki rolüne yeni bir bakış açısı getirilmesi amaçlanmıştır.

YÖNTEM: NMU(Nitrozometilüre) aracılı kimyasal meme kanseri modeli kullanılarak 21-günlük dişi Sprague-Dawley sıçanlara NMU enjeksiyonları yapılmıştır. Steril koşullarda çıkarılan meme tümörlerinden KİF'ler, sağlıklı meme dokularından NF'ler (normal fibroblastlar); Kollajenaz/Hyaluronidaz aracılı yöntemle izole edilmiştir. KİF'ler ve NF'ler; α SMA(α Smooth-Muscle-Actin) ve vimentin gibi yüzey belirteçlerindeki ekspresyon farklılıklarının gösterilmesi için immünsitokimya ile değerlendirilmiştir. NMU'ya bağlı olası DNA hasarı, Comet analizleriyle incelenmiştir. KİF'ler, splenositlerle kokültür edilmiş ve CFSE(Carboxyfluorescein-succinimidyl-ester) proliferasyon deneyleriyle fonksiyonel analizler yapılmıştır. KİF-splenosit etkileşiminin T hücre immün fenotipi üzerine etkileri, kokültür sonrası T hücrelerinde immün aktivasyon belirteçlerinden CD25'in yüzey, IFN- γ 'nın hücre-içi ekspresyonunun akım-sitometrik analiziyle incelenmiştir. KİF'lerin, sitokin sekresyon profili üzerine etkileri KİF-splenosit kokültür süpernatantlarından IFN- γ ,IL4,IL10,IL17A,TGF β ,TNF α düzeyleri incelenerek yapılmıştır. KİF'lerde TGF β ,PDL1,VEGF,IFN γ ; KİF ile kokültür yapılmış splenositlerde de aktivasyon belirteçleri CD25,CD69; kostimülatör moleküller CD28,CD40L,CD95, 4-1BB-L; sitotoksisite belirteçleri perforin,granzim B gen ekspresyonları incelenmiştir.

BULGULAR: İmmünsitokimya, KİF'lerde α SMA ekspresyonunun NF'lerden belirgin olarak daha yüksek olduğunu göstermiştir. Histolojik incelemeler bu 2 hücre tipi arasında belirgin morfolojik farklar göstermiştir. Comet analizlerinde, NMU enjeksiyonundan 2 ay sonraki DNA hasarı, kontrol düzeyine benzer bulunmuştur. CFSE proliferasyon deneyleriyle yapılan fonksiyonel analizler, KİF'lerin splenositler üzerinde immünsupresif etkileri olduğunu göstermiştir. KİF'lerle kokültürleri yapılan T hücrelerinin immün aktivasyon belirteçlerinden IFN γ 'nın hücre içi ekspresyonunun azaldığı izlenmiştir. KİF-splenosit kokültür süpernatantlarından yapılan incelemelerde de, IL4 düzeyleri artmış olarak gözlenmiştir. Ayrıca KİF ile kokültür yapılmış splenositlerde kostimülatör moleküllerin gen ekspresyonlarında düşüş olduğu izlenmiştir.

SONUÇ: Sıçan kimyasal meme karsinogenez modeli başarıyla uygulanmış, KİF izolasyonları stabil olarak gerçekleştirilmiştir. T hücrelerinde meydana gelen değişikliklerin hem fonksiyonel incelemeler hem de gen ve protein düzeyinde analizlerle gösterildiği bu araştırma sonucunda KİF'lerin anti-tümör immün yanıtlar üzerinde baskılayıcı etkiye sahip olduğu düşünülmektedir.

Anahtar Kelimeler: fibroblast, kimyasal karsinogenez, meme kanseri, mikroçevre, T hücre, tümör immünolojisi

Detaylar

Statü	: Baş Hakemde
Tercih Edilen Sunuş Şekli	: Sözlü Sunum
Bildiri Grubu	: Tümör İmmünolojisi
Dili	: Türkçe
Saved:	: 10.03.2013 20:16:14
Submit:	: 10.03.2013 20:29:57

Yazar ve Editöre Özel Bilgiler

Sunan Yazar : Gürçan Günaydın (gurcangunaydin@hacettepe.edu.tr)

Sıçan kimyasal meme kanseri modelinde Kanserle İlişkili Fibroblastların tanımlanması ve bu hücrelerin tümörün immün kaçış mekanizmalarındaki fonksiyonel rollerinin araştırılması

Gürcan Günaydın, Yusuf Dölen, Sacit Altuğ Kesikli, Dicle Güç
Hacettepe Üniversitesi Kanser Enstitüsü, Temel Onkoloji Anabilim Dalı, Ankara

Amaç: Fibroblastlar, tümör mikroçevresinde KİF'lere (Kanserle ilişkili fibroblast) dönüşürler. Tümöre karşı gelişen yetersiz T hücre yanıtlarında KİF'lerin önemli rolü olduğu düşünülmektedir, ancak bu konuda çalışmalar kısıtlıdır. Bu çalışmayla KİF'lerin efektör T hücre yanıtları üzerindeki etkilerinin aydınlatılması ve böylece tümör mikroçevresinin tümöre karşı immün yanıtlardaki rolüne yeni bir bakış açısı getirilmesi amaçlanmıştır.

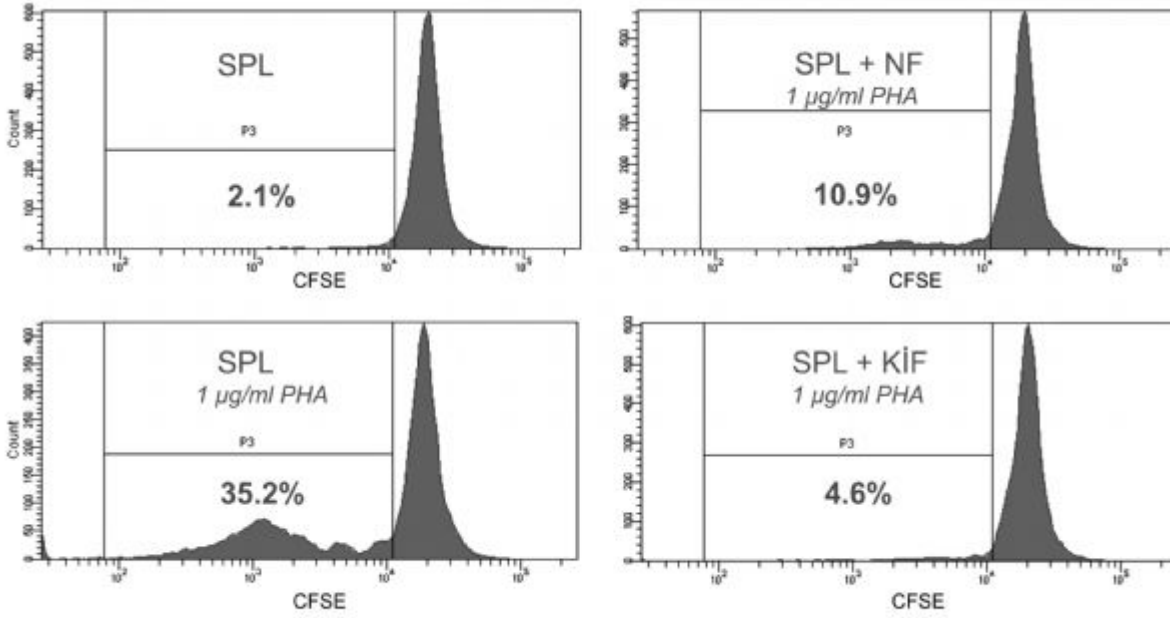
Yöntem: NMU (Nitrozometilüre) aracılı kimyasal meme kanseri modeli kullanılarak 21 günlük dişi Sprague Dawley sıçanlara NMU enjeksiyonları yapılmıştır. Steril koşullarda çıkarılan meme tümörlerinden KİF'ler, sağlıklı meme dokularından da NF'ler (normal fibroblastlar); Kollajenaz/Hyaluronidaz aracılı yöntemle izole edilmiştir. KİF'ler ve NF'ler; α SMA (α Smooth Muscle Actin) ve vimentin gibi yüzey belirteçlerindeki ekspresyon farklılıklarının gösterilmesi için immünsitokimya ile değerlendirilmiştir. NMU'ya bağlı olası DNA hasarı, Comet analizleriyle incelenmiştir. KİF'ler, splenositlerle kokültür edilmiş ve CFSE (Carboxyfluorescein succinimidyl ester) proliferasyon deneyleriyle fonksiyonel analizler yapılmıştır. KİF-splenosit etkileşiminin T hücre immün fenotipi üzerine etkileri, kokültür sonrası T hücrelerinde immün aktivasyon belirteçlerinden CD25'in yüzey, IFN- γ 'nın hücre içi ekspresyonunun akım sitometrik analiziyle incelenmiştir. KİF'lerin, sitokin sekresyon profili üzerine etkileri KİF-splenosit kokültür süpernatantlarından IFN- γ , IL4, IL10, IL17A, TGF β , TNF α düzeyleri incelenerek (ELISA) yapılmıştır. KİF'lerde TGF β , PDL1, VEGF, IFN γ ; KİF ile kokültür yapılmış splenositlerde de aktivasyon belirteçleri CD25, CD69; kostimülator moleküller CD28, CD40L, CD95, 4-1BB-L; sitotoksikite belirteçleri perforin, granzim B gen ekspresyonları incelenmiştir.

Bulgular: İmmünsitokimya, KİF'lerde α SMA ekspresyonunun NF'lerden belirgin olarak daha yüksek olduğunu göstermiştir. Histolojik incelemeler bu 2 hücre tipi arasında belirgin morfolojik farklar göstermiştir. Comet analizlerinde, NMU enjeksiyonundan 2 ay sonraki DNA hasarı, kontrol düzeyiyle aynı bulunmuştur. CFSE proliferasyon deneyleriyle yapılan fonksiyonel analizler, KİF'lerin splenositler üzerinde immünsupresif etkileri olduğunu göstermiştir (Şek). KİF'lerle kokültürleri yapılan T hücrelerinin immün aktivasyon belirteçlerinden IFN γ 'nın hücre içi ekspresyonunun azaldığı izlenmiştir. KİF-splenosit kokültür süpernatantlarından yapılan incelemelerde de, IL4 düzeyleri artmış olarak gözlenmiştir. Ayrıca KİF ile kokültür yapılmış splenositlerde kostimülator moleküllerin gen ekspresyonlarında düşüş olduğu izlenmiştir.

Sonuç: Sıçan kimyasal meme karsinogenez modeli başarıyla kullanılarak stabil bir şekilde KİF izolasyonu gerçekleştirilmiştir. T hücrelerinde meydana gelen değişikliklerin hem fonksiyonel incelemeler hem de gen, protein düzeyinde analizlerle gösterildiği bu araştırma sonucunda KİF'lerin anti-tümör immün yanıtlar üzerinde baskılayıcı etkiye sahip olduğu düşünülmektedir.

Anahtar Kelimeler: fibroblast, kimyasal karsinogenez, meme kanseri, T hücre, tümör mikroçevresi

CFSE Proliferasyon Deneyi Sonuçları



Şek.: CFSE Proliferasyon Deneyi Sonuçları

SPL: Splenosit, NF: Normal fibroblast, KİF: Kanserle ilişkili fibroblast

Detaylar

Statü : Kaydedildi. Bilim Kuruluna Gönderilmedi
Tercih Edilen Sunuş Şekli : Sözlü Sunum
Bildiri Grubu : B.03 Tümör biyolojisi
Dili : Türkçe
Saved: : 17.02.2013 10:10:40
Submit: :

Yazar ve Editöre Özel Bilgiler

Sunan Yazar : Gürcan Günaydın (gurcangunaydin@hacettepe.edu.tr)

[Kapat](#)

[Yazdır](#)